



HAL
open science

Stellar Evolution Beyond the Standard Picture

Ana Palacios

► **To cite this version:**

Ana Palacios. Stellar Evolution Beyond the Standard Picture. Astrophysics [astro-ph]. UNIVERSITÉ MONTPELLIER II ÉCOLE DOCTORALE I2S Information-Structures-Systèmes, 2014. tel-02009628

HAL Id: tel-02009628

<https://hal.science/tel-02009628>

Submitted on 6 Feb 2019

HAL is a multi-disciplinary open access archive for the deposit and dissemination of scientific research documents, whether they are published or not. The documents may come from teaching and research institutions in France or abroad, or from public or private research centers.

L'archive ouverte pluridisciplinaire **HAL**, est destinée au dépôt et à la diffusion de documents scientifiques de niveau recherche, publiés ou non, émanant des établissements d'enseignement et de recherche français ou étrangers, des laboratoires publics ou privés.

UNIVERSITÉ MONTPELLIER II

ÉCOLE DOCTORALE I2S

Information - Structures - Systèmes

CANDIDATURE AU TITRE
HABILITATION À DIRIGER DES RECHERCHES

Dr. Ana PALACIOS

Spécialité : **PHYSIQUE**

**Stellar Evolution
Beyond the Standard Picture**

présentée le 31 mars 2014 devant le jury composé de

Dr. Jérôme BOUVIER	Rapporteur
Pr. Magali DELEUIL	Rapporteur
Dr. Achim WEISS	Rapporteur
Dr. Sophie VAN ECK	Examinatrice
Dr. Nicolas MAURON	Examineur
Dr. Jérôme BALLOT	Examineur

Laboratoire Univers et Particules de Montpellier - UMR 5299 - CNRS / UM2



Contents

1	Curriculum Vitae and Duties	1
1.1	Curriculum Vitae	1
1.2	List of Publications	5
1.2.1	Refereed Journals	5
1.2.2	Conference Proceedings	7
1.3	Teaching Duties	10
1.4	Scientific Duties	10
1.5	Outreach	11
2	Introduction	13
2.1	Classical and Standard Stellar Evolution Modelling	13
2.1.1	Standard Solar Model	16
2.2	Outline	18
3	News on stellar evolution from the observational point of view	21
3.1	Direct probes of the existence of non-standard physical processes in stars	21
3.1.1	Measurements of stellar rotation	21
3.1.2	Magnetic fields	26
3.2	Indirect evidences of the action of non-standard physical processes in stars	31
3.2.1	Activity	31
3.2.2	Abundance patterns	32
3.3	Summary	36
4	Stellar evolution modelling beyond the standard picture	37
4.1	1-D non-standard stellar evolution modelling	38
4.1.1	Modifying the stellar structure equations	40
4.1.2	Modelling the transport of angular momentum and chemicals	42
4.1.3	Personal implication	46
4.2	2-D and 3-D stellar structure modelling	46
4.2.1	Multi-D stellar "evolution" codes	47
4.2.2	(M)HD codes as fine-tooth combs to explore physical processes	48
5	The evolution of solar-type stars	55
5.1	Evolution from the pre-main sequence to the age of the Sun	55
5.1.1	Modelling the interaction of the star with its environment	55
5.1.2	The rotational and chemical evolution from observations	56
5.1.3	Self-consistent non-standard models of solar-type stars including rotation and rotation-induced mixing	59
5.1.4	Self-consistent non-standard models of solar-type stars including rotation, rotation-induced mixing and IGW	63

5.1.5	Self-consistent non-standard models of solar-type stars including rotation, rotation-induced mixing and Tayler-Spruit dynamo	66
5.2	Red Giant Branch stars	68
5.2.1	Rotating models of low-mass RGB stars	68
5.2.2	News from asteroseismology	69
6	Conclusion	73
6.1	Summary	73
6.2	Future prospects	74
A	Constants and Formulae	77
A.1	Units and Constants	77
A.2	Nomenclature	78
B	Selected papers	79

Curriculum Vitae and Duties

Contents

1.1 Curriculum Vitae	1
1.2 List of Publications	5
1.2.1 Refereed Journals	5
1.2.2 Conference Proceedings	7
1.3 Teaching Duties	10
1.4 Scientific Duties	10
1.5 Outreach	11

1.1 Curriculum Vitae

ANA PALACIOS

ASSISTANT ASTRONOMER / ASTRONOME ADJOINT

Date of Birth November 22, 1976
 Place of Birth Montpellier (FRANCE)
 Nationality French / Spanish
 Address : LUPM - UMR 5299
 Université Montpellier II - CC072
 Place Eugène Bataillon
 F-34095 Montpellier cedex 5
 Phone : 33 (0)4 67 14 41 27
 email : ana.palacios@univ-montp2.fr
 webpage : http://www.graal.univ-montp2.fr/hosted/palacios

Research interests

- Stellar evolution
 - Nucleosynthesis
 - Transport processes
 - Hydrodynamics
-

Education

1999-2002 **PhD in Astrophysics**
 University Paul Sabatier, Toulouse, France
 Under supervision of Dr. C. Charbonnel and Dr. M. Forestini
 1998-1999 **D.E.A. (Master) of Astrophysics, Planetology and Space Sci-**
 ences and Technics
 University Paul Sabatier, Toulouse, FRANCE

Research Experience

2007 - present **Assistant Astronomer**
 LUPM - UMR 5299, Montpellier, France
 CNAP duty as responsible of the POLLUX database of synthetic stellar
 spectra
 2005 - 2006 **CEA Post-doctoral research associate**
 CEA/DMS/IRFU/SaP, Saclay, France
 Topic : Hydrodynamical simulation of the convective envelope
 of a rotating RGB star - Effects of rotation on solar models
 2002 - 2005 **ESA Post-doctoral research associate**

I.A.A. - U.L.B. Brussels, Belgium

Topic : ^{26}Al nucleosynthesis in massive stars - Stellar evolution with rotation

Research Projects

- 2012-2016** co-I of the ANR project TOUPIES
TOwards the Understanding of the sPIn Evolution of Stars
- 2012-2014** member of the ANR project TUMSE
TOwards the Understanding of Massive Stars Evolution
- 2012-2013** PI of the PNPS project
Understanding red giant stars and their role on galactic chemical evolution
-

Responsibilities

- PI of the database of synthetic stellar spectra POLLUX (<http://www.pollux.graal.univ-montp2.fr>)
 - Nominated member of the council of the LUPM (CNRS/Université Montpellier II laboratory)
 - Regular referee for Astronomy & Astrophysics, Astrophysical Journal, Science
 - Member of international boards for telescope allocation time
 - Responsible for the recruitment for the Master of Physics of Montpellier II University
 - Responsible of a national working group on Red Giant Stars
 - Organizer of the 2013 Annual Meeting of the French Astronomical Society (SF2A) and editor of the proceedings
-

Academic Supervision

- 2012- present** co-supervisor of Mr Louis AMARD, PhD student in astrophysics
Modelling the angular momentum evolution of young solar-type stars
- 2010-2013** co-supervisor of Mr Abdelaziz MAALEJ, PhD student in computer sciences
Interactive visualization of scientific data in astrophysics
- 2012** supervisor of Mr Daniel EISMANN, Master 2 trainee in astrophysics
Evolution of the angular momentum of solar-type stars from the PMS to the MS
- 2011** supervisor of Mrs Katrin BROSEIT, Master 1 trainee in physics
Impact of helium on the evolution of stars
-

Long Term Academic Stays

- 2009** Invited researcher at UFRN Universidade Federal do Rio Grande do Norte , Natal, Brazil
- 2000** Invited researcher at CERCA Montreal University , Montreal, Canada
-

Schools

- 2013** Invited lecturer at the second OPTICON Awareness Conference, Bucharest, Romania
- 2012** Invited lecturer at the Evry Schatzman School, Aussois, France
- 2008** Invited lecturer at the Nordic-Baltic Research School, Moletai, Lithuania
-

Observing programs

- 2013** PI of the observing program proposal 093.D-0567
Assessment of the dispersion of the rotation period among CoRoT solar analogs
10 h requested on UVES (ESO/Paranal)
Status Pending
- 2011** PI of the observing program proposal 089.D-0189
Weak G band stars : Understanding the puzzle
Status 3 nights granted during Period 89A on FEROS (ESO/La Silla)
- 2008** co-I of the observing program proposal 383.D-0412
Unveiling the origin of fast rotation among horizontal branch stars
Status 10h granted during period 83A on FLAMES (ESO/Paranal)
-

Numerical Codes

Developer of the **STAREVOL** stellar evolution code and regular user of the 3D MHD code Anelastic Spherical Harmonics **ASH**.

1.2 List of Publications

To date, I have published 25 papers in international refereed journals and 30 papers in conference proceedings.

These works are cited in about 460 unique papers, for a h-index of 13.

1.2.1 Refereed Journals

1. F. Martins & **A. Palacios**, *A comparison of evolutionary tracks for single Galactic massive stars*, *Astronomy & Astrophysics*, 560, 16 (2013)
2. C. Charbonnel, T. Decressin, L. Amard, **A. Palacios** & S. Talon, *Impact of internal gravity waves on the rotation profile inside pre-main sequence low-mass stars*, *Astronomy & Astrophysics*, 554, 40 (2013)
3. S. Meibom, S.A. Barnes, K. Covey, R.D. Jeffries, S. Matt, J. Morin, **A. Palacios**, A. Reiners, A. Sicilia-Aguilar & J. Irwin, *Angular momentum evolution of cool stars: Toward a synthesis of observations and theory before and after the ZAMS*, *Astronomische Nachrichten*, 334, 168 (2013)
4. J.P. Marques, M.-J. Goupil, Y. Lebreton, S. Talon, **A. Palacios**, K. Belkacem, R.-M. Ouazzani, B. Mosser, A. Moya, P. Morel et al., *Seismic diagnostics for transport of angular momentum in stars. I. Rotational splittings from the pre-main sequence to the red-giant branch*, *Astronomy & Astrophysics*, 549, 74 (2013)
5. N. Lagarde, T. Decressin, C. Charbonnel; P. Eggenberger, S. Ekstroem & **A. Palacios**, *Thermohaline instability and rotation-induced mixing. III. Grid of stellar models and asymptotic asteroseismic quantities from the pre-main sequence up to the AGB for low- and intermediate-mass stars of various metallicities*, *Astronomy & Astrophysics*, 543, 108 (2012)
6. **A. Palacios**, M. Parthasarathy, Y. Bharat Kumar, G. Jasiewicz, *Weak G-band stars on the H-R diagram: clues to the origin of the Li anomaly*, *Astronomy & Astrophysics*, 538, A68 (2011)
7. S. Turck-Chièze, S. Couvidat, V. Duez, S. Mathis, J.P. Marques, **A. Palacios** & L. Piau, *The dynamics of the radiative zone of the Sun*, *Journal of Physics: Conference Series*, Volume 271, Issue 1 (2011)
8. B.L. Canto Martins, A Lèbre, **A. Palacios**, P. de Laverny, O. Richard, C. H. F. Melo, J. D., Jr. Do Nascimento, J.R., de Medeiros, *Lithium abundances and extra mixing processes in evolved stars of M 67*, *Astronomy & Astrophysics*, 527, A94 (2011)
9. S. Turck-Chièze, **A. Palacios**, J.P. Marques & P.A.P. Nghiem, *Seismic and Dynamical Solar Models I. The Impact of the Solar Rotation History on Neutrinos and Seismic Indicators*, *Astrophysical Journal* 715, 1539 (2010)

10. **A. Palacios**, M. Gebran, E. Josselin, F. Martins, B. Plez, M. Belmas & A. Lèbre, *POL-LUX : a database of synthetic stellar spectra*, *Astronomy & Astrophysics*, 516, A13 (2010)
11. A. S. Brun & **A. Palacios**, *Numerical simulations of a rotating red giant star I. 3-D Models of turbulent convection and associated mean flows*, *Astrophysical Journal*, 720, 1078 (2009)
12. T. Decressin, C. Charbonnel, L. Siess, **A. Palacios**, G. Meynet & C. Georgy, *CNO enrichment by rotating AGB stars in globular clusters*, *Astronomy & Astrophysics*, 505, 727 (2009)
13. A. Lèbre, **A. Palacios**, J. D. do Nascimento Jr, R. Konstantinova-Antova, D. Kolev, M. Aurière, P. de Laverny, J. R. De Medeiros, *Detection of magnetic fields in giants. HD 232 862 : a magnetic and Lithium-rich giant field star*, *Astronomy & Astrophysics* (2009)
14. T. Decressin, S. Mathis, **A. Palacios**, L. Siess, S. Talon, C. Charbonnel & J.-P. Zahn, *Diagnoses to unravel secular hydrodynamical processes in rotating main sequence stars*, *Astronomy & Astrophysics*, 495, 271 (2009)
15. **A. Palacios** & A.S. Brun, *Simulation of turbulent convection in a slowly rotating red giant star*, *Astronomische Nachrichten*, 328, 1114 (2007)
16. S. Mathis, T. Decressin, **A. Palacios** et al., *Meridional circulation in the radiation zones of rotating stars: Origins, behaviours and consequences on stellar evolution*, *Astronomische Nachrichten*, 328, 1062 (2007)
17. S. Mathis, **A. Palacios**, J.-P. Zahn, *Erratum: On shear-induced turbulence in rotating stars*, *Astronomy & Astrophysics*, 462, 1063 (2007)
18. **A. Palacios**, C. Charbonnel, S. Talon, L. Siess, *Rotational mixing in low-mass stars II. Self-consistent models of Pop II RGB star*, *Astronomy & Astrophysics*, 453, 261 (2006)
19. **A. Palacios**, M. Arnould, G. Meynet, *The thermonuclear production of ^{19}F by Wolf-Rayet stars revisited*, *Astronomy & Astrophysics*, 443, 243 (2005)
20. **A. Palacios**, G. Meynet, C. Vuissoz, J. Knoedlseder, D. Schaerer, M. Cerviño, N. Mowlavi, *New estimates of the contribution of Wolf-Rayet stellar winds to the Galactic ^{26}Al* , *Astronomy & Astrophysics*, 429, 613 (2005)
21. S. Mathis, **A. Palacios**, J.-P. Zahn, *On shear-induced turbulence in rotating stars*, *Astronomy & Astrophysics*, 426, 243 (2004)
22. **A. Palacios**, S. Talon, C. Charbonnel, M. Forestini, *Rotational mixing in low-mass stars. I Effect of the μ -gradients in main sequence and subgiant Pop I stars*, *Astronomy & Astrophysics*, 399, 603 (2003)
23. **A. Palacios**, J. Bolmont, C. Charbonnel, F. Thévenin, *Abundance anomalies in RGB stars: field vs GCs*, *Astrophysics and Space Science*, 281, 213-214 (2002)
24. C. Charbonnel, **A. Palacios**, *Abundance anomalies in RGB stars as probes of galactic chemical evolution*, *Astrophysics and Space Science Journal*, 277, 157-160 (2001)

25. **A. Palacios**, C. Charbonnel, M. Forestini, *The Lithium Flash - Thermal instabilities generated by Li burning in RGB stars*, *Astronomy & Astrophysics*, 375, L9 (2001)

1.2.2 Conference Proceedings

1. **A. Palacios**, A.S. Brun, *On dynamo action in the giant star Pollux : first results*, to appear in the proceedings of the IAU Symposium 302 on "Magnetic Fields Throughout the HR diagram", held in Biarritz (France) in August 2013, 2014
2. **A. Palacios**, *Influence of Rotation on Stellar Evolution*, EAS Publications Series, Volume 62, p.227-287, 2013
3. N. Lagarde, P. Eggenberger, C. Charbonnel, T. Decressin, S. Ekstroem, **A. Palacios**, *Thermohaline instability and rotation-induced mixing in low and intermediate mass stars: Consequences on global asteroseismic quantities*, 40th Liège International Astrophysical Colloquium, Ageing Low Mass Stars: From Red Giants to White Dwarfs, Liège, Belgium, EPJ Web of Conferences vol. 43, p. 1006, 2013.
4. A. Lèbre, **A. Palacios**, M. Sanguillon, P. Maeght, *Automatic comparison between observed and computed stellar spectra with tools and protocols from the Virtual Observatory*, SF2A-2012: Proceedings of the Annual meeting of the French Society of Astronomy and Astrophysics, p. 365, 2012
5. **A. Palacios**, *3D Picture of the Convective Envelope of a Rotating RGB Star*, Red Giants as Probes of the Structure and Evolution of the Milky Way, Astrophysics and Space Science Proceedings, 2012, P. 105, 2012.
6. **A. Palacios**, A. Lèbre, M. Sanguillon, P. Maeght, *The POLLUX database of synthetic stellar spectra*, International Workshop on Stellar Libraries, Proceedings of a conference held 5-9 December, 2011 at University of Delhi, India. Astronomical Society of India Conference Series, Vol. 6, 2012, p. 63, 2012.
7. **A. Palacios**, A. Lèbre, J.D. do Nascimento, R. Konstantinova-Antova, D. Kolev, M. Aurière, P. de Laverny, J.R. de Medeiros, *HD 232 862 : a magnetic and lithium-rich giant star*, Light Elements in the Universe, Proceedings of the International Astronomical Union, IAU Symposium, Volume 268, p. 347, 2010
8. A. Lèbre, **A. Palacios**, J.D. do Nascimento, J.R. de Medeiros, R. Konstantinova-Antova, D. Kolev, M. Aurière, *HD 232862: a magnetic and Lithium-rich giant field star*, Cosmic Magnetic Fields: From Planets, to Stars and Galaxies, Proceedings of the International Astronomical Union, IAU Symposium, Volume 259, p. 435, 2009
9. **A. Palacios** & A.S. Brun, *Hydrodynamical Simulations of Turbulent Convection in a Rotating Red Giant Star*, The Art of Modeling Stars in the 21st Century, Proceedings of the International Astronomical Union, IAU Symposium, Volume 252, p. 175-182, 2008

10. **A. Palacios**, E. Josselin, A. Lèbre, F. Martins, R. Monier, B. Plez, M. Belmas, *POL-LUX: a database of stellar spectra - First step : SED and High Resolution Synthetic Spectra*, Astronomical Spectroscopy and Virtual Observatory, Proceedings of the EURO-VO Workshop, held at the European Space Astronomy Centre of ESA, Villafranca del Castillo, Spain, 21-23 March, 2007, ESA Publications p. 217, 2008
11. **A. Palacios**, A.S. Brun, *On the interactions of turbulent convection and rotation in RGB stars*, Convection in Astrophysics, Proceedings of IAU Symposium 239 held 21-25 August, 2006 in Prague, Czech Republic, p. 431, 2007
12. S. Mathis, P. Eggenberger, T. Decressin, **A. Palacios**, L. Siess, C. Charbonnel, S. Turck-Chièze, J.-P. Zahn, *Advances in Secular Magnetohydrodynamics of Stellar Interiors Dedicated to Asteroseismic Spatial Missions*, EAS Publications Series, Volume 26, p.65-78, 2007.
13. Goupil, M. J.; Moya, A.; Suarez, J. C.; Lochard, J.; Barban, C.; Dias Do Nascimento, J.; Dupret, M. A.; Samadi, R.; Baglin, A.; Zahn, J. P.; Hubert, A. M.; Brun, S.; Boisnard, L.; Morel, P.; Garrido, R.; Mathis, S.; Michel, E.; Renan de Medeiros, J.; **Palacios, A.**; Lignières, F.; Rieutord, E. M., *Why Bothering to Measure Stellar Rotation with CoRoT?*, Proceedings of "The CoRoT Mission Pre-Launch Status - Stellar Seismology and Planet Finding" (ESA SP-1306), P. 51, 2006
14. **A. Palacios**, S. Talon, S. Turck-Chièze, C. Charbonnel, *Dynamical processes in the solar radiative interior*, Proceedings of SOHO 18/GONG 2006/HELAS I, Beyond the spherical Sun (ESA SP-624). 7-11 August 2006, Sheffield, UK. Editor: Karen Fletcher. Scientific Editor: Michael Thompson, Published on CDROM, p.38, 2006
15. S. Mathis, T. Decressin, **A. Palacios**, L. Siess, C. Charbonnel, S. Turck-Chièze, J.-P. Zahn, *Dynamical processes in stellar radiation zones: secular magnetohydrodynamics of rotating stars*, Proceedings of SOHO 18/GONG 2006/HELAS I, Beyond the spherical Sun (ESA SP-624). 7-11 August 2006, Sheffield, UK. Editor: Karen Fletcher. Scientific Editor: Michael Thompson, Published on CDROM, p.36, 2006.
16. S. Mathis, T. Decressin, **A. Palacios**, L. Siess, C. Charbonnel, S. Turck-Chièze, J.-P. Zahn, *Dynamical processes in stellar radiation zones*, Highlights of Recent Progress in the Seismology of the Sun and Sun-Like Stars, 26th meeting of the IAU, Joint Discussion 17, 23 August 2006, Prague, Czech Republic, JD17, 18, 2006
17. S. Mathis, T. Decressin, **A. Palacios**, L. Siess, C. Charbonnel, S. Turck-Chièze, J.-P. Zahn, *Dynamical processes in stellar radiation zones: secular magnetohydrodynamics of rotating stars*, SF2A-2006: Proceedings of the Annual meeting of the French Society of Astronomy and Astrophysics, p. 491, 2006
18. **A. Palacios**, ²⁶Al and ¹⁹F nucleosynthesis in Wolf-Rayet and AGB stars, EAS Publications Series, Volume 19, p.67-84, 2006.
19. **A. Palacios**, C. Charbonnel, S. Talon, L. Siess, *Rotation-induced mixing in red giant stars*, ESO-Arcetri Workshop on "Chemical abundances and mixing in stars in the Milky

- Way and its satellites" held in Castiglione della Pescaia, Italy, September 2004, ESO ASTROPHYSICS SYMPOSIA, p. 304, 2006.
20. A. Lèbre, **A. Palacios**, G. Jasniewicz, P. de Laverny, C. Charbonnel, A. Recio-Blanco, F. Thévenin, *Li abundance evolution as probe of extra-mixing in 47 Tuc RGB stars*, Proceedings of " From Lithium to Uranium: Elemental Tracers of Early Cosmic Evolution", IAU Symposium 228, Held in Paris, France, May 23-27, 2005, Proceedings of the International Astronomical Union, v. 228, p. 339, 2005.
 21. **A. Palacios**, C. Charbonnel, S. Talon , L. Siess, *Meridional circulation and shear turbulence in low-mass RGB stars*, EAS Publications Series, Volume 17, p.337-340, 2005
 22. T. Decressin, C. Charbonnel, L. Siess, **A. Palacios**, *The role of low metallicity AGB stars in globular cluster evolution*, SF2A-2004: Semaine de l'Astrophysique Française , meeting held in Paris, France, June 14-18. EdP-Sciences, Conference Series, 283, 2004
 23. T. Decressin, C. Charbonnel, L. Siess, **A. Palacios**, *Rotating models of low metallicity AGB stars with STAREVOL*, Memorie della Società Astronomica Italiana, v.75, p.682, 2004
 24. **A. Palacios**, G. Meynet and C. Vuissoz, *Nucleosynthesis of ^{26}Al in rotating Wolf-Rayet stars*, 5th INTEGRAL workshop "The Integral Universe", held in Munich (Germany) in february 2004, ESA Special Publication SP-552, 111, 2004
 25. C. Charbonnel, **A. Palacios**, *Rotating models for evolved low- and intermediate-mass stars*, invited review paper, Symposium IAU 215 "Stellar rotation" held in Cancun (Mexico) in november 2002, Astronomical Society of the Pacific, p. 440, 2004
 26. **A. Palacios**, *Production of ^{26}Al by Wolf-Rayet stars*, Proceedings of the " Semaine de l'Astrophysique Française", held in Bordeaux (France) in june 2003, eds F. Combes, D. Barret and T. Contini., EdP-Sciences, Conference Series, p. 231, 2003
 27. C. Vuissoz, G. Meynet, J. Knoedlseder, M. Cervino, D. Schaerer, **A. Palacios**, N. Mowlavi, *^{26}Al yields from rotating Wolf-Rayet star models*, "Astronomy with radioactivities IV", held in Seon (Germany) in may 2003, New Astronomy Reviews, 48, p. 7-11, 2004
 28. **A. Palacios**, C. Charbonnel, *RGB stars as clues of galactic chemical evolution*, Cosmic Evolution symposium, held in Paris (France) in november 2000, eds E. Vangioni-Flam, R. Ferlet, and M. Lemoine, New Jersey: World Scientific, p. 217, 2001
 29. **A. Palacios**, C. Charbonnel, *^3He and ^7Li in low and intermediate mass stars*, Euroconference of "The evolution of galaxies", held in Granada (Spain) in may 2000, Astrophysics and Space Science Journal, 277, p. 207-207, 2000.
 30. **A. Palacios**, F. Leroy, C. Charbonnel & M. Forestini, *Nucleosynthesis in evolved stars with the NACRE compilation*, Proceedings of the 35th Liege International Astrophysics Colloquium, held in Liège (Belgium) in July 1999, p. 67, 2000

1.3 Teaching Duties

I **have** a teaching duty attached to my position. It consists of 64h ETD¹ per year, that I have been giving at the Montpellier II University. Since my hiring in January 2007, I have been giving the following lectures :

2007 - present	Numerical Methods for Physicists -Master 1 lecture
2007- 2011	Introduction to Astronomy and Astrophysics within the module " <i>Planet Earth</i> " - First year undergraduate lecture
2009-2010	Stellar structure and evolution within the module " <i>Astrophysics</i> " - Master 1 lecture
2007-2008	Project on the evolution of the Sun within the module " <i>Maniplab</i> " - Third year undergraduate project supervision

Since 2011, I have taken the responsibility of the selection and hiring of the first year master students for the physics speciality, and I am thus released of part of my on-site teaching duty. This administrative duty is concentrated from April to July and concerns both the selection of foreign students applying to the master via the Campus France Embassy network, and that of students coming from french universities. My on-site teaching is concentrated from September to December. It consists of lectures and numerical labs on "Numerical Methods for Physics" at the Master 1 level. Having only one class in charge allowed me to experiment several teaching and evaluation methods over the past 3 years. I have in particular used a series of didactic papers (Cline 2005; Sagert et al. 2006) to set up a non-standard evaluation process based on personal projects rather than a final classroom test. This resulted in a greater implication of the students, who eventually managed to better understand the use and purpose of the numerical tools they are taught.

In addition to my teaching duty, I have also been invited to give lectures on stellar astrophysics in several national and international schools as mentioned in my curriculum vitae.

I **have** also supervised several undergraduate trainees for projects lasting over 1 week to 4 months.

1.4 Scientific Duties

As an assistant astronomer, I have a community duty referred to as an observing service, that should occupy 25 % of my time. The main task I assume in this framework is the responsibility of the POLLUX database of high-resolution stellar synthetic spectra and spectral energy distributions.

This work consists in managing the data that are made available in the database through a dedicated web interface, and make these data interoperable within the framework of the Astronomical Virtual Observatory. I work in tight collaboration with A. Lèbre, Astronomer at the LUPM who is the initiator of the development of this database, and Michèle Sanguillon, a research engineer who deals with all the technical aspects (software development).

Since my hiring on the project, I have worked on the definition of a specific header describing

¹ETD stands for "Equivalent Travaux Dirigés", meaning on-site teaching.

in details each data in POLLUX. This dedicated DataModel was the first step to make the data interoperable. We have further made the database VO-compliant with the support of P. Maeght, a research engineer from the *Observatoire Virtuel Grand Sud Ouest*², an administrative and logistic structure in which POLLUX is identified. The other aspects of my work have been to verify the quality of the data in POLLUX, to advertise the database at an international level, to coordinate the integration of new data.

POLLUX is currently accessible via this webpage

<http://www.pollux.graal.univ-montp2.fr>

It can also be queried through the VIZIER Catalog Service at the Centre de Données de Strasbourg, and using specific VO-tools such as VOSpec, through the registries of the Virtual Observatory.

We are currently working on further developments of the database within the Virtual observatory. We have for now developed an application, VOSPECFLOW³ that allows to compare within the VO an observed spectrum from the TBLLegacy database⁴ with theoretical spectra from POLLUX. The next step will be to propose to the community a spectral convolution service.

1.5 Outreach

I have been involved in scientific outreach ever since I started as a PhD. Here is a list of the main activities of outreach I have organized or participated to:

- Photography exhibition "Infinités Plurielles" by Marie-Hélène Le Ny sponsored by the Ministère de l'Enseignement Supérieur et de la Recherche - 2013
- Presentation of personal career at a Springboard meeting organized by the "Action Sociale et Culturelle" department of the Montpellier II University - December 2013
- Organization of the contest " Découvrir l'Univers" organized in parallel of the Annual Meeting of the French Astronomical Society (SF2A) - June 2013
- Participation to a " Café des Métiers" organized by the city of Montpellier and the local radio station AVIVA for the International Women's Day - March 2013
- Participation to several annual national " Fête de la Science" events - 2007 to 2009, 2013
- Invited speaker to the radio show "La tête dans les étoiles" on the local radio station radio AVIVA - 2012
- Regularly consulted as an expert by journalists from the french astronomy magazine "Ciel & Espace" - 2008 to 2013

²<http://ov-gso.irap.omp.eu/doku.php>

³<http://cdab.bagn.obs-mip.fr/vospecflow/>

⁴<http://tblegacy.bagn.obs-mip.fr/>

- Conference at the Planetarium Galilée - 2009
- Responsible for the IYA 2009 activities of the GRAAL - 2008-2009
Design and creation of a planetary path for the university of Montpellier II (still on location); design and creation of an astronomy pictures exhibition "Univers Morceaux Choisis"
- Public conference in Montpellier suburbs - 2008
- Outreach in schools - 2007 to 2009, 2014
- Scientific Supervision for the EPOS (European Project On the Sun) - 2000

Introduction

Contents

2.1	Classical and Standard Stellar Evolution Modelling	13
2.1.1	Standard Solar Model	16
2.2	Outline	18

Stellar evolution and stellar evolution models are a cornerstone not only for stellar astrophysics but also for galactic physics, planet formation, cosmology, ... Stellar evolution models are used in many aspects of astrophysics, to evaluate masses, radii and ages of stars but also of their surrounding planets, to constrain the formation and structure of the associations, clusters and galaxies they are found in, to evaluate galactic and extragalactic distances and ages, to understand the cosmic evolution of nuclides. Understanding how stars evolved from their birth to their state of remnant is thus of prime importance.

2.1 Classical and Standard Stellar Evolution Modelling

A star is a continuous plasma that should be described by fully three-dimensional hydrodynamical equations - namely the continuity equation, the equation of motion, the energy conservation equation, the heat transfer equation and the abundance conservation equation - that all describe the temporal evolution of key quantities and thus give the necessary framework¹ to study the evolution of stars.

In practice, it is not possible as of today to follow both the dynamical evolution of a star, on small time and spatial scales, and its secular evolution, on long time and large spatial scales. This is illustrated by Fig 2.1 from [Decressin et al. \(2009\)](#).

To solve the problem of stellar *evolution*, the classical models rely on two main simplifying complementary approaches : reduce the 3D problem to a 1D problem and neglect all the hydrodynamical processes (and scales) but convection. In the case of non-rotating, weakly or non-magnetic single stars, pressure and gravity are the only forces acting on a mass element. The resulting spherically symmetric configuration allows to reduce the problem of stellar evolution to the resolution of a set of equations that only depend on time and one spatial coordinate

¹They should be supplemented by an equation of state for the plasma, an equation for other thermodynamical quantities such as the specific heats, by an equation for the opacity of the plasma and by a network of nuclear reactions.

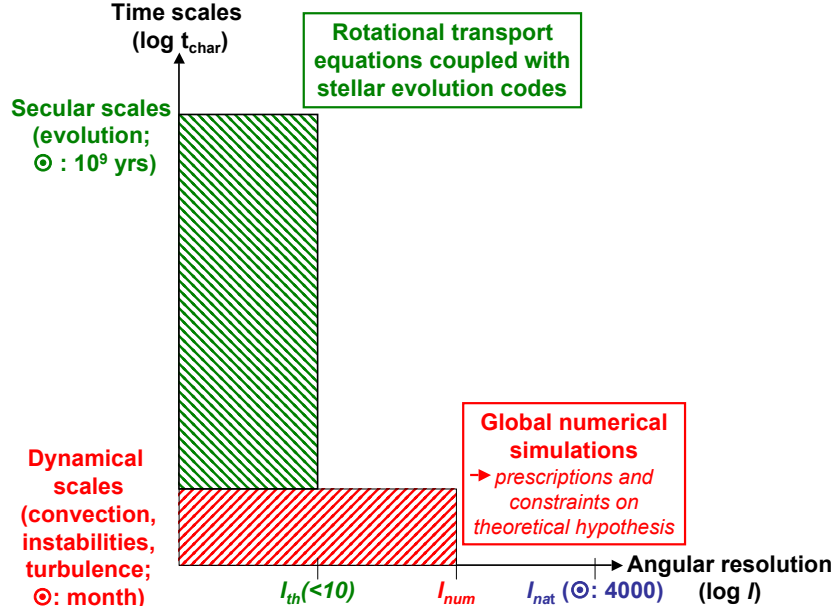


Figure 2.1: Modelling strategy to study dynamical stellar evolution. The diagram presents time scales of the typical physical processes as a function of the angular resolution needed to properly describe these processes. The angular resolution is expressed in terms of the ℓ index of the spherical harmonics $Y_{\ell,m}(\theta, \phi)$. ℓ_{num} 600 indicates the maximum angular resolution (in terms of spherical harmonics nodes) presently achieved in global numerical simulations. *From Decressin et al. (2009)*

as illustrated in Fig. 2.2. This considerably simplifies the numerics of the problem and allowed for the first stellar evolution codes and model outputs to be published in the late 1950's (Henyey et al. 1959a,b; Tayler 1954; Kushwaha 1957).

The typical time scales governing such an idealized star are the Kelvin-Helmoltz ($t_{KH} = GM_*^2/R_*L_*$) and the thermonuclear time scales. Dynamical time scales are completely neglected as are the small scales at which they occur. The convective instability is defined according to the Schwarzschild or the Ledoux criterion, and the simplified approach of the Mixing Length Theory (hereafter MLT) first proposed by Böhm-Vitense (1958) is used according either to Kippenhahn's formalism (Kippenhahn et al. 2013) or to Cox & Giuli's (Weiss et al. 2004). The convective regions are supposed to be instantaneously homogenized, an approach that remains valid as long as the thermonuclear time scales are much longer than the convective turnover time τ_{conv} .

Instead of the natural eulerian formulation that would derive from expressing the general conservation equations as a function of the radius r only, the Lagrangian formulation is normally preferred. In that case, the spatial coordinate is thus the mass m associated to a radius r^2 and time derivatives become Lagrangian derivatives defined by

² m is the mass contained in a concentric sphere of radius r at a given time t .

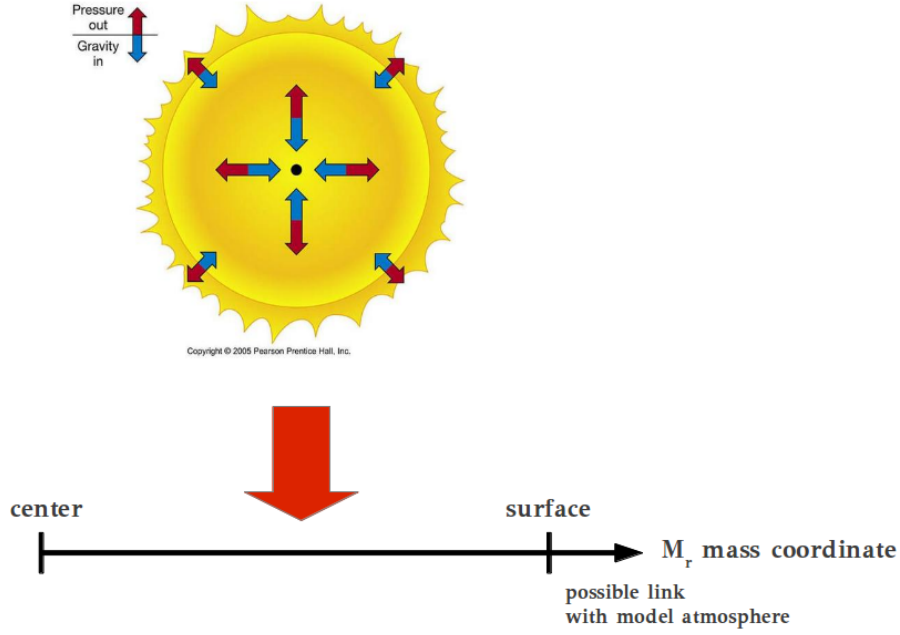


Figure 2.2: Illustration of the hydrostatic equilibrium in a non-rotating, non-magnetic single star and of the 1D stellar model used in stellar evolution

$$\left. \frac{D}{Dt} \right|_m = \frac{\partial}{\partial t} + v \frac{\partial}{\partial r}. \quad (2.1)$$

The resulting set of stellar structure equations is the following:

$$\frac{\partial r}{\partial m} = \frac{1}{4\pi r^2 \rho} \quad (2.2)$$

$$\frac{\partial P}{\partial m} = -\frac{1}{4\pi r^2} \left(\frac{Dv}{Dt} + \frac{\partial \Phi}{\partial m} \right) = -\frac{1}{4\pi r^2} \left(\frac{Dv}{Dt} + \frac{Gm}{r^2} \right) \quad (2.3)$$

$$\frac{\partial L}{\partial m} = \varepsilon_n - \varepsilon_\nu - C_p \frac{\partial T}{\partial t} + \frac{\delta}{\rho} \frac{\partial P}{\partial t} = \varepsilon_n - \varepsilon_\nu + \varepsilon_g \quad (2.4)$$

$$\frac{\partial T}{\partial m} = -\frac{GmT}{4\pi r^4 P} \left. \frac{d \ln T}{d \ln P} \right|_{\text{medium}} = -\frac{GmT}{4\pi r^4 P} \nabla \quad (2.5)$$

$$\frac{\partial X_i}{\partial t} = \frac{m_i}{\rho} \left(\sum_j r_{ji} - \sum_k r_{ik} \right) \quad \forall i \quad (2.6)$$

The meaning of the different symbols are as usual and are detailed in Appendix A. The luminosity L is defined by :

$$L = 4\pi r^2 (F_{\text{conv}} + F_{\text{rad}}) = \frac{16\pi ac GmT^4}{3\kappa P} \nabla_{\text{rad}} \quad (2.7)$$

These equations need to be complemented by

1. an equation of state $\rho = \rho(P, T, \mu)$
2. an expression for the mean Rosseland opacity of the plasma, $\kappa = \kappa(P, T, \mu)$
3. a network of nuclear reactions rates r_{ij}
4. an equation for energy production/losses by neutrinos ε_ν
5. a description of the energy transport by convection to obtain F_{conv}

The **convective** flux, hence the temperature gradient ∇ , can be formulated as follows within the framework of the MLT (Kippenhahn et al. 2013) :

$$F_{conv} = \rho C_p T \sqrt{g \delta} \frac{l^2}{4\sqrt{2}} H_p^{-3/2} (\nabla - \nabla_e)^{1/2} \quad (2.8)$$

where H_p is the pressure scale height. $l = \alpha_{\text{MLT}} H_p$ is the so-called “*mixing length*” over which a fluid element dissolves completely into its surroundings, with α_{MLT} a parameter of order unity that is calibrated by having a $1 M_\odot$ model reproducing the Sun’s radius, luminosity and temperature at the age of the Sun. $\nabla_e = \left. \frac{d \ln T}{d \ln P} \right|_e$ is the temperature gradient of the fluid element.

Solving the set of equations Eq. (2.2) to Eq. (2.6) leads to the computation of what we will refer to as a **standard stellar evolution model**. This denomination indicates that the only hydrodynamical mechanism leading to transport of matter (nuclides) in such models is the convective instability. It manifests in particular by the absence of the a velocity or diffusion term in the equation for the evolution of the nuclides mass fractions Eq.(2.6).

This denomination is however changing, and models including what is called *microscopic diffusion* are considered to be standard, in particular when considering the case of the Sun. Indeed a calibrated solar model computed using this standard set of equations is referred to as a *classical solar model*

2.1.1 Standard Solar Model

The **denomination of standard solar model** is commonly used for models that include microscopic diffusion. This process derives from first principles and should thus naturally be included in any stellar evolution model. The necessity of its inclusion in solar models was strongly impulsed by helioseismology and the direct comparison of the soundspeed profile as inverted from helioseismic data and that predicted by stellar evolution models (see e.g. Bahcall & Pinsonneault 1992; Christensen-Dalsgaard et al. 1996; Richard et al. 1996; Brun et al. 1998).

The **denomination "microscopic diffusion"** is used to describe slow transport mechanisms occurring in stellar radiative regions generated by the relative drift of the different species with respect to each other due to concentration, pressure and temperature gradients in the stellar plasma and to collisions between species (Chapman & Cowling 1970; Burgers 1969).

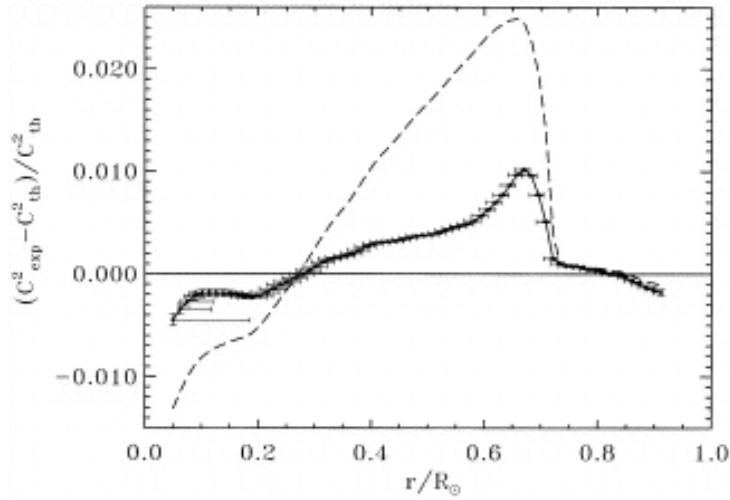


Figure 2.3: Sound-speed square difference between the Sun as measured by GOLF + LOWL experiments and models without (dashed line) and with diffusion (solid line with experimental error bars). From *Brun et al. (1998)*

According to the Fick law³ the presence of a local radial concentration gradient for a given species a implies that the nuclides a will *diffuse* at a speed v_a to reduce this gradient. The separation of charges (electrons and ions) in stellar plasmas will also induce a radial electric field E that will modify the impact of the pressure gradient on the velocity of nuclides a (*Montmerle & Michaud 1976*). This effect is often referred to as the *gravitational settling*. As noted before, collisions between nuclides will compete with their drifting and should also be included (*Chapman & Cowling 1970; Paquette et al. 1986*). They will in particular be generated by temperature gradients in the plasma.

Finally one should also take into account the momentum transfer between photons and ions that represents yet another source of nuclides movement, called *radiative acceleration* (see e.g. *Michaud et al. 1976; Turcotte et al. 1998; Richard et al. 2001*).

Considering these effects, and applying the so-called *test atom* formalism that is based on the fact that all nuclides diffuse with respect to the population of the most abundant species, 1 , we can give the following expression for the *microscopic diffusion velocity* of nuclides a :

3

$$\vec{j}_a = -\mathcal{D}\vec{\nabla}n_a$$

where $\vec{\nabla}n_a$ is the local composition gradient for species a and \vec{j}_a is the flux appearing in order to reduce such gradient. \mathcal{D} is called diffusion coefficient and measures the efficiency of the transport of species a in order to reduce the gradient.

$$v_{1a} = \mathcal{D}_{1a} \left\{ - \underbrace{\nabla \ln c_a}_{\text{concentration gradient}} + \underbrace{k_p \nabla \ln P}_{\text{gravitational settling}} + \underbrace{\alpha_{1a} \ln T}_{\text{thermal diffusion}} + \underbrace{\frac{mF}{kT}}_{\text{external forcing}} \right\} \quad (2.9)$$

where \mathcal{D}_{1a} is the molecular diffusion coefficient, ∇ is the partial radial derivative $\partial/\partial r$, c_a is the concentration of nuclides a , α_{1a} is the thermal diffusion coefficient of species a with respect to the most abundant one 1 in the [Paquette et al. \(1986\)](#) formalism, and the external forcing term can be identified to the radiative acceleration term. The gravitational settling term can be expressed as

$$k_p \ln P = \left(A_a - \frac{Z_a}{2} - \frac{1}{2} \right) \left(\frac{m_p}{kT} \frac{Gm_r}{r^2} \right) \quad (2.10)$$

where m_p is the proton mass.

Taking microscopic diffusion into account modifies the evolution of the mass fraction (hence the concentration) of nuclides of type i described by Eq. (2.6) in classical models. Its new expression is of the form :

$$\frac{\partial c_i}{\partial t} = \mathcal{D}'_{1i} \frac{\partial^2 c_i}{\partial m^2} + \left(\frac{\partial \mathcal{D}'_{1i}}{\partial m} - v'_{1i} \right) \frac{\partial c_i}{\partial m} - \left(\frac{\partial v'_{1i}}{\partial m} + \lambda_i \right) c_i \quad (2.11)$$

where c_i is the concentration of nuclides i , λ_i is the nuclear variation rate (of the form of the right-hand side of Eq. (2.6)), $v'_{1i} = 4\pi\rho r^2 v_{1i}$ is the microscopic diffusion velocity of species i in the lagrangian framework and $\mathcal{D}'_{1i} = (4\pi\rho r^2)^2 (\mathcal{D}_{macro} + \mathcal{D}_{1i})$ is the total diffusion coefficient for nuclides of type i , with \mathcal{D}_{macro} the diffusion coefficient associated to *macroscopic* transport processes (that will be detailed further on).

The introduction of microscopic diffusion and the definition of a new standard for solar model greatly improved the comparison to the inverted soundspeed profile from helioseismic data as shown in Fig. 2.3 from [Brun et al. \(1998\)](#).

Beyond the solar model, microscopic diffusion combined to radiative acceleration has proved to be a key mechanism to understand the abundance patterns of stars with radiative envelopes (typically A and early F type stars) ([Richer et al. 2000](#); [Richard et al. 2001](#); [Théado et al. 2012](#)). Microscopic diffusion is thus usually included in standard stellar evolution models but can be neglected during specific evolutionary phases or in the modelling of certain types of stars, when its effects are known to be negligible.

2.2 Outline

The standard stellar evolution models have been used ever since the 1950's with great success to interpret and understand numerous observational data, allowing for a good understanding of the structure and evolution of stars to a zero level. However, numerous evidences of departures from the standard models predictions have also been exposed by a large and increasing variety

of observations. This motivated the need to *go beyond the standard modelling* already in the late 1970's but it is not until the last decade that *non-standard* stellar evolution models really became more commonly used.

In this document, I intend to give a review of our understanding of stellar evolution beyond the standard picture and to summarize my contribution to this field.

As a start, a state-of-the-art review of the observational facts evidencing the need for more physics in the stellar evolution models is presented in Chap. 3. Chap. 4 will give some keys to the non-standard stellar evolution modelling, focusing both on the improvement of the 1D stellar evolution models, and on the efforts made to move to a multi-dimensional more realistic picture of the stellar structure at different evolutionary points and for different types of stars. Having mainly worked on the modelling of solar-type stars at different stages of their evolution, I will use these stars to present selected results of non-standard stellar evolution models in Chap. 5. A conclusion and some perspectives are finally given in Chap. 6.

News on stellar evolution from the observational point of view

Contents

3.1 Direct probes of the existence of non-standard physical processes in stars	21
3.1.1 Measurements of stellar rotation	21
3.1.2 Magnetic fields	26
3.2 Indirect evidences of the action of non-standard physical processes in stars	31
3.2.1 Activity	31
3.2.2 Abundance patterns	32
3.3 Summary	36

Our understanding of stellar evolution and of the way the different locations in the Hertzsprung-Russell diagram are connected, entirely relies on our ability to make the connection between theoretical and models predictions and observational facts.

It is observational facts that have been driving the new advances in stellar evolution modelling in the past ten years. We present here an overview of the main observational evidences, both direct and indirect, that the standard evolution models presented in the introduction need to be revised.

3.1 Direct probes of the existence of non-standard physical processes in stars

3.1.1 Measurements of stellar rotation

The rotation of stars was first evidenced by Galileo Galilei ([Galilei et al. 1613](#)) in the case of the Sun, and in the late nineteenth - early twentieth century, the development of spectroscopy allowed astronomers to first envision to measure the rotation of stars by studying the broadening of the spectral lines that should result from it ([Abney 1877](#); [Monck 1890](#); [Souleyre 1898](#); [Fowler 1900](#)).

Direct measurements of the rotation rate of stars are accessible via

- *photometry* light curve modulation by rotation allows to derive rotation periods P_{rot} ;

- *spectroscopy* spectral lines broadening is partly due to surface rotation and an estimation of the projected surface velocity on the line of sight, $v \sin i$ can be obtained from spectral analysis;
- *spectropolarimetry and Doppler imaging* modulation of the polarized signal by rotation allowing to derive rotation periods P_{rot} and surface latitudinal differential rotation $\delta\Omega$;
- *asteroseismology* splitting of oscillation modes due to rotation allows the reconstruction of the internal rotation profile of some stars in addition to the Sun;
- *interferometry* direct imaging of rapidly rotating non-spherical stellar surfaces allows to estimate the mean rotation rate as a fraction of the break-up velocity.

The **rotational study** of stars based on these measurements allows us to draw some sort of rotational HR diagram :

O and B-type stars (Fig. 3.1, ab):

$v \sin i$ **measurements** in the Galaxy and in the Magellanic Clouds indicate that these are rapidly rotating stars, with a mean projected velocity of about 130 km.s^{-1} for B-type stars (Bragança et al. 2012; Hunter et al. 2008; Mokiem et al. 2006; Abt et al. 2002), and about 110 km.s^{-1} for O-type stars (Penny 1996; Penny & Gies 2009). Some stars in the On subtype (with nitrogen enrichment) can reach projected velocities of about 420 km.s^{-1} (Walborn et al. 2011) but the number of these very rapid rotators is actually limited.

A and F-type stars (Fig. 3.1c)

A **large survey** of A and F type stars allowed Royer and collaborators (see Royer et al. 2007, and references therein) to establish a good statistic for their typical rotation. These are generally rapid rotators, $\langle v \sin i \rangle \approx 150 \text{ km.s}^{-1}$, although the velocity distribution is more complex when going into more details for each subtype. For instance, a significant fraction of late A-type stars rotate at more than 50% of their break-up velocity. Actually part of the fast rotating oblate stars imaged with interferometry and rotating near the break-up limit are A-type stars (see e.g. Zhao et al. 2011).

G, K and M-type giants (Fig. 3.2)

The **spectral lines** broadening of red giants and red supergiants is dominated by surface convection, which makes the spectroscopic determination of rotation velocity somewhat challenging. **Overall, red giant** stars are generally slow rotators, with surface velocities lower than about 10 km.s^{-1} (de Medeiros 2004; Carlberg et al. 2011). However, some of them present unusually higher projected velocities ($\gtrsim 10 \text{ km.s}^{-1}$) as evidenced by Rucinski (1990); Barnbaum et al. (1995); Carlberg et al. (2011, 2012). Also evidenced from asteroseismic data, they have been interpreted as the result of some peculiar events that may occur during this phase.

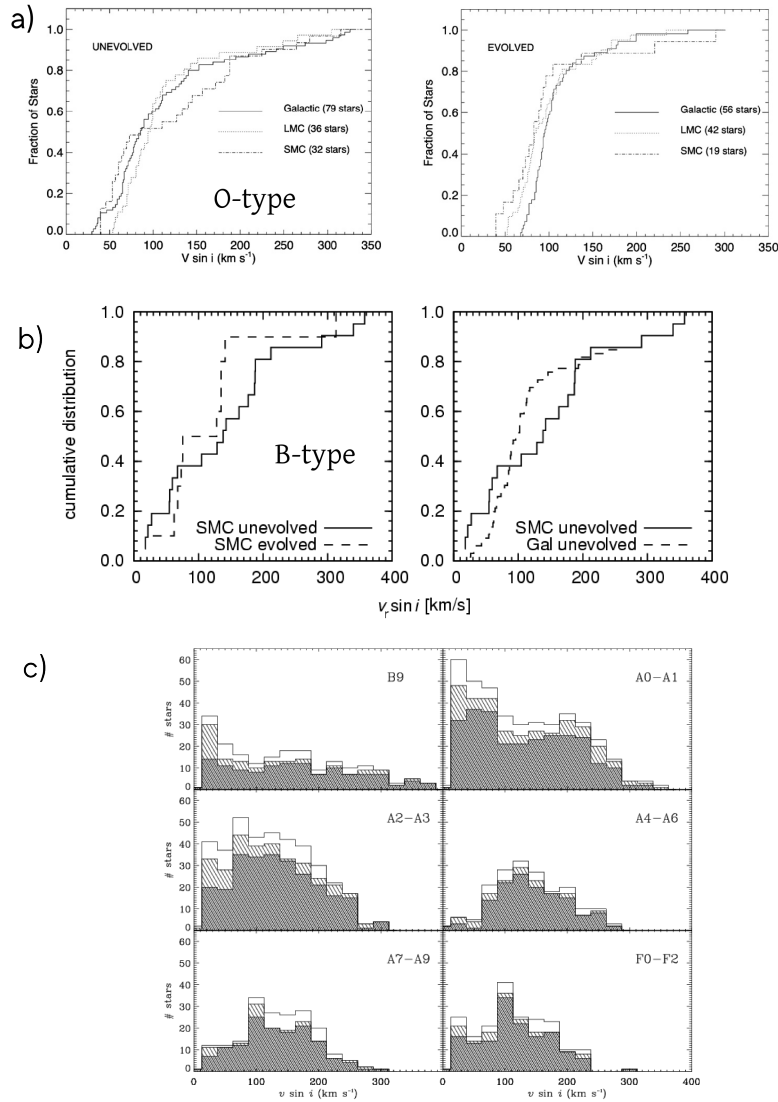


Figure 3.1: Rotation of early-type stars. *a)* Projected velocity distribution of O-type stars (From *Mokiem et al. (2006)*); *b)* Projected velocity distribution of B type stars (From *Penny & Gies (2009)*); *c)* Projected velocity distribution for A-type stars (From *Royer et al. (2007)*)

Low-mass pre-main sequence and main sequence stars (Fig. 3.2)

A large effort has been dedicated to measure rotation periods via photometric surveys of open clusters sampling a wide range of ages (see MONITOR project for instance). These studies show that from an essentially bi-modal distribution of P_{rot} at young ages, the rotation converges to a single low P_{rot} (for solar-type stars) or high P_{rot} (for very low-mass stars - M-type) at the age of the Hyades.

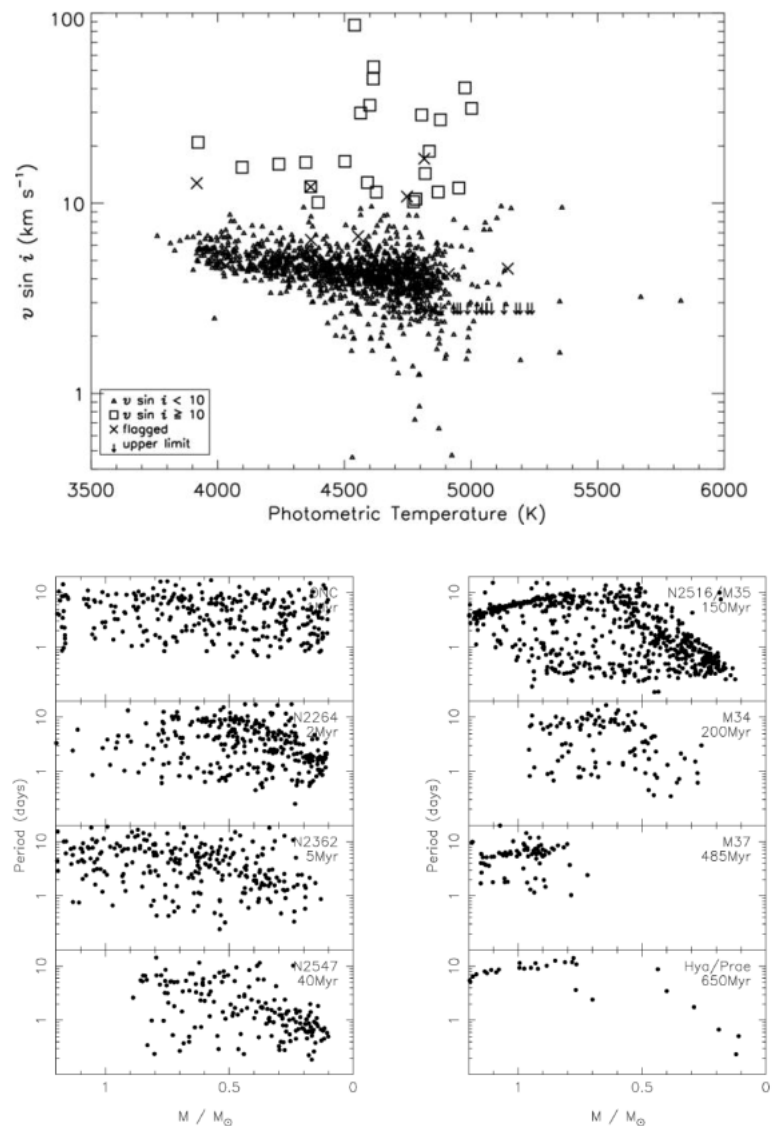


Figure 3.2: Rotation of cool stars . Upper panel Projected velocity as a function of surface temperature for a sample of K-type giants (From *Carlberg et al. (2011)*); Lower panels Rotation periods as a function of mass and age in a set of open clusters (From *Irwin & Bouvier (2009)*).

These direct measurements testify the ubiquity¹ of stellar rotation and indicate in some cases that it can lead to significant departures from the spherical symmetry. They also show that the stellar angular velocity (and angular momentum) differs according to spectral type, which implies differences according to stellar mass and evolutionary status.

¹I did not mention here the case of stellar remnants as white dwarfs and neutrons stars, which are also known to experience rotation.

Internal rotation of the Sun and of red giants (Fig. 3.3)

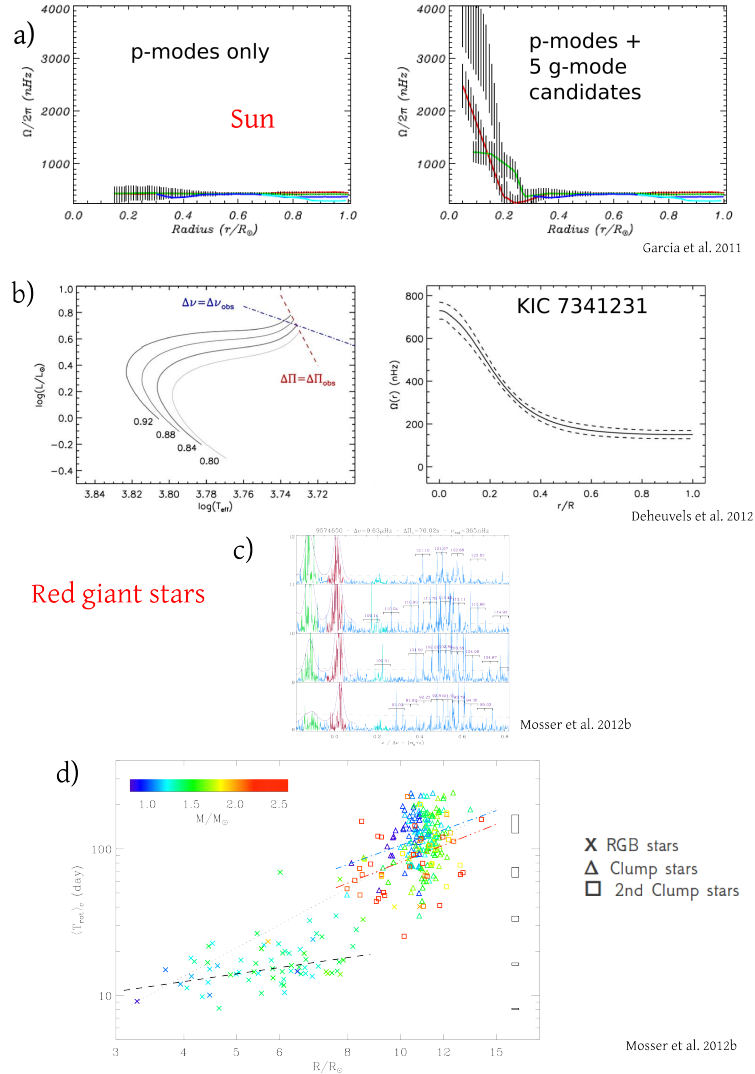


Figure 3.3: Probing the internal rotation of stars through solar-like oscillations : a) Inversion of the internal rotation profile of the Sun using 4608 days of MDI and GOLF data; b) Evolutionary status and internal rotation profile as deduced from mixed-modes for the subgiant KIC 7341231; c) Rotational splittings of the mixed modes corresponding to radial orders 8 to 11 in the giant KIC 9574650; d) Mean period of core rotation as a function of the asteroseismic stellar radius for about 300 Kepler giants.

Thanks to helioseismic data from the SoHO satellite (García et al. (2011)) and much more recently to the instruments on-board the CoRoT and KEPLER satellites (De Ridder et al. (2009); Beck et al. (2012); Deheuvels et al. (2012); Mosser et al. (2012b,a)), an insight to the *internal rotation profile* of the Sun and of a large number of red giant stars has become available. This opens a completely new road for our understanding of stellar structure and angular momentum distribution and constitutes extremely valuable constraints to stellar models.

Solar-like oscillations are due to the trapping of sound waves excited by convection. Assuming a spherical star, such oscillations appear as a discrete spectrum of degenerate modes characterized by their radial order n and their spherical harmonic degree l . The azimuthal number m is degenerated, a degeneracy that is completely lifted by rotation as well as other aspherical perturbations.

In the Sun, the pressure modes (p -modes) are trapped in relatively superficial cavities and probe the convective envelope and part of the underlying radiative interior, the solar core remaining unprobed. Gravity modes on the other hand (g -modes) are generally confined to inner cavities, and scarcely appear at the surface. They could probe the solar core but do not appear at the solar surface and are extremely difficult to detect : after 14 years of SoHO data integration, only g -mode candidates have been tentatively identified (García et al. (2011)). In red giant stars, the situation was discovered to be unexpectedly simpler, since mixed gravity/pressure modes have been detected. These modes correspond to the coupling of gravity waves in the interior to pressure waves in the envelope and give unprecedented insight on the internal properties of red giant stars.

Figure 3.3 displays the inverted radial rotation profile of the Sun (García et al. (2011)) and of the subgiant named Otto from the Kepler fields (Deheuvels et al. (2012)), as well as a core rotation period versus asteroseismic stellar radius plot for a sample of about 300 red giants from the Kepler field (Mosser et al. (2012a)). Red giants appear to experience differential rotation in their interior, and hints exist that a similar behaviour could exist in the solar central regions as can be seen from panels a) and b).

Another important point coming out of these data is a clear distinction between clump (e.g. core helium burning stars) and red giant stars (e.g. shell hydrogen burning stars) in terms of core rotation period (panel d)). This provides a new powerful tool to discriminate between stars belonging to these very different evolutionary phases that occupy overlapping regions in the Hertzsprung-Russell diagram and are thus very difficult to distinguish from classical surface parameters as temperature or magnitude.

3.1.2 Magnetic fields

Magnetic fields are ubiquitous in the Universe and stars make no exception. The magnetized nature of stars was revealed for the first time in the case of the Sun at the beginning of the 20th century by Hale. Magnetic fields affect the structure and energies of atomic/molecular energy levels and thus the profiles and polarisation properties of stellar spectral lines.

They are detected through the Zeeman effect and marginally (because it is up to now only detected for the Sun), the Hanle effect. The Zeeman effect is generated by a splitting of energy levels in atoms/ molecules in presence of a magnetic field. The spectral signature of the Zeeman effect is a splitting of specific lines when the field is strong enough (about 1 kG at optical wavelengths), or a broadening of these lines when the field is weaker and the splitting cannot be resolved. The Zeeman splitting is illustrated in Fig. 3.4.

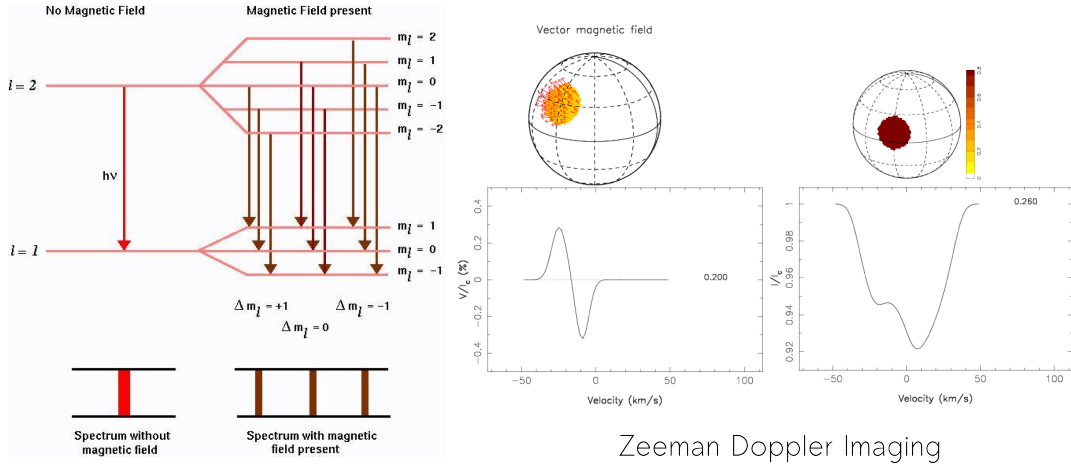


Figure 3.4: *Left* Zeeman line splitting . *Right* Zeeman Doppler Imaging. Based on *J.-F. Donati's* images.

Associated to the splitting of energy levels is the light polarisation. The Zeeman polarization depends on the properties of the magnetic field vector and is insensitive to weak tangled fields for which it cancels out. While the direct broadening or splitting of lines gives information on the field intensity, the analysis of the polarization allows to infer the intensity of the longitudinal magnetic field and gives information on the large scale structures of the magnetic field.

The polarisation of stellar light is described in terms of the Stokes vector : I represents the total specific intensity of light, Q and U the linear polarisation and V the circular polarisation of the beam. IQUV profiles can be directly obtained thanks to spectropolarimetry in full Stokes mode. The Stokes V profile is particularly used to measure the longitudinal component of the field. Using specific spectral masks that allow to average the polarized signal over thousands of spectral lines, it is possible to probe (longitudinal) field intensities as low as 1 gauss. Finally, using the deformation of the Stokes I and V profiles by the presence of magnetized spots at the surface of stars, it is possible to infer the position of these spots and the field orientation using Zeeman Doppler Imaging (ZDI, e.g. Semel 1989; Donati 2001), see Fig. 3.4.

The use of spectropolarimetry and in particular the operation of the high-resolution spectropolarimeters ESPaDOnS@CFHT and NARVAL@TBL, has opened the path to an in depth characterization of stellar magnetism all over the HR diagram. Donati & Landstreet (2009) give a recent overview of the main results obtained for non-degenerate stars.

Let us summarize the present panorama of direct measurements of magnetic fields found for the different spectral types.

O, B and A type stars

- From the large sample of 554 OB stars observed and analysed within the MiMeS consortium studying the magnetism of massive stars, only about 7% of O and B-type stars have a detected magnetic field (Wade et al. 2013). Values in the range 200 G to 5 kG are derived for the longitudinal field B_l in massive stars. The large scale fields are organised in simple and steady structures. The magnetic early type stars are mostly slow rotators. Of?p stars are

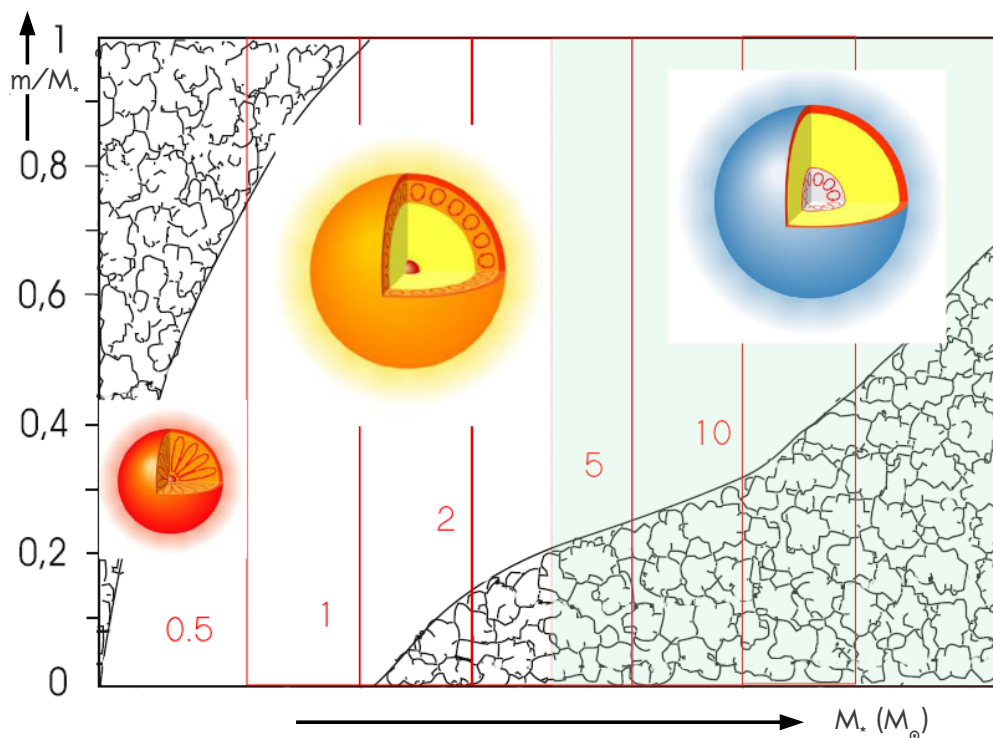


Figure 3.5: Internal structure of main sequence stars as a function of mass at solar metallicity. *Adapted from (Kippenhahn et al. 2013).*

slow rotators and have all been found to have very strong large scale magnetic fields of the order of $\simeq 10$ kG.

- In the intermediate-mass range, about 10% of A-type stars are identified as Ap stars and present surface magnetic fields with a longitudinal component in the range 200G to 30 kG . The fields of these slow rotators are organized on a large scale and remain steady over decades. On the other hand very weak fields ($B_l \approx 0.5G$) have been detected for two main-sequence A stars, Vega (Lignières et al. 2009; Petit et al. 2010) and Sirius A (Petit et al. 2011). This seems to indicate that A stars have a bimodal distribution in terms of magnetism, with very weak fields of the order of 1 G on one side, then a gap with no detection, and then Ap stars with fields intensities larger than 200 G.

Examples of surface magnetic field reconstructions of early-type stars are shown in Fig. 3.6. Due to their similar structure as shown in Fig. 3.5, it is thought that the magnetic fields observed in O, B and Ap stars have the same origin. It is still under debate whether they are generated by a core dynamo (Brun et al. 2005; MacGregor & Cassinelli 2003) or if they are the reminiscence of the magnetic field of the protostellar clouds these stars have formed from (e.g. Mathis et al. 2011).

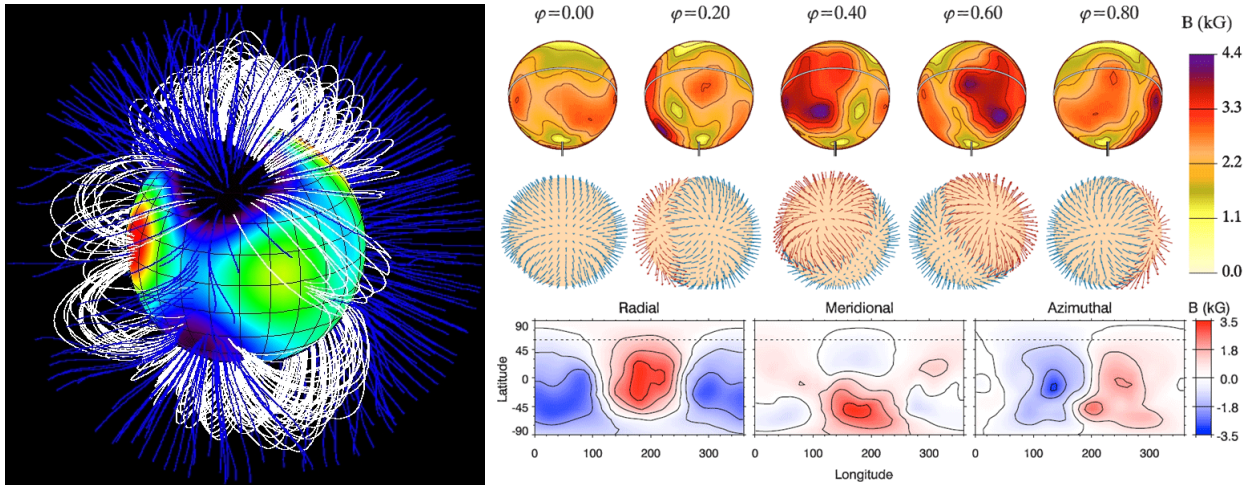


Figure 3.6: *Left* Reconstruction of the magnetic field lines and topology of the massive star τ Sco from ZDI imaging (*Credits : P. Petit*). *Right* Surface magnetic field distribution of the Ap star α^2 CVn derived from the Stokes IQUV profiles of the Fe II and Cr II lines at five equidistant rotational phases. The lower panel shows the orientation (blue pointing inwards, red pointing outwards). (*From Kochukhov & Wade (2010).*)

F,G,K type stars

The magnetism of solar-type stars is first evidenced by that of the Sun which manifestations have been monitored for several centuries, allowing for instance to build the so-called butterfly diagram representing the number and latitude of sunspots as a function of time (see panel a) of Fig. 3.7). In the Sun, activity indicators (coronal mass ejections, sunspots, etc... see below) and magnetic field are intimately correlated as can be seen from magnetograms indicating the field and polarity of sunspots as a function of time. The common scenario invoked to explain solar magnetism is the $\alpha - \Omega$ dynamo process, where the magnetic field is generated by a dynamo process at the interface between the convective envelope and the radiative interior, in a highly sheared region called the tachocline, and cyclically emerges at the surface in the form of sunspots (panel b) Fig. 3.7).

In other F,G and K type stars, the spectropolarimetric studies indicate similar dynamo processes with highly variable magnetic fields (Donati & Landstreet 2009). As the structure of these stars is similar to that of the Sun (see Fig. 3.5), the same type of dynamo is expected in these stars. Morgenthaler et al. (2011) studied a sample of 19 solar-type stars and showed the existence of short magnetic cycles with clear polarity reversals, as seen in the Sun, and a dependence of the cycle lengths on mass and rotation period (see panel c) from Fig. 3.7). More generally, there are some clear trends between stellar mass, field topology and rotation period, with more massive rapidly rotating stars exhibiting large-scale fields of moderate intensity and complex non-axisymmetric topologies (see panel d) Fig. 3.7). The Rossby number, defined as the ratio of the rotation period to the convective turnover time, $Ro = P_{rot} / \tau_{conv}$ is actually found to be a good proxy for the connection between magnetic fields topologies and strengths and rotation rate (see e.g. Donati & Landstreet 2009, for detailed review).

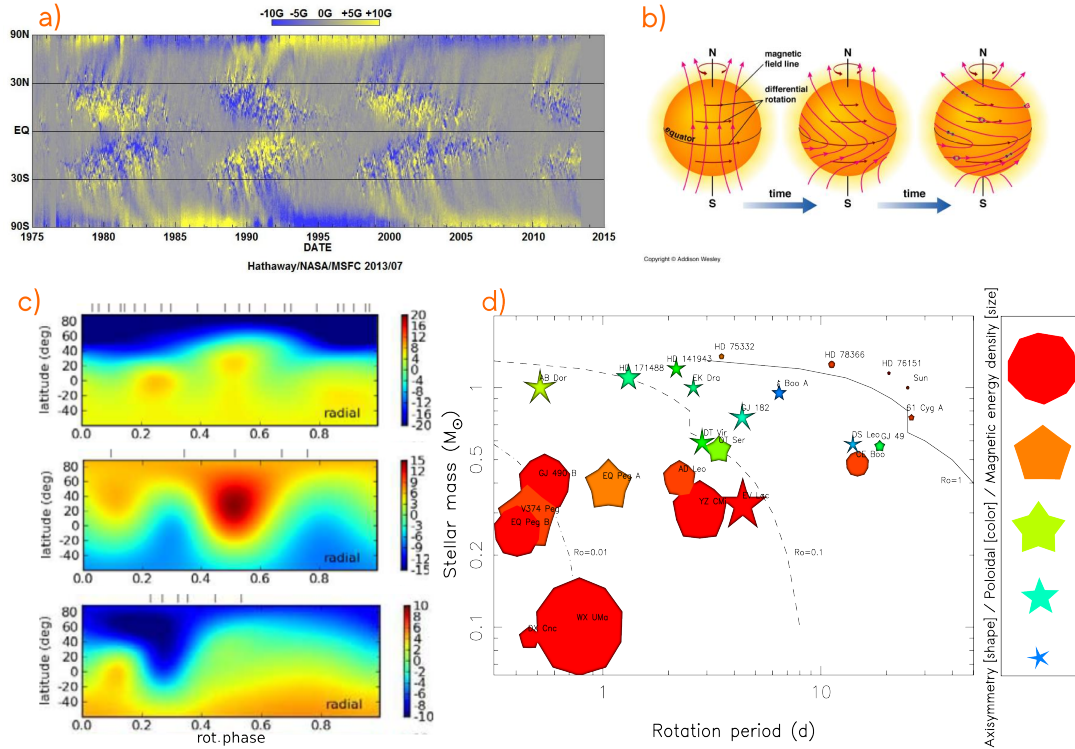


Figure 3.7: **Magnetism of solar-type stars** a) Synoptic magnetogram of the radial component of the solar surface magnetic field. b) Sketch of the $\alpha - \Omega$ dynamo process. c) Magnetic maps of HD 78366, derived from 2008.09, 2010.04, and 2011.08 observations, with magnetic field strength expressed in Gauss. *From Morgenthaler et al. (2011)*. d) Basic properties of the large-scale magnetic topologies of cool stars, as a function of stellar mass and rotation rate. Large scale field strengths vary between 3 G and 1.5 kG. Blue and red refer to toroidal and poloidal fields respectively. *Adapted from Donati & Landstreet (2009)*.

M dwarfs

For the lowest mass main sequence stars ($M_* \leq 0.8 M_\odot$), there is a global dichotomy between fully convective stars ($M_* \leq 0.5 M_\odot$) and partially convective ones ($M_* \geq 0.5 M_\odot$), with the latter having weaker and less organized fields as shown in Fig. 3.8. As there is no such thing as a tachocline in the fully convective less massive M dwarfs, the magnetic field generation cannot be attributed to a solar-type dynamo. It was shown by Browning (2008) that strong magnetic fields can nevertheless be generated and maintained in fully convective stars. However, a few very low-mass fully convective stars present the same behaviour as the early-type M dwarfs (weak non-axisymmetric fields), and introduce a dichotomy in the possible magnetic fields configuration among fully convective stars which remains to be explained (Morin et al. 2011).

3.2. Indirect evidences of the action of non-standard physical processes in stars31

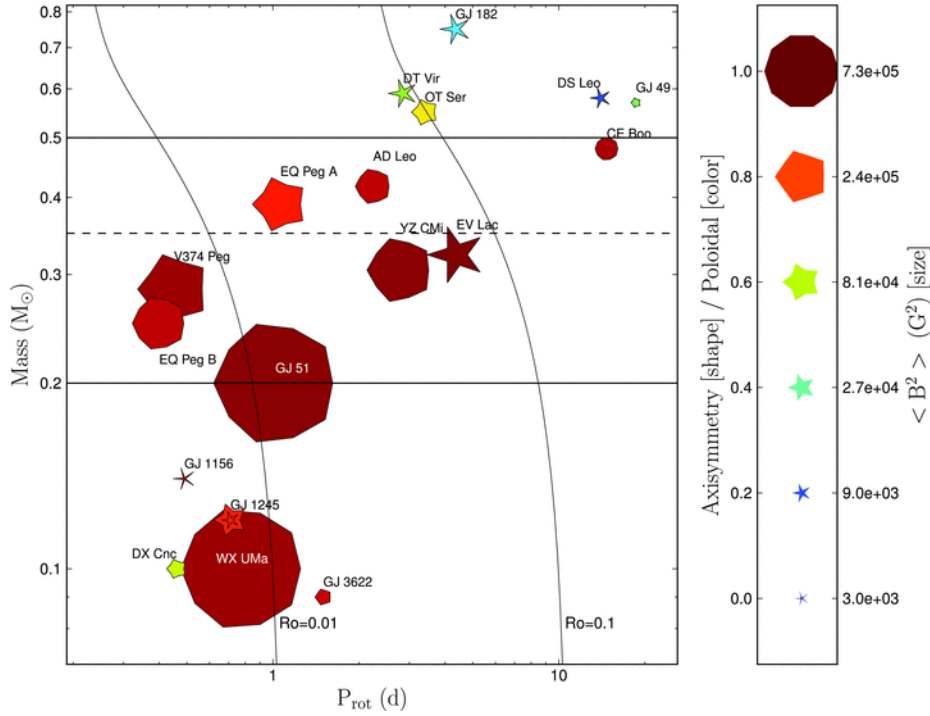


Figure 3.8: Large-scale magnetic field characteristics for M dwarfs from spectropolarimetric studies. (*From Morin et al. (2008)*).

3.2 Indirect evidences of the action of non-standard physical processes in stars

3.2.1 Activity

Indirect evidence of stellar magnetism is given by activity indicators (flares, protuberances, dark spots, ...) that are observed in cool stars developing subsurface convective regions similarly to the Sun. The observations of the emission cores of CaIIK and HK chromospheric lines were first identified as a good proxy for averaged magnetic field strength on the Sun, in particular with [Babcock & Babcock \(1955\)](#) showing that regions with increasing magnetic field strength correlate well with enhanced chromospheric emission. Such spectral signatures have since then been observed in many cool stars, and by analogy, the hot chromosphere they evidence is also interpreted as the result of an underlying magnetic activity. Using chromospheric lines integrated over the full solar disc, [Livingston et al. \(2007\)](#) further showed the very nice correlation between full disc integration of the CaII K 3933 Å line and the 11 years magnetic cycle based on sunspot number.

Other activity indicators similar to those that are observed in the Sun with a clear link to magnetic features, such as flares, dark spots, coronal mass ejections, are also evidenced in other stars by fine structures in their optical light curve ([Maehara et al. 2012](#)) or by X-ray emissions ([Wright et al. 2011](#)).

3.2.2 Abundance patterns

In addition to the direct measurements, the analysis of the surface chemical properties of stars and their confrontation to the predictions of the standard stellar evolution models may provide evidences for transport processes occurring inside the stars.

"**Abundance anomalies**", e.g. departures from the predictions of standard stellar evolution models, are powerful diagnostic tools to probe the efficiency of transport processes that yield a modification of the expected abundance patterns in the stellar atmospheres. Such transport can be of internal origin and connect the surface to regions where efficient nucleosynthesis occurs, or be generated by an external source, for instance when material of different chemical composition is accreted onto the star.

It is important to keep in mind that the nature itself of the "non-standard" transport processes responsible for such deviations cannot be directly inferred. The processes described in the previous section that are known to occur in stars will nevertheless naturally be considered in the first place to explain the discrepancies between abundance observations and predictions of classical and standard stellar evolution models.

Those abundance variations observed at the surface of stars that reflect nucleosynthetic processes occurring inside these very same stars can be considered as evidences for transport / mixing processes connecting the surface to the regions where the nucleosynthesis occurs. Indeed, the abundances of the products of hydrogen burning via the pp-chains and the *extended* CNO cycle (including NeNa- and MgAl- chains) can be used to trace internal mixing when variations are observed at evolutionary phases where they are not expected from standard stellar evolution models². In red giant stars, the presence of *s*-process³ at the surface may also be considered as evidence for internal mixing.

Figure 3.9 presents a set of observed abundance patterns that are used as indirect probes for internal mixing.

Helium

Helium enrichment of the surface layers in main sequence massive stars as observed in O-type stars at low-metallicity (Mokiem et al. (2006)) is a strong indicator of internal mixing in these stars with moderate wind and huge radiative envelopes.

Lithium

Lithium is one of the products of the Big Bang nucleosynthesis (hereafter BBN). It is also produced by spallation in the ISM. The rate of the thermonuclear reaction ${}^7\text{Li}(p, \gamma)2\alpha$ responsible for lithium destruction becomes rapidly high at temperatures $\gtrsim 2.5 \times 10^6$ K even at low densities ($\lesssim 1 \text{ g.cm}^{-3}$) leading to a very easy destruction of this nuclide in stellar interiors already during the PMS phase.

²This essentially concerns the abundance variations that do not appear to be concurrent to a convective dredge-up event.

³The *s*-process is a nucleosynthesis path that involves the production of heavy elements by slow neutron captures (Clayton 1984).

3.2. Indirect evidences of the action of non-standard physical processes in stars 33

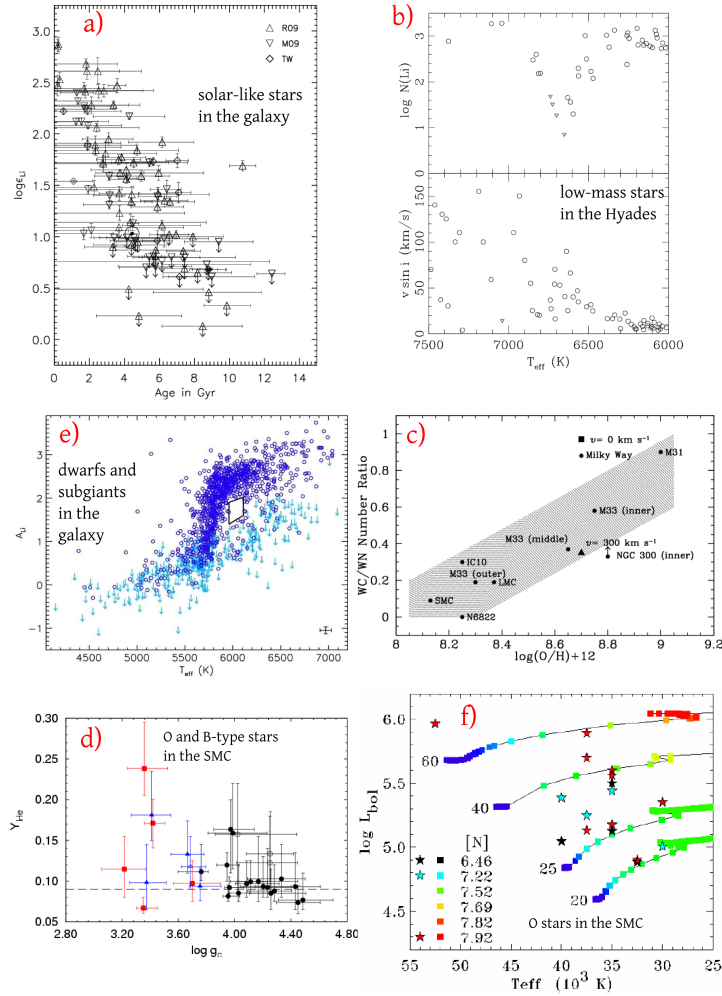


Figure 3.9: **a)** Lithium abundances in solar-type stars as a function of age (*from Baumann et al. (2010)*); **b)** Lithium abundances and projected rotation velocities as a function of T_{eff} in stars of the Hyades (*from Talon & Charbonnel (1998)*); **c)** Number population of two types of Wolf-Rayet stars as a function of metallicity traced by the oxygen abundance (*from Meynet & Maeder (2003)*); **d)** He overabundances in O-type stars of the Magellanic Clouds (*from Mokiem et al. (2006)*); **e)** Li abundances as a function of T_{eff} for a sample of dwarfs and subgiants in the Galaxy (*from Mishenina et al. (2012)*); **f)** Nitrogen abundances in O-type stars of the SMC (*from Heap et al. (2006)*)

Lithium abundance is thus expected to decrease at the surface of stars as they evolve (whatever their mass and metallicity), and more specifically each time the convective envelope reaches down into regions where lithium is destroyed.

The surface lithium depletion observed in low and intermediate-mass stars on the main sequence or on the red giant phase, when no convective dredge-up is expected, is thus considered as strong evidence of internal mixing (Boesgaard & Budge (1989); Boesgaard & Tripicco (1986); Gratton et al. (2000); Baumann et al. (2010); Canto Martins et al. (2011); Mishenina et al. (2012)). Such mixing can be partly attributed to microscopic diffusion (gravitational settling and radiative acceleration) (Korn et al. 2006; Nordlander et al. 2012), which derives from first

principles and is a *standard* process. However [Richard et al. \(2005\)](#); [Richard \(2012\)](#) have shown that its efficiency needs to be moderated by the inclusion of an additional non-standard process in order to match observations.

Although lithium is mainly destroyed in stars, it can also be produced via the Cameron-Fowler mechanism at the bottom of the deep convective envelopes of thermally pulsating intermediate-mass Asymptotic Giant Branch (i.e. AGB) stars. The lithium produced by the ${}^7\text{Be}$ decay during the episodes of Hot Bottom Burning, will show up at the surface as an overall increase of the lithium abundance. This phase is however short-lived and exists in a limited number of objects since it is strongly dependent on the temperature at the base of the convective envelope. The fact that *lithium rich* stars are observed among Red Giant Branch (i.e. RGB) stars of low and intermediate-mass ([Charbonnel & Balachandran \(2000\)](#); [Lèbre et al. \(2009\)](#)), at a phase where the standard stellar evolution models do not allow for Hot Bottom Burning, can be interpreted as the signature of efficient non-standard transport processes occurring in their radiative interiors.

Beryllium and Boron

${}^7\text{Be}$ is also produced during the BBN, while heavier isotopes and boron result essentially from spallation nucleosynthesis in the interstellar medium. Similarly to lithium, beryllium and boron are destroyed in stars for temperatures typically higher than 3×10^6 K and 5×10^6 K respectively. Standard stellar evolution models predict that the surface abundances of these nuclides are modified in low- and intermediate mass stars during the dredge-up episodes only. Signs of depletion in main sequence or post-dredge-up RGB stars again point to efficient internal transport processes ([Boesgaard 2005](#); [Boesgaard et al. 2005](#); [Boesgaard & Krugler Hollek 2009](#)).

Carbon

The carbon participates to the hydrogen burning at high temperature via proton captures within the CNO bi-cycle. The net result of this cycle is the production of ${}^4\text{He}$ from H, and the transformation of the C, N and O isotopes mostly into ${}^{14}\text{N}$ as a result of the relative slowness of ${}^{14}\text{N}(p,\gamma){}^{15}\text{O}$ with respect to the other involved reactions. The CN cycle is the first to reach equilibrium at low temperatures ([Arnould et al. 1999](#)). This equilibrium translates into an anti-correlation of the carbon and nitrogen abundances and leads to carbon isotopic ratio ${}^{12}\text{C}/{}^{13}\text{C}$ values of about 5. In low and intermediate mass stars, the deepening of the convective envelope at the base of the red giant branch reaches in zones that have been partially processed through this chain and standard stellar evolution models predict a decrease of the surface abundance of ${}^{12}\text{C}$ by about 30% (in solar type stars at solar metallicity) and of the carbon isotopic ratio ${}^{12}\text{C}/{}^{13}\text{C}$ from its initial value of 90 to 20-30 depending on the mass and metallicity.

Surface carbon abundance variations are only predicted to occur as a result of dredge-up episodes. **Most of the** luminous RGB stars in the galactic field, whatever their metallicity, and a large proportion of globular clusters RGB stars beyond the luminosity bump present low carbon isotopic ratio (${}^{12}\text{C}/{}^{13}\text{C} \simeq 10$) and low carbon abundance (e.g. [Charbonnel & Do Nascimento 1998](#); [Gratton et al. 2000](#); [Carretta et al. 2005](#)), as shown in Fig. 3.10. These variations are seen above the *bump* luminosity, when the mean molecular weight barrier left behind by the retreating convective envelope at the end of the first dredge-up is erased by the advancing

3.2. Indirect evidences of the action of non-standard physical processes in stars 35

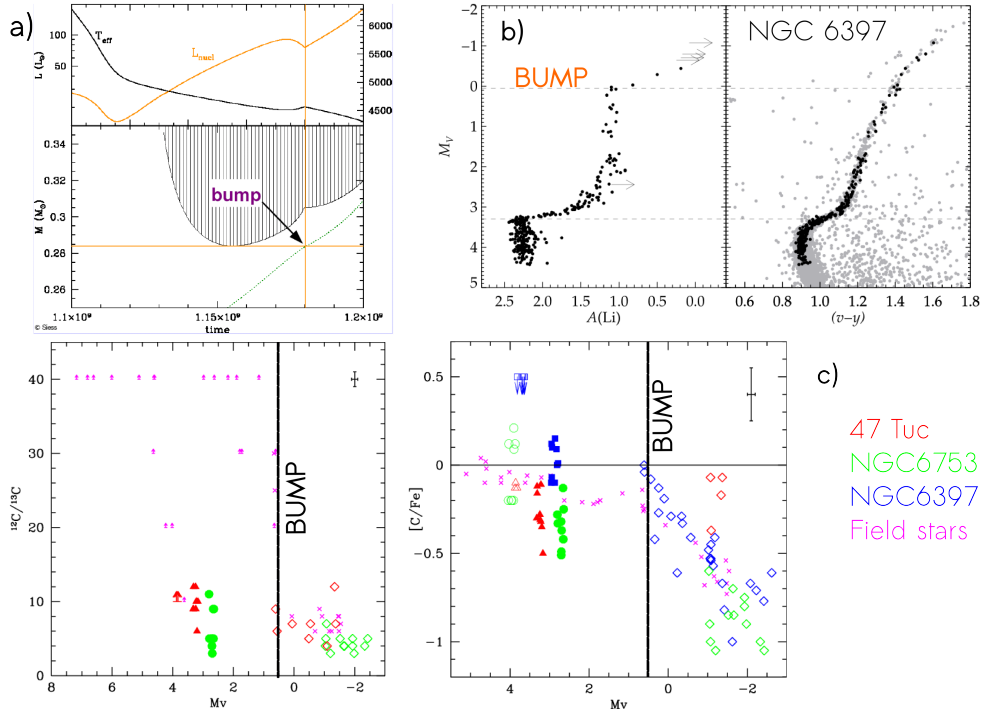


Figure 3.10: **a)** Illustration of the internal structure readjustment in a low-mass RGB stars when it reaches the luminosity bump in terms of effective temperature and nuclear luminosity (top panel) and internal structure with the Kippenhahn diagram (lower panel). **b)** Lithium abundances as a function of magnitude and colour-magnitude diagram for the globular cluster NGC 6397. (From *Lind et al. (2009)*). **c)** Carbon abundance and carbon isotopic ratio for red giants in 4 globular clusters and in the field. (From *Carretta et al. (2005)*).

hydrogen burning shell (see Fig. 3.10). As mean molecular weight barriers are thought to be strong inhibitors for mixing processes, and considering that the carbon abundance variations are generally anti-correlated with the variations of the nitrogen surface abundances, they are commonly interpreted as the signature of deep extra-mixing connecting the deep convective envelope to the surroundings of the hydrogen burning shell, where the CN cycle operates.

Nitrogen

According to standard stellar evolution models, surface abundance variations of nitrogen are expected to occur at the same evolutionary points as those of carbon, and anti-correlation between carbon (^{12}C) and nitrogen (^{14}N) abundances is a clear signature of nuclear processing via the CNO cycle. It is then interesting to observe surface nitrogen abundance variations anti-correlated with those of carbon in upper RGB stars, interpreted as yet another signature of extra-mixing processes (e.g. *Gratton et al. 2000; Carretta et al. 2005*). Unexpected variations of the surface nitrogen abundances are also observed in main sequence and post main sequence massive stars (see panel e). Fig. 3.9), that could be due to the action of non-standard transport processes (*Frebel et al. 2005; Heap et al. 2006; Martins et al. 2009*).

Heavy elements

The nucleosynthesis occurring during the thermally pulsating AGB phase is very rich due to the structural configuration consisting of a periodically unstable thin He burning shell surrounded by the hydrogen burning shell which is closer to the base of the convective envelope. In addition to the aforementioned Hot Bottom Burning, the thermal pulses mix the HeBS ashes with those of the HBS in the intershell region, leading to specific nucleosynthesis. In particular, if enough protons from the envelope can be injected within the carbon-rich layers left behind the pulse-driven convective shell, region, a so-called ^{13}C pocket can be formed via the $^{12}\text{C}(p,\gamma)^{13}\text{N}(\beta^+)^{13}\text{C}$ reaction. The $^{13}\text{C}(\alpha,n)^{22}\text{Ne}$ reaction then generates neutrons that can be captured by iron seeds and form s-process elements. The fact that such nuclides are observed at the surface of TP-AGB stars validates this phenomenological scenario, but the nature of the process allowing of proton leakage from the convective envelope during the interpulse is still to be assessed (Lambert et al. 1995; Abia et al. 2002; Karakas & Lugaro 2010).

3.3 Summary

I have reviewed some of the numerous observational evidences of the occurrence of non-standard physical processes in stars, and also of the action of transport processes that lead to abundance patterns evolution that are not predicted by standard models, and indicate that the angular momentum of stars evolves in a more intricate manner than that resulting from a simple conservation law.

Stellar evolution modelling beyond the standard picture

Contents

4.1	1-D non-standard stellar evolution modelling	38
4.1.1	Modifying the stellar structure equations	40
4.1.2	Modelling the transport of angular momentum and chemicals	42
4.1.3	Personal implication	46
4.2	2-D and 3-D stellar structure modelling	46
4.2.1	Multi-D stellar "evolution" codes	47
4.2.2	(M)HD codes as fine-tooth combs to explore physical processes	48

The overview of the previous chapter indicates that there is a discrepancy between predictions of the standard stellar evolution models and observations for stars of all spectral types. Considering that some obvious physical processes as rotation or magnetic fields are overlooked in these models, and that these ingredients have an impact on the stellar structure and can generate (M-)HD instabilities able to transport angular momentum and matter in stellar interiors, important efforts have been devoted to their inclusion in stellar evolution models from the end of the 1970's (Kippenhahn & Thomas 1970; Endal & Sofia 1976). Most of the theoretical efforts to derive prescriptions and formalisms for the transport processes that could be used in 1-D stellar evolution codes were made in the 1990's and early 2000's (e.g. Zahn 1992; Maeder & Zahn 1998; Lydon & Sofia 1995; Heger et al. 2000), leading to a real advance beyond the standard stellar evolution models in the last ten years or so.

In this chapter I will present an overview of the formalisms and codes that implement ingredients and processes beyond the standard picture. I will also present the efforts to go beyond the unidimensional models either using 3-D codes to constrain 1-D models or directly solving the stellar structure in 2-D or 3-D.

4.1 1-D non-standard stellar evolution modelling

Non-standard stellar evolution models are those introducing processes that may efficiently transport angular momentum and/or chemical species in the radiative interiors of stars. Microscopic diffusion is not considered in the list of *non-standard* processes as explained in Chap. 2, as these processes result from first principles and should be seen as standard ingredients¹.

Rotation and magnetic fields are present all over the HR diagram and can modify the structure of stars, so that these are two physical ingredients that can be added in non-standard stellar evolution models.

Associated to these are (M)-HD instabilities triggered by differential rotation and/or magnetic fields that can transport both angular momentum and nuclides when reaching a non-linear regime, and these constitute another family of processes that can be found in non-standard stellar evolution codes.

More "standard" mechanisms such as convective-type double-diffusive instabilities that can develop in stellar interiors depending on the thermal and composition gradients and independently of rotation or magnetic fields, are treated as non-standard transport processes as they may lead to extra-mixing in regions that are stable with respect to convection.

Finally most of stars appear to present oscillations as evidenced by the results of the CoRoT and Kepler missions, some of them directly triggered by sub-surface convection. It is the case of internal gravity waves (hereafter IGW) that propagate in the stably stratified regions surrounding the convective regions at the edge of which they are triggered. This propagation may lead to efficient transport of angular momentum and nuclides, putting IGW in the section of *non-standard* transport processes.

In Tab. 4.1, I have identified and listed the 13 stellar evolution codes incorporating one or more of these non-standard processes as of 2013.

Rotation was the first non-standard process to be included in stellar evolution computations (Kippenhahn & Thomas 1970; Endal & Sofia 1976, 1978). In the late 1990's, detailed formalisms describing the structural effects on one side, and some rotation-driven transport processes on the other side, were available for the community to test and confront to observations. I devoted my PhD thesis to the introduction of the formalism developed by Zahn (1992) and Maeder & Zahn (1998) in the STAREVOL code and to confront it to the observational constraints available for solar-type stars at different metallicities and evolutionary phases (Palacios et al. 2003, 2006).

The magnetism is still marginally accounted for in stellar evolution codes. Its structural effects are generally neglected, and it was introduced in some codes via the Tayler-Spruit dynamo and Tayler instability proposed by Spruit (1999) (see also Spruit 2002) as a possible important transport process in rotating stars.

¹In many cases however, the time-scales over which they can develop are too long with respect to the evolutionary time-scale of the star considered, and they can be neglected without any important impact.

Code	Process	References	Formalism
YREC	R RIM	Endal & Sofia (1978) Pinsonneault et al. (1989)	Endal & Sofia (1978)
STERN	R RIM MHD	Heger et al. (2000)	Endal & Sofia (1978) Sprit (2002)
KEPLER	R RIM MHD	Heger et al. (2000)	Endal & Sofia (1978) Sprit (2002)
ATON	R RIM MAG	Mendes et al. (1999) Landin et al. (2006) Mendes et al. (2013)	Endal & Sofia (1978) Lydon & Sofia (1995)
FRANEC	R RIM	Chieffi & Limongi (2013)	Endal & Sofia (1978) Maeder & Zahn (1998)
MESA	R RIM MHD	Paxton et al. (2013)	Endal & Sofia (1978) Sprit (2002)
GENEC	R RIM MHD	Meynet & Maeder (1997) Eggenberger et al. (2008)	Zahn (1992) Maeder & Zahn (1998) Sprit (2002)
TGEC	RIM TM	Hui-Bon-Hoa (2008)	Maeder & Zahn (1998) Vauclair & Théado (2003) Vauclair & Théado (2012) Vauclair (2004)
STAREVOL	R RIM TM IGW	Palacios et al. (2006) Decressin et al. (2009) Charbonnel & Lagarde (2010) Charbonnel et al. (2013)	Zahn (1992) Maeder & Zahn (1998) Kippenhahn et al. (1980) Charbonnel & Zahn (2007) Talon & Charbonnel (2003)
CESTAM	R RIM MHD	Marques et al. (2013)	Zahn (1992) Maeder & Zahn (1998) Sprit (2002)
MONSTAR	TM	Angelou et al. (2011)	Kippenhahn et al. (1980) Charbonnel & Zahn (2007)
STARS	TM	Stancliffe et al. (2007) Stancliffe & Eldridge (2009)	Kippenhahn et al. (1980) Charbonnel & Zahn (2007)
DSEP	MAG	Feiden & Chaboyer (2012)	Lydon & Sofia (1995)

Table 4.1: Census of 1-D stellar evolution codes including non-standard processes. **R** stands for structural effects of Rotation, **RIM** stands for rotation-induced mixing, including transport of angular momentum and chemical species, **MAG** designates structural effects of magnetic fields, **MHD** stand for Magneto-HydroDynamical Tayler-Spruit instability, **TM** stands for Thermohaline Mixing and **IGW** for Internal gravity Waves. The Reference column gives the bibliographic reference concerning the introduction of the processes in the code concerned and the Formalism column indicates the bibliographic references for the formalisms adopted.

The **double-diffusive** thermohaline instability, which can occur independently of rotation and magnetic fields, was introduced in stellar evolution codes to consistently treat some cases where the configuration favours its development (Vauclair 2004; Charbonnel & Zahn 2007). It is introduced as a diffusive process for chemical elements and is easy to implement in the diffusion equation for chemical concentrations (Eq. 2.11).

IGW are also very marginally included in stellar evolution codes due to the complexity of the formalism and the lack of a full description of the excitation mechanisms (Talon & Charbonnel 2003, 2004; Pantillon et al. 2007; Talon & Charbonnel 2008).

In the following, I give a brief overview of the formalisms and prescriptions used in *non-standard* stellar evolution models to account for the processes listed above in stellar evolution codes. I have written a detailed review on rotation and rotation-induced mixing modelling for the lectures I gave at the Evry Schatzman School 2012 (Palacios 2013), and I refer to it for a more extensive description of the different rotation-driven instabilities and of the IGW.

4.1.1 Modifying the stellar structure equations

Magnetism and rotation have a direct impact on the stellar structure as they modify the basic stellar structure equations:

- The presence of a magnetic field (or magnetic perturbation) in the stellar plasma impacts (1) the hydrostatic equilibrium with the introduction of the Lorentz force and of the magnetic pressure, (2) the energy balance through the ohmic heating (3) and the convection efficiency and stability criterion (Lydon & Sofia 1995; Duez et al. 2010; Feiden & Chaboyer 2012).
- Rotation impacts the mechanical and radiative equilibrium of stars and implies (1) a deformation of the equipotential surfaces, (2) a modification of the effective gravity due to the centrifugal acceleration (3) and a variation of the radiative flux on equipotential surfaces with a possible strong impact on the mass-loss of early-type fast rotating massive stars (Kippenhahn & Thomas 1970; Endal & Sofia 1976; Meynet & Maeder 1997).

In stellar evolution codes, the effects of rotation on the stellar structure and radiative equilibrium equations are introduced using the formalism first developed by Kippenhahn & Thomas (1970) for uniform rotation cases², and later extended by Meynet & Maeder (1997) to non-uniform rotation cases³ as the shellular rotation. These formalisms consist in modifying the total gravity to take into account the centrifugal acceleration and to project the structure equations on equipotentials (or isobars). Doing so, the form of the standard stellar structure equations is preserved and rotation is treated as a perturbation, an approach that is justified when considering that the equipotential deformation becomes important only for rotation rates larger than 60% of the critical angular velocity, as shown in Fig 4.1 for the case of a Roche potential.

²This corresponds to **barotropic** stars in which isobars, isotherms and isodensity coincide with equipotentials.

³This corresponds to **baroclinic** stars in which isobars and isotherms do not coincide with equipotentials anymore.

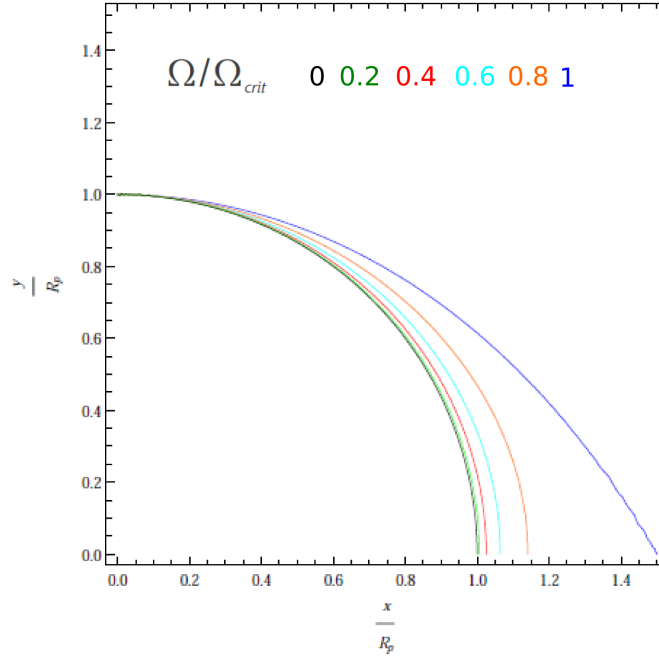


Figure 4.1: Distortion of a rotating star with the Roche model. Each color corresponds to the mentioned values of the ratio $\omega = \Omega/\Omega_{\text{crit}}$ with $\Omega_{\text{crit}} = \sqrt{\frac{8GM}{27R_p^3}}$, M the stellar mass, Ω the angular velocity at the surface and R_p the polar radius. From [Potter \(2012\)](#).

I have computed models of different masses solely including these effects under the assumption of solid-body rotation, and the resulting Hertzsprung-Russell diagrams are shown in Fig. 4.2. These effects are expected to modify the evolutionary path (and time scales) of low-mass PMS stars and to impact the evolution of massive main-sequence stars although in that case, the transport processes associated with rotation will rapidly take over in more realistic models.

The introduction of magnetic fields as a perturbing process has been poorly explored up to now, essentially limited by the important approximations on the field geometry ([Lydon & Sofia 1995](#); [Feiden & Chaboyer 2012](#)) due to the lack of observational constraints, and also by the complexity of its implementation ([Duez et al. 2010](#)). [Feiden & Chaboyer \(2013\)](#) have computed some models including a magnetic perturbation to explain the inflation of low-mass stars in detached binaries systems, with some encouraging yet very exploratory results.

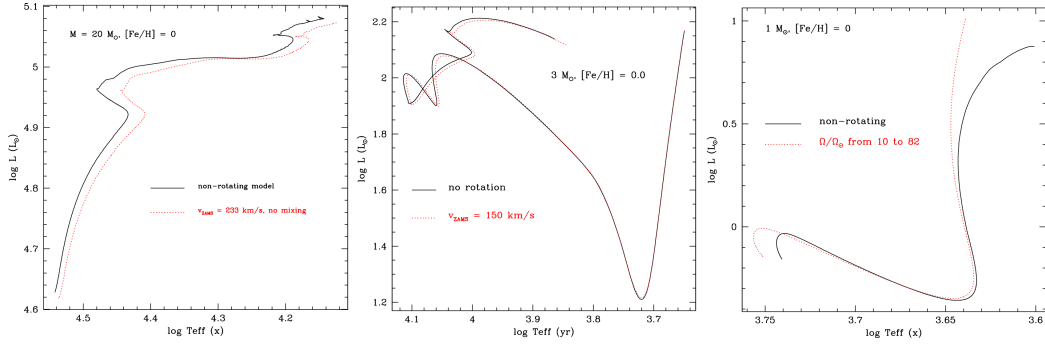


Figure 4.2: Effect of the centrifugal acceleration on the main sequence evolutionary track of a $20 M_{\odot}$ model at solar metallicity, on the evolutionary track of a $3 M_{\odot}$ model at solar metallicity, and on the pre-main sequence evolutionary track of a $1 M_{\odot}$ model at solar metallicity. Black solid lines are for the non-rotating models and red dotted lines for the models including the modifications of the stellar structure equations and radiative equilibrium according to Endal & Sofia (1976). No rotational mixing is included. Rotating models are assumed to experience solid-body rotation.

4.1.2 Modelling the transport of angular momentum and chemicals

The second important point of non-standard stellar evolution models is to account for the processes that can transport angular momentum and chemical species in regions that are stable with respect to convection. As mentioned above, it is the case of hydrodynamical instabilities in the non-linear regime, of the Tayler-Spruit dynamo associated to the Tayler MHD instability, and of IGW.

Including additional transport processes for the chemical species is the easier part to implement. In the simplest approach in which the action of all processes can be described by a diffusion equation and are assumed to have an additive impact with no explicit mutual interaction, it essentially consists in introducing new diffusion coefficients into the equation describing the time evolution of a nuclide concentration or mass fraction (Eq. 2.11).

For the transport of angular momentum associated to rotation-driven instabilities, IGW and MHD instabilities, it is necessary to solve an additional equation at each time-step : the equation for the angular momentum evolution. Two formalisms have been developed to describe the angular momentum evolution and to allow for it to be taken into account in 1-D stellar evolution models :

Endal & Sofia 1978 : Diffusive approach

The angular momentum and nuclides profiles evolution due to secular rotation-driven instabilities are described by a set of two diffusion equations, which have the advantage to be computationally easy to implement :

$$\frac{\partial \Omega}{\partial t} = \frac{1}{\rho r^4} \frac{\partial}{\partial r} \left(\rho r^4 \nu \frac{\partial \Omega}{\partial r} \right) \quad (4.1)$$

$$\frac{\partial X_i}{\partial t} = \frac{1}{\rho r^2} \frac{\partial}{\partial r} \left(\rho r^2 D \frac{\partial X_i}{\partial r} \right) \quad (4.2)$$

where X_i is the mass fraction of nuclide i , ν and D are respectively the total viscosity and the total diffusion coefficient defined as a sum of all diffusion coefficients associated to the transport processes taken into account. I have omitted the terms corresponding to nuclear reaction and microscopic diffusion in Eq. 4.2. Each of these diffusion coefficients is built as the product of a velocity v and the path length l of the redistribution currents with

$$l = \min \left(r, \left| \frac{\partial r}{\partial \ln v} \right| \right). \quad (4.3)$$

$\left| \frac{\partial r}{\partial \ln v} \right|$ is the velocity scale height. The time-scale associated to the *redistribution* over path scale is then simply $l^2/D = l/v$.

With this description, the viscosity ν is given by

$$\nu = D_{\text{conv}} + D_{\text{sem}} + D_{\text{SSI}} + D_{\text{DSI}} + D_{\text{SHI}} + D_{\text{ES}} + D_{\text{GSF}} \quad (4.4)$$

and the diffusion coefficient is usually written as the following sum (Heger et al. 2000)

$$D = D_{\text{conv}} + D_{\text{sem}} + f_c \times (D_{\text{SSI}} + D_{\text{DSI}} + D_{\text{SHI}} + D_{\text{ES}} + D_{\text{GSF}}) \quad (4.5)$$

Eq. 4.1 and Eq. 4.2 are solved in the entire star so that the viscosity and diffusivity include the diffusion coefficients associated to the standard convective instability (D_{conv} and D_{sem}), and diffusion coefficients associated to hydrodynamical instabilities that develop in rotating stellar radiation zones : secular shear instability D_{SSI} , dynamical shear instability D_{DSI} , Eddington-Sweet meridional circulation (treated as a diffusive process) D_{ES} , baroclinic Goldreich-Schubert-Fricke instability D_{GSF} . A detailed description of these instabilities is found in Heger et al. (2000); Palacios (2013).

f_c is one of the efficiency parameters entering the diffusive formalism. It is defined as the ratio of the diffusion coefficient to the turbulent viscosity $f_c \equiv D/\nu$ and it is calibrated on observations (solar lithium abundance in Pinsonneault et al. (1989), nitrogen abundances at the surface of B-type in the LMC in Brott et al. (2011)). Another parameter, f_μ ($\in [0; 1]$) is introduced to mimic the sensitivity of the rotationally induced mixing to μ -gradients, i.e., ∇_μ is replaced by $f_\mu \nabla_\mu$.

These parameters were introduced by Pinsonneault et al. (1989) to account for the “considerable uncertainties” (s explicitly written in Heger et al. 2000) associated to diffusion coefficient used as they derive from order-of-magnitude considerations.

In stellar evolution codes implementing this formalism, the transport of angular momentum by the Tayler instability via the Tayler-Spruit dynamo formalism (Spruit 1999, 2002) is naturally included as an additional diffusion coefficient in both equations Eq. 4.4 and Eq. 4.5 (see Heger et al. 2005), and the thermohaline convection is introduced in Eq. 4.5 also in the form of an additional diffusion coefficient (see e.g. Stancliffe et al. 2007).

The equation for the angular momentum evolution describes the angular velocity at all radii inside the star, with no distinction between radiative and convective regions. In the latter, solid-body rotation is assumed and actually results from the very large convective diffusion coefficient D_{conv} associated to the very short time-scales characterizing convection.

Zahn 1992 and Maeder & Zahn 1998 : advective/diffusive approach

The other family of stellar evolution models including rotation adopts the formalism developed by Chaboyer & Zahn (1992), Zahn (1992) and Maeder & Zahn (1998). This formalism entirely relies on the hypothesis of shellular rotation enforced by highly anisotropic shear turbulence (horizontal shear develops without any hindering force contrary to vertical shear). Only the transport of nuclides is modelled with a diffusion equation. The evolution of the angular momentum obeys an advection/diffusion equation.

The transport equations governing the evolution of angular momentum and nuclides *in the radiative interior* read :

$$\rho \frac{d}{dt} [r^2 \Omega] = \underbrace{\frac{1}{5r^2} \frac{\partial}{\partial r} [\rho r^4 \Omega U]}_{ADVECTION} + \underbrace{\frac{1}{r^4} \frac{\partial}{\partial r} [\rho \nu_v r^4 \frac{\partial \Omega}{\partial r}]}_{DIFFUSION} + \underbrace{\frac{3}{8\pi r^2} \frac{\partial \mathcal{L}_J}{\partial r}}_{IGW} \quad (4.6)$$

$$\rho \frac{dc}{dt} = \left[r^2 \rho (D_{\text{eff}} + D_v) \frac{\partial c}{\partial r} \right]. \quad (4.7)$$

where U is the vertical component of the meridional circulation velocity, ν_v is the vertical component of the turbulent viscosity associated to the secular shear instability, c_i is the concentration of nuclide i , D_{eff} is the effective diffusion coefficient associated with the meridional circulation (Zahn 1992; Maeder & Zahn 1998; Mathis et al. 2004), $D_v \approx \nu_v$ is the diffusion coefficient associated with the secular shear instability (Talon & Zahn 1997; Maeder 1997).

We have here again omitted to quote the abundance variations due to nuclear terms and microscopic diffusion processes.

These equations need to be complemented by an equation describing the evolution of the mean molecular weight relative fluctuations $\Lambda = \frac{\tilde{\mu}}{\bar{\mu}}$ on an isobar. As for the nuclides abundances/concentrations/mass fractions, we can write a diffusion equation for the evolution of the mean molecular μ on an isobar provided that we write it using the perturbative approach $\mu = \bar{\mu} + \tilde{\mu} P_2(\cos \theta)$:

$$\frac{\partial \tilde{\mu}}{\partial t} + U_2 \frac{\partial \tilde{\mu}}{\partial r} = \frac{6}{r^2} D_h \tilde{\mu} \quad (4.8)$$

which can be re-written into an equation for Λ :

$$\frac{\partial \Lambda}{\partial t} = \frac{U_2}{H_P} \nabla_\mu - \frac{6}{r^2} D_h \Lambda \quad (4.9)$$

With this advective/diffusive description of the angular momentum transport in the *radiative stellar interiors*, at each evolutionary time-step, it is necessary to solve a coupled system of five non-linear differential equations resulting from the splitting of the 4th order in Ω of the angular momentum transport equation (Eq. 4.6) + the equation for mean molecular weight fluctuations evolution (Eq. 4.9). This set of equations is complemented by boundary conditions describing

the meridional circulation and the rotation profile at the edges of the radiative domain, including a description of the angular momentum distribution in the convective envelope when present.

The convective regions are assumed to have a solid-body rotation, they are treated as a bulk by integrating their inertia momentum at each time-step, and serve as boundary conditions to the radiative interior equations.

Thermohaline mixing only affects the transport of nuclides and is included in Eq. 4.7 as an additional diffusion coefficient (Charbonnel & Zahn 2007; Charbonnel & Lagarde 2010). The Tayler-Spruit dynamo and associated MHD instability is treated as a magnetic viscosity adding to the turbulent shear viscosity in Eq. 4.6, and as a magnetic diffusivity adding to the other diffusion coefficients in Eq. 4.7 (Meynet & Maeder 2003; Maeder & Meynet 2004). The introduction of IGW is trickier since to get the last term in the right-hand side of Eq. 4.6, $\frac{\partial \mathcal{L}_J}{\partial r}$, it is necessary to first compute the waves excitation⁴, then the net flux of waves that actually propagate inside the radiation zone (Talon & Charbonnel 2008; Mathis et al. 2013; Charbonnel et al. 2013).

Surface torques for young stellar models

During the PMS evolution of low and intermediate-mass stars, and in particular when the star decouples from its surrounding accretion disk during the weak T-Tauri phase, the torque exerted on the stellar surface by the (weak) stellar winds can be described analytically and is introduced as a boundary condition to the angular momentum transport equation in both the formalisms described above.

Several prescriptions exist based on fits to observations (Skumanich 1972) or on elaborated simulations (Kawaler 1988; Reiners & Mohanty 2012; Matt et al. 2012). The more recent ones are based on the simple assumption that the stellar surface and the disk are in co-rotation at a specific radius, the Alfvén radius r_A beyond which the wind velocity becomes Alfvénic and the wind is free to flow. The torque then depends on the mass and radius of the star, but also on the angular velocity and on the magnetic configuration at the stellar surface.

Kawaler (1988) derived an analytical prescription that is widely used in stellar evolution codes. When assuming a field with a geometry close to the radial geometry (but slightly more complex) and a total surface field strength that is directly proportional to the rotation rate, it writes :

$$j = -K\Omega\Omega^2 \left(\frac{R}{R_\odot}\right)^{1/2} \left(\frac{M}{M_\odot}\right)^{-1/2} \quad \text{for } \Omega < \Omega_{\text{sat}} \quad (4.10)$$

$$\dot{j} = -K\Omega\Omega_{\text{sat}}^2 \left(\frac{R}{R_\odot}\right)^{1/2} \left(\frac{M}{M_\odot}\right)^{-1/2} \quad \text{for } \Omega \geq \Omega_{\text{sat}} \quad (4.11)$$

It depends only on the saturation value for rotation, Ω_{sat} , which is associated with a saturation of the stellar magnetic field and usually taken in the range $[8 \Omega_\odot; 20 \Omega_\odot]$. The

⁴As of now, only the excitation by Reynolds stresses is included in STAREVOL, based on the formalism by Goldreich & Kumar (1990); Goldreich et al. (1994); Zahn et al. (1997)

parameter K is a free parameter that needs to be calibrated on observations. It is typically of the order of 10^{47} for solar-mass stars.

The more recent prescriptions by [Reiners & Mohanty \(2012\)](#); [Matt et al. \(2012\)](#) include an explicit dependence to the magnetic field geometry and strength and to mass loss. This implies some assumptions on the magnetic field and the introduction of a mass-loss prescription at a phase where this process is usually fully neglected ([Hartigan et al. 1995](#)). The recipe given by [Canto Martins et al. \(2011\)](#) for cool stars can be used during the weak T-Tauri phase.

4.1.3 Personal implication

I have been personally involved in the development of prescriptions used in the [Zahn \(1992\)](#)' formalism ([Mathis et al. 2004, 2007](#)), and my collaborators and I have developed diagnosis tools to be able to analyse the outcome of stellar evolution models including rotation and other transport processes ([Decressin et al. 2009](#); [Mathis et al. 2013](#)).

The development of the STAREVOL code beyond the standard picture that I have initiated with my PhD work is still undergoing with the work undertaken with the other developers of the code. I am in particular involved in the more in-depth exploration of the impact of adding IGW to rotating models through the supervision of Mr Louis AMARD PhD work within the ANR funded project TOUPIES (ANR-11-BS56-0020) on the understanding of the spin evolution of solar-type stars.

4.2 2-D and 3-D stellar structure modelling

As indicated in Chap. 2, a star is a three-dimensional object and if going to 1-D by advocating spherical symmetry in the case of non-rotating, non-magnetic isolated stars is fairly justified, the question of the validity of doing so for rotating and magnetic stars is risen.

The non-standard processes described in the previous section are intrinsically three-dimensional or have effects in the three spatial dimensions. To model their effect in 1-D requires a number of approximations, including their treatment as perturbations and their averaging to extract an overall effect along the radial direction. These approximations are based on theoretical developments but also on results extracted from 3-D (magneto-)hydrodynamical simulations that are able to follow the small spatial scales but also the dynamical scales over which the instabilities develop, and that cannot be captured in a stellar evolution model.

To move from 1-D stellar evolution to 2-D or 3-D thus requires being able to treat processes acting on dynamical time-scales (convection, turbulence, waves, ...) over the secular evolution of the stars dictated by the nuclear reactions. Despite the challenge this represents, some efforts have been made to develop 2-D and 3-D codes that consistently solve the stellar structure equations in 2-D or 3-D and also include the evolution due to nuclear reactions.

4.2.1 Multi-D stellar "evolution" codes

I have identified 5 codes with published results in the past decade, that clearly develop an effort for moving to multi-dimensional stellar evolution.

- DJEHUTY (Bazán et al. 2003; Dearborn et al. 2006) is a project of the Lawrence Livermore National Laboratory to model stars in 3-D. The structure of the code has been developed but due to the lack of computing power, it has not been applied to 3-D stellar evolution per se as of present. Dearborn et al. (2006) used Djehuty to compute the He flash event in a $1 M_{\odot}$ stellar model using an initial structure coming from a 1-D stellar evolution code. These computations do not follow the entire event and do not include the entire star (only the Helium and Hydrogen burning shells were the energetics come from).
- 2-D version of YREC (Li et al. 2006, 2009) is developed since 2006 and incorporates rotation and magnetic fields with the clear objective of modelling the magnetic fields evolution in the solar convective envelope over time-scales of about 1 year. This code includes a simplified nuclear reaction network and has yet not been fully used beyond a test phase to produce evolutionary sequences.
- ESTER (Espinosa Lara & Rieutord 2007, 2011, 2013) is a project to compute full bi-dimensional stellar evolution models of stars that self-consistently incorporate the effects of rotation (structural and transport processes) at any rate, in particular fast rotating stars for which rotation cannot be considered as a perturbation any more. The typical objects that the ESTER project aims to reproduce are very rapidly rotating oblate objects like Achernar, Regulus or Vega. Espinosa Lara & Rieutord (2013) have published what is the closest to a multi-D evolutionary computation to date, looking at fast rotating $5 M_{\odot}$ model evolving on the main sequence. The secular evolution is mimicked by the core hydrogen mass fraction proxy.
- ROTORC (Deupree 1990, 1995, 1998, 2011) is a two-dimensional code designed to study stellar evolution with arbitrary rotation laws. It allows the calculation of the evolution due to nuclear burning and also to the redistribution of angular momentum by selected instabilities. If most of the published papers using ROTORC are focused on providing a sound 2-D background to the study of stellar convection, pulsation and mass loss, Deupree (1995) has also applied it to directly compute the secular evolution of $8.75 M_{\odot}$ rotating and non-rotating models on the main sequence.
- MUSIC (Viallet et al. 2011, 2013) is not an evolutionary code⁵ per se, but it is proposed as a first step towards multi-D stellar evolution with a special emphasis on the development of numerical techniques that set a framework within which multi-D secular stellar evolution can be considered in the future. As of present, the MUSIC code is a multi-D (solves 2-D and 3-D structures) hydrodynamical code devoted to the modelling of stellar interiors using an implicit numerical scheme for time evolution. It has essentially been applied to study convection in stellar interiors.

⁵I refer here to a code in which the evolution is driven by nuclear burning.

All these efforts open the path to what will probably be stellar evolution in a long-term future, but still appear to be in their infancy and do not allow for now to compute proper multi-D stellar evolution models.

4.2.2 (M)HD codes as fine-tooth combs to explore physical processes

Another path to go is to pave the secular evolution of stars with 3-D simulations in order to have a better description of the hydrodynamical (and MHD) processes at phases that can be separated by several million years, and to use the outputs of these simulations to improve the stellar evolution models.

I have been involved in such an approach in collaboration with A.S. Brun for several years now, to study the angular momentum redistribution in the extended envelopes of red giant stars with the ASH code (Palacios & Brun 2007; Brun & Palacios 2009; Palacios & Brun 2013). The ASH code has also been used to simulate the interior of stars of different masses and evolutionary stages as shown in Fig. 4.3 illustrating the 3-D MHD simulation efforts made within the STARS² ERC project lead by A.S. Brun.

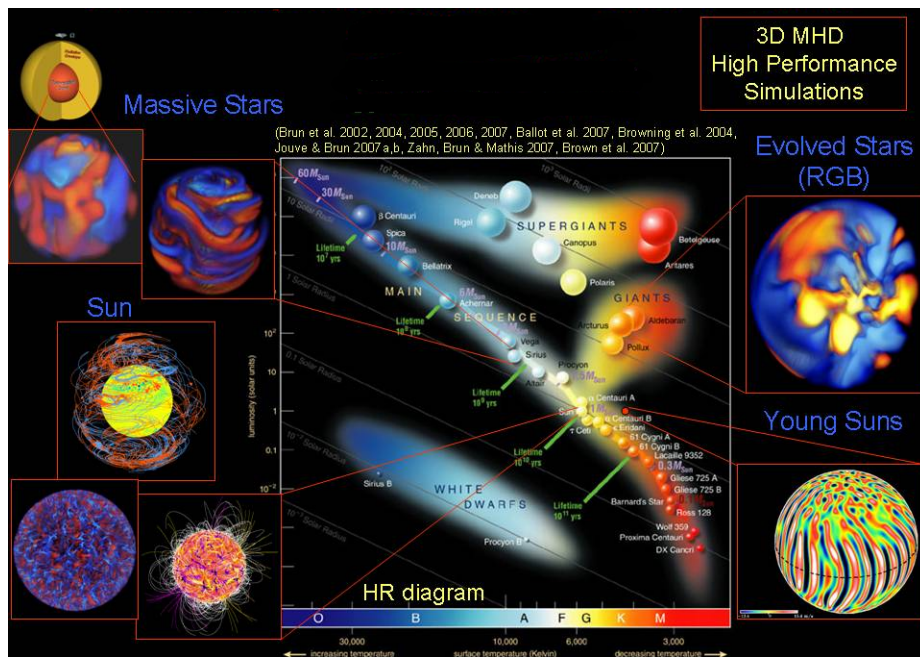


Figure 4.3: Illustration of the HR diagram coverage using 3-D MHD simulations with the ASH code. *Courtesy of A.S. Brun.*

As in the multi-D codes presented above, the principle of this approach is to start the 3-D MHD simulation using "realistic" stratifications and initial set-up coming from a 1-D stellar evolution model evolved to the point of interest. The difference with the previous codes is that the simulations exclusively focus on dynamical processes evolving on dynamical time-scales, with no feedback on the structure whatsoever, and no energy generation by a nuclear reaction

network.

4.2.2.1 Convection and rotation in red giants envelopes

Turbulent convection is poorly known and understood in the extended envelopes of giant stars. Its interaction with rotation needs to be more deeply understood. As described previously, some 1-D stellar evolution models include a sophisticated description of the angular momentum transport in radiative interiors (Zahn 1992), but no similar formalism exists for convective regions that are in most cases roughly described by the phenomenological approach of the mixing length theory in 1-D stellar evolution codes.

The problem of how to describe the angular momentum distribution and angular velocity profile in convective regions arose already in the 70s. Tayler (1973) studied the effects of rotation in stellar convective zones and came to the conclusion that meridional currents could develop and alter the rotation law in stellar convective regions. In that case the rotation regime could approach a uniform specific angular momentum in the convective regions ($j \propto r^2\Omega(r)$). Another limiting case would be that of uniform angular velocity profile ($\Omega(r) = \text{const}$), and for long no real constrain was available in favour of one or another of these approaches so that the simplest was often adopted, that is uniform angular velocity, e.g. solid-body rotation. The inversion of the solar angular velocity profile from helioseismology later comforted this hypothesis: the Sun presents a fairly uniform *radial* angular velocity within its convective envelope (Kosovichev et al. 1997). However the structure and plasma characteristics of the moderately deep solar convective envelope and that of the deep extended convective envelope of red giant stars should be quite different and we may expect a different interaction between convection and rotation in the latter than in the Sun.

Using the ASH code I have performed a series of numerical experiments to evaluate for the first time the rotational state achieved in the envelope of red giants stars. ASH is an anelastic magneto-hydrodynamical code that has been successfully applied to study convection in different types of stars as shown in Fig. 4.3, and I refer to Brun et al. (2004) for more details on the code.

To build the 3-D non-linear simulations I used a 1-D red giant stellar model computed with STAREVOL as initial state. It was chosen to be representative of a low-mass upper RGB star with a luminosity and a radius of about $400 L_{\odot}$ and $40 R_{\odot}$ respectively. In order to lower the density contrast to a value that could be numerically handled by ASH version 1.4 (e.g. $\rho_{\text{bottom}}/\rho_{\text{top}} = 100$)⁶, I only considered the inner 50% of the convective envelope, e.g. $r \in [0.05 R_*, 0.5 R_*]$. This choice was also driven by the fact that getting too close to the surface would imply large Mach numbers that are not compatible with the anelastic assumption. The convective envelope initially rotates as a solid-body, and two different initial rotation rates are used in the simulations: a tenth solar (cases A,B), corresponding to $v_{eq,surf} \simeq 7$ km/s and a fiftieth solar (cases C,D) corresponding to $v_{eq,surf} \simeq 2$ km/s. The characteristics of the models published in Brun & Palacios (2009) are recalled in Table 4.2, and present a first exploration of

⁶This has been greatly improved in the ASH version 2.0, allowing us to compute density contrast of up to 3 orders of magnitude.

Table 4.2: Parameters for the four simulations

Case	A	B	C	D
N_r, N_θ, N_ϕ	257, 256, 512	257, 512, 1024	257, 256, 512	257, 768, 1536
$R_a \dots$	8.25×10^5	3.18×10^6	7.45×10^5	2.69×10^6
$T_a \dots$	1.32×10^6	4.89×10^6	5.44×10^4	1.96×10^5
$P_r \dots$	1	1	1	1
$R_{oc} \dots$	0.791	0.806	3.703	3.703
$\nu_{\text{top}} \dots$	1.2×10^{15}	5×10^{14}	1.2×10^{15}	5×10^{14}
$\kappa_{\text{top}} \dots$	1.2×10^{15}	5×10^{14}	1.2×10^{15}	5×10^{14}
$\tilde{R}e' \dots$	400	895	419	958
$\tilde{P}e' \dots$	400	895	419	958
$\tilde{R}o' \dots$	0.281	0.284	2.17	2.07

Table 4.3: Characteristics of the 3-D hydrodynamical simulations of the convective envelope of an RGB star computed with the ASh code. All simulations have an inner radius $r_{bot} = 1.36 \times 10^{11}$ cm, an outer radius $r_{top} = 1.36 \times 10^{12}$ cm, with $L = 1.22 \times 10^{12}$ cm ($\simeq 17.6 R_\odot$). The number of radial, latitudinal and longitudinal mesh points are N_r , N_θ and N_ϕ respectively. The higher degree of turbulence in cases B and D was obtained maintaining the Prandtl number at 1 and lowering both the eddy viscosity ν and eddy diffusivity κ at the top edge of the domain. ν and κ are given in units of $cm.s^{-2}$. The characteristic numbers evaluated at midlayer depth are the Rayleigh number $R_a = (\partial\rho/\partial S)\Delta SgL^3/\rho\nu\kappa$, the Taylor number $T_a = 4\Omega_0^2L^4/\nu^2$, the Prandtl number $P_r = \nu/\kappa$, the convective Rossby number $R_{oc} = \sqrt{R_a/T_a P_r}$, the rms Reynolds number $\tilde{R}e' = \tilde{v}'L/\nu$, the rms Péclet number $\tilde{P}e' = \tilde{R}e'P_r$, and the rms Rossby number $\tilde{R}o' = \tilde{\omega}'/2\Omega_0 \approx \tilde{v}'/2\Omega_0L$. The rms convective velocity \tilde{v}' at midlayer depth was used to compute these quantities.

the parameters space.

The main results that I obtained are summarized in the different panels of Fig. 4.4. Despite the relative simplicity of our models, they can give a first hint on the intricate dynamics of these extended convective envelopes and of the subtle interplay between convection and rotation. Convection displays a rich dynamics in red giant stars. This already appeared in earlier works that did not include rotation (Woodward et al. 2003; Porter & Woodward 2000). The achieved convective patterns are characterized by broad upflows surrounded by a complex network of downflow lanes as shown in Fig. 4.4a with a 3-D rendering of the radial velocity fluctuations. Associated to these convective cells are large temperature and velocity fluctuations. They lead to a huge enthalpy, e.g. convective, flux reaching up to 200% and more of the total flux emerging at the top edge of the shell, thus compensating for the large downward flux of kinetic energy due to the high degree of stratification assumed in our simulations. This appears on the flux balance presented in Fig. 4.4b for the case B. The importance of this downward flux of kinetic energy has also been observed in other simulations of turbulent convection (Chan & Sofia 1989; Cattaneo et al. 1991; Woodward et al. 2003), and indicates a clear contradiction with one of the main assumptions of the Mixing Length Theory used in 1-D stellar evolution codes, according to which the kinetic energy flux can be neglected and the convective luminosity is set to be the total luminosity (i.e. $L_{conv} = L_{tot} = L_*$) in convection zones.

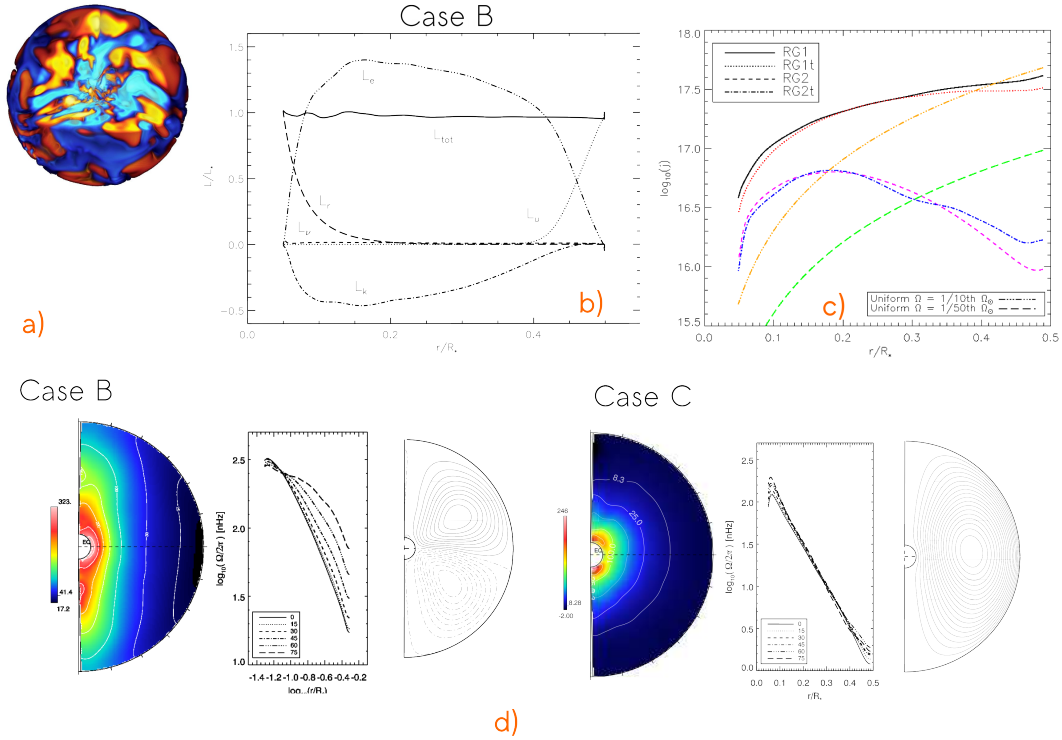


Figure 4.4: Main results of the first 3-D hydrodynamical simulations of the rotating deep convective envelope of a red giant star. See text for further details. *Adapted from Brun & Palacios (2009).*

In the slowly rotating cases a large $\ell = 1$ temperature dipole is established that leads to the separation of the convective shell in two zones of respectively divergence and convergence of the horizontal flow. Such a dipolar configuration also shows through the radial velocity of the fluid, and is very similar to the dipolar behaviour observed in non-rotating simulations of turbulent convection (e.g. Woodward et al. 2003). When accelerating to a bulk rotation of a tenth solar, the dipole no more dominates the energy spectra.

The bulk rotation rate also affects the resulting large scale flows, namely differential rotation and meridional circulation. Meridional circulation is found to possess two large cells (one per hemisphere) or one large cell encompassing the overall domain when rotation is slow as can be seen from Fig. 4.4d, right panel. This structure is associated to the temperature dipole existing in these slowly rotating cases, for which the rotational influence is not large enough yet to shape (constrain) the turbulent convection.

Finally Fig. 4.4d also shows the rotation achieved in cases B and C : differential rotation possesses large radial gradients in both faster and slower cases, and the achieved profile does not vary when changing the Reynolds number by a factor of about 3. When turning to the average specific angular momentum displayed in Fig. 4.4c, it appears that the rotation achieved in the simulations differs greatly from solid-body generally used in 1-D stellar evolution codes, and is not equivalent to a constant specific angular momentum either.

4.2.2.2 MHD simulations of the intermediate-mass subgiant star Pollux

Keeping in mind the necessity to test the validity of these idealized 3-D simulations by comparing them to observational data, I recently turned to the simulation of the star Pollux. This K0III giant has a mass of about $2.5 M_{\odot}$ (Aurière et al. 2009), and its surface velocity was estimated by Takeda et al. (2008) to $v \sin i = 1.61 \text{ km.s}^{-1}$. The original observational campaign using both Narval and ESPaDOnS spectropolarimeters reported in Aurière et al. (2009), led to the first detection of a sub-Gauss magnetic field ($\approx 0.7 \text{ Gauss}$) in a giant star. A follow-up campaign allowed to confirm this first detection and also to precisely determine a rotation period P_{rot} of about 590 days (Aurière et al. 2013), significantly slower than the period that could be derived from the $v \sin i$ of Takeda et al. (2008) and the radius deduced from 1-D stellar evolution models tailored to reproduce the fundamental parameters of Pollux.

I performed a first MHD simulation with a bulk rotation rate based on the data from Takeda et al. (2008). To do so, I have first evolved an hydrodynamical simulation for 6000 days, with a bulk rotation corresponding to $v \sin i \approx 1.3 \text{ km.s}^{-1}$, until it reached a turbulent convective steady state. I then initialized the magnetic field with a multipole $l = 3$, $m = 2$ seed field, with an initial total magnetic energy ME less than 10^{-3} of the total kinetic energy. The magnetic Prandtl number of the simulation is $P_m = 3$.

After evolving for 320 days, the magnetic energy is still in the linear exponential growth phase, and the magnetic field has not yet affected the rotation. The convective pattern and energy transport have an overall behaviour similar to that described above (Fig. 4.5a), but the rotation is radically different, due to different stellar structure and fluid parameters⁷ (Fig. 4.5c).

Over this same time-scale, the simulation has evolved from an initial magnetic field seed to build a dipolar configuration, as shown in Fig. 4.5b .

This is an ongoing work and these first results were presented at the IAU Symposium 302 on "Magnetic Fields Throughout the HR diagram" in August 2013 (Palacios & Brun 2013).

⁷The stellar parameters associated with the 1-D evolutionary model of the star Pollux correspond to $L \approx 40 L_{\odot}$ and $R = 9 R_{\odot}$.

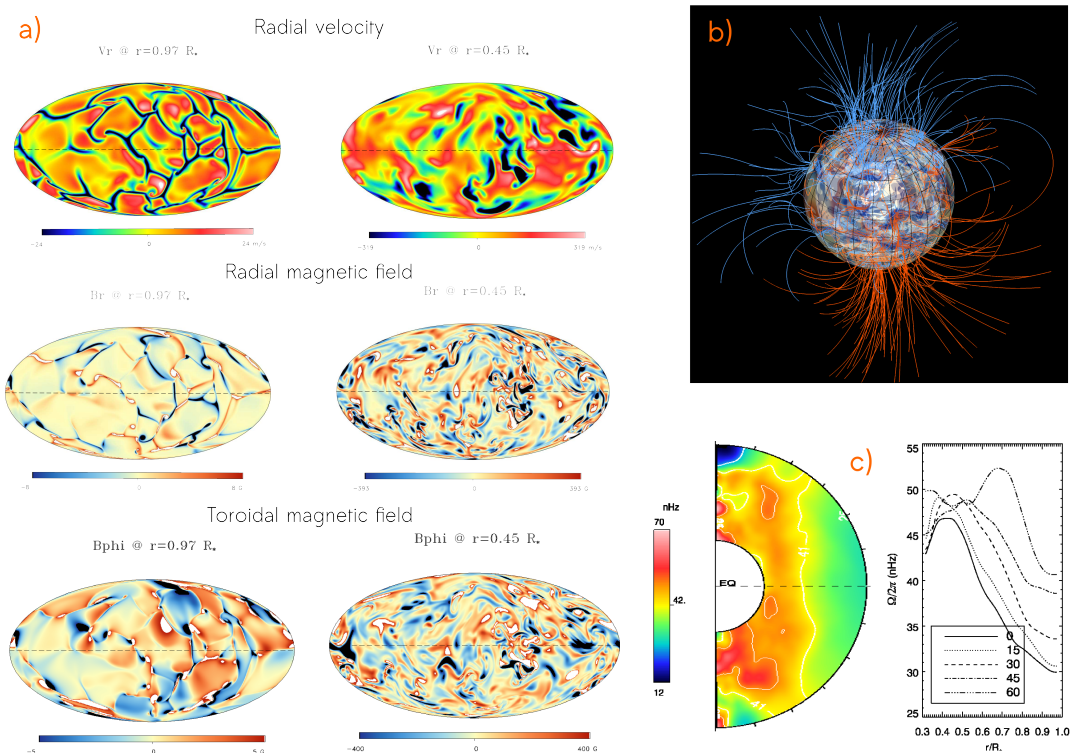


Figure 4.5: **a)** Fluctuations of the radial velocity (convective patterns upper row), the radial magnetic field (middle row) and the toroidal magnetic field (lower row) at three different depths after the simulation has been evolved for 320 days. **b)** 3-D rendering of the magnetic field in the convective envelope of Pollux and of the extrapolated magnetic field at $t = 320$ days. The lines represent magnetic field lines and the surface is a spherical cut in the convective zone. The colours blue and orange represent negative and positive values of B_r . **c)** *Right* Temporal and longitudinal average of the angular velocity profiles achieved in the simulation over 320 days. *Left* Associated radial profiles of angular velocity for selected latitudes (0, 15, 30, 45, and 60 deg).

With these works in collaboration with A.S. Brun, I have assessed how 3-D hydrodynamical simulations can help constrain the prescriptions used in 1-D stellar evolution codes and be used to gain insight on the mechanisms responsible for the magnetic configuration observed in some giant stars.

These simulations are an important first step on the road of paving the evolutionary path of solar-type stars with 3-D simulations. They however need to be complemented and to be put into perspective considering the recent results obtained on the rotation of red giant stars from the asteroseismology missions CoRoT and Kepler.

The evolution of solar-type stars

Contents

5.1	Evolution from the pre-main sequence to the age of the Sun	55
5.1.1	Modelling the interaction of the star with its environment	55
5.1.2	The rotational and chemical evolution from observations	56
5.1.3	Self-consistent non-standard models of solar-type stars including rotation and rotation-induced mixing	59
5.1.4	Self-consistent non-standard models of solar-type stars including rotation, rotation-induced mixing and IGW	63
5.1.5	Self-consistent non-standard models of solar-type stars including rotation, rotation-induced mixing and Tayler-Spruit dynamo	66
5.2	Red Giant Branch stars	68
5.2.1	Rotating models of low-mass RGB stars	68
5.2.2	News from asteroseismology	69

Now that the observational constraints and the ingredients included in non-standard stellar evolution models have been described, I have chosen to focus on the work I have done on solar-type stars (spectral types F, G and K on the main sequence) to illustrate the use of non-standard stellar evolution modelling. I present a summary of the new insight I gained on the evolution of solar-type stars and discuss the new questions that have appeared along the way.

5.1 Evolution from the pre-main sequence to the age of the Sun

5.1.1 Modelling the interaction of the star with its environment

During the classical T-Tauri phase (hereafter CTT), the star is surrounded by a disk with which it strongly interacts. Moreover young stars appear to be highly magnetized, which reinforces the star-disk interaction and deeply influences the stellar winds (Donati et al. 2007, 2008, 2010, 2011, 2013). Facing the profound complexity of these processes, which undoubtedly play a major role in the angular momentum evolution during the early evolution phases, we lack from a consistent formalism to incorporate them in stellar evolution codes.

Accretion of matter (and of angular momentum) from the disk onto the star is an important process that can alter the evolutionary paths, the ages and the angular momentum evolution of low-mass stars on the pre-main sequence. Yet this process is generally not accounted for when computing stellar evolution models for stars with $M_{\text{ini}} \geq 0.6 M_{\odot}$ with some exceptions

(Palla & Stahler (1992, 1993); Siess & Forestini (1996); Siess et al. (1997, 1999); Tout et al. (1999); Baraffe et al. (2009)). Note that for accretion rates of about $10^{-7} M_{\odot} \text{yr}^{-1}$, the influence of this process is negligible on the stellar tracks and ages. Its influence on the global angular momentum evolution is on the other end yet to be explored.

To put it in a nutshell, *the CTT phase is not properly taken into account in stellar evolution codes as far as the angular momentum evolution is concerned.* During this phase, and based on observational evidence (Irwin & Bouvier 2009; Gallet & Bouvier 2013; Bouvier et al. 2013) stellar evolution models just enforce the surface angular velocity to remain constant for a variable duration corresponding to what is abusively called "disk-coupling".

When reaching the more advanced weak T-Tauri phase and all the way to the early main sequence, the prescriptions presented in Chap. 4 can be used to describe the torque exerted by the stellar wind at the stellar surface.

5.1.2 The rotational and chemical evolution from observations

I already briefly mentioned in Chap 3 the case of solar-type stars, and I give here a more focused review of the available observational constraints to the non-standard stellar evolution models.

Special attention has been put in the past five to seven years in determining accurate rotation periods P_{rot} for thousands of stars in open clusters and young associations to provide tight constraints on the problem of the angular momentum evolution of low-mass and in particular solar-mass stars. A compilation of these surveys was published by Irwin & Bouvier (2009) (see Fig. 3.2 lower panel) and recently updated in Bouvier et al. (2013); Gallet & Bouvier (2013), from which it is reproduced in Fig. 5.1 upper panel. From basic considerations of angular momentum conservation, as the star contracts one would expect its surface to accelerate (and its rotation period to decrease). However photometric observations show that the average surface velocity does not increase significantly from the Orion Nebula Cluster (ONC) at 1 Myr to NGC 2363 at 5 Myr, even if there is a large dispersion of rotation periods among stars about the solar mass. This is taken as an indication that some mechanisms prevent the stellar surfaces from accelerating. This is what I referred to earlier as "disk-coupling". As a matter of fact, due to the strong interaction still existing between the accretion disk and the star during the CTT phase, the conservation of angular momentum should not be considered for the star *alone*, but for the star-disk system. Changing to this point of view, the fact that the *stellar surface alone* does not accelerate becomes much less astonishing.

After 5 Myrs, the dispersion of P_{rot} is maintained for the other PMS clusters up to the ZAMS (h Per), and the different percentiles defined on Fig. 5.1a all reach their maximum value. Beyond the ZAMS, the dispersion decreases to be almost null when the stars reach an age of 1 Gyr (in NGC 6811).

The rotational spin down experienced by solar mass stars on the main sequence is thought to result from the braking effect of magnetically-driven stellar winds. While the major physical processes impacting on the rotational evolution of solar-type stars are probably identified

(magnetized winds, star-disk interaction, internal transport of angular momentum) none is fully understood yet.

Let us mention the special case of the Sun, for which a great wealth of data is available. Helioseismic data are particularly important and the analysis of the rotational splitting of p-modes has given access to the rotation profile in the solar radiative interior down to $r = 0.2 R_{\odot}$, putting very strong constraints on models treating the angular momentum transport (Eggenberger et al. 2005; Charbonnel & Talon 2005; Turck-Chièze et al. 2010; García et al. 2011). The profile deduced from these data is presented in Fig. 3.3 in Chap. 3.

Turning now to the lithium abundances in PMS and the early main sequence, which can be used as tracers of extra-mixing processes connecting the convective envelopes of stars to the region where it is destroyed by proton capture, we display the compilation of data from the literature made by Sestito & Randich (2005) for young open clusters between 5 Myr and 100 Myr. Advancing in ages within the range defined by these clusters, lithium becomes more depleted at low temperatures, and the mean value of the surface lithium abundance $\varepsilon(Li) = \log(N(Li)/N(H)) + 12$ is reduced by 0.2 dex. This trend continues when moving to older clusters, and at the age of the Sun (solar value and data from the open cluster M67) the initial abundance has decreased by about a factor 140, evidencing the action of mixing in the radiative regions. In addition to that Soderblom et al. (1993) found a correlation between Li equivalent widths and surface rotation in stars of the Pleiades ZAMS open cluster : stars that rotate faster seem to be less depleted in lithium than slow rotators.

To gain some insight on the efficiency and action of the transport processes of angular momentum responsible of the behaviour previously described, parametric models based on standard evolution models outputs have been developed to solve the equation for the evolution of angular momentum (Allain 1998; Bouvier 2008; Gallet & Bouvier 2013). They include a treatment of the internal variation of angular momentum by separating the star into the convective envelope and the radiative interior, each region rotating at a constant rate that may differ, and being coupled by an arbitrary process that will eventually lead to solid-body rotation. They also include the star-disk coupling and angular momentum losses via magnetized stellar winds. The results of the last generation of these models is reproduced from Gallet & Bouvier (2013) in Fig. 5.2. The best fit models shown in this figure are obtained for an increasing coupling time between the radiative interior and the convective envelope with decreasing initial rotation rate. The angular momentum transport is thus more efficient in fast rotators, leading more rapidly to a small amount of differential rotation (as evidenced by the difference between the solid and dotted blue lines on Fig. 5.2), while a stronger differential rotation is maintained also on the early main sequence in slow rotators. Bouvier (2008) interpreted this result within the framework of shear mixing, invoking that the small amount of shear apparently present in fast rotators should lead to a lesser decrease of the lithium abundances, in agreement with the results of Soderblom et al. (1993) in the Pleiades.

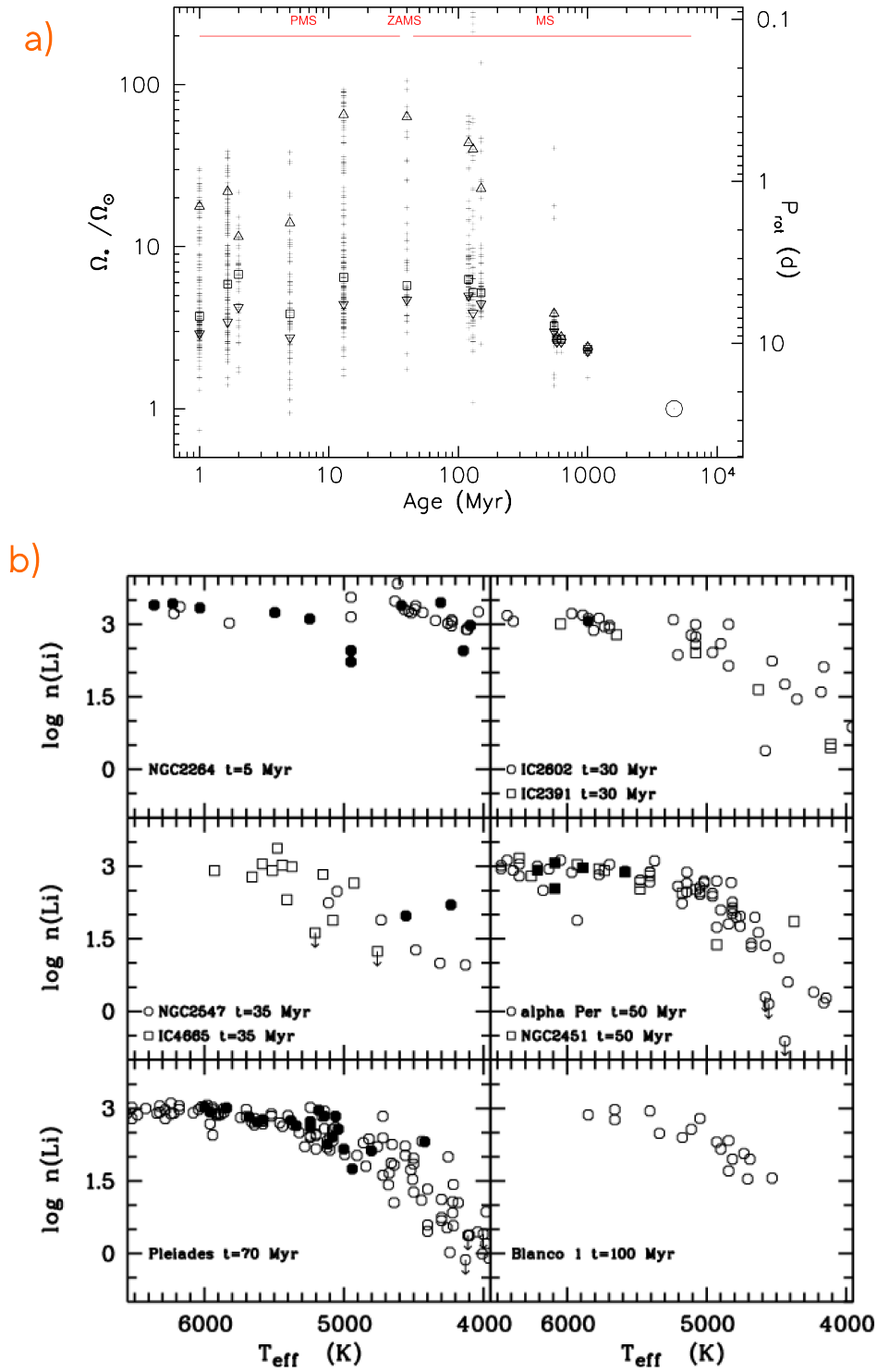


Figure 5.1: Rotation periods and lithium abundances in young open clusters. **a)** Surface rotation rate and P_{rot} of stars in the mass range $[0.9 M_{\odot}; 1.1 M_{\odot}]$ as a function of time for a series of open clusters in the age range from 1 Myr (ONC) to the age of the Sun. At each age, the inverted triangle, the square and the triangle represent the 25th percentile, the median and the 90th percentile of the observed distributions, respectively. *From Gallet & Bouvier (2013).* **b)** Compilation of lithium abundances as a function of T_{eff} in several young open clusters. *From Sestito & Randich (2005).*

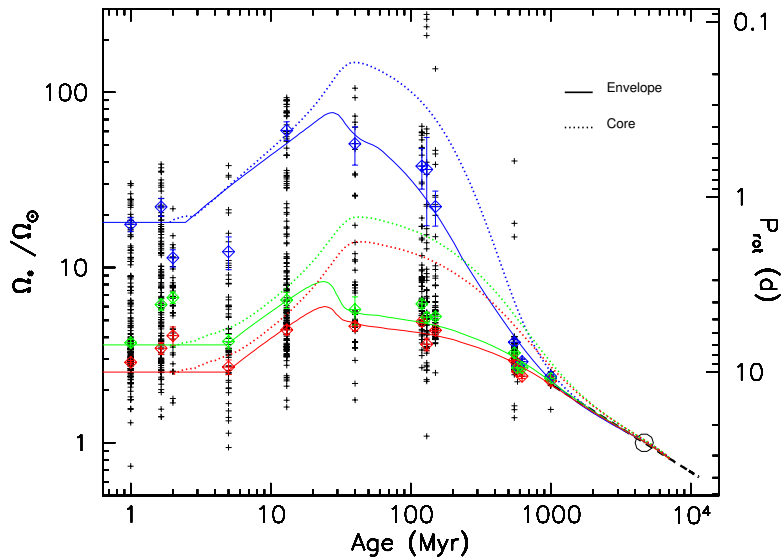


Figure 5.2: Angular velocity of the radiative core (dashed lines) and of the convective envelope (solid lines) as a function of time for fast (blue), median (green), and slow (red) rotator models. These lines result from the computation of the angular momentum evolution based on stellar structures from Baraffe (priv. comm.) and assuming that the convective envelope and the radiative interior rotate at two distinct rates at the beginning. A coupling time corresponding to the time necessary to have both rotating at the same rate is introduced as a parameter and adjusted in order to find the best fit to observations. The torque used here is adapted from [Matt et al. \(2012\)](#). The dashed black line illustrates the Skumanich relationship, $\Omega \propto t^{-1/2}$. From [Gallet & Bouvier \(2013\)](#).

5.1.3 Self-consistent non-standard models of solar-type stars including rotation and rotation-induced mixing

Within the project TOUPIES, I am the coordinator of the stellar evolution modelling task. Our goal is to go beyond the parametric, even if sophisticated, studies as that of [Gallet & Bouvier \(2013\)](#), and to look for the physical mechanisms that can develop in stellar interiors during the PMS phase and both generate the strong rotational coupling between the core and the convective envelope necessary to match the rotation periods of young solar-mass stars, and reproduce the surface lithium abundances evolution up to 5 Gyr.

This work is part of the PhD thesis of Louis Amard, which I supervise together with C. Charbonnel.

The first step was to compute evolutionary models including angular momentum transport and mixing due to meridional circulation and turbulent shear as described by [Zahn \(1992\)](#). This way, we were able to quantify the amount of transport these processes can generate during the early evolution of solar-type stars.

Figures 5.3 and 5.4 present the predicted evolution of the surface rotation and lithium abundances coming from these models. Looking first at Fig. 5.3, it appears very difficult to have models that fit the same percentile values (red, green and blue stars) at all clusters ages at once, contrary to what is achieved by the bi-zonal model of [Gallet & Bouvier \(2013\)](#) presented

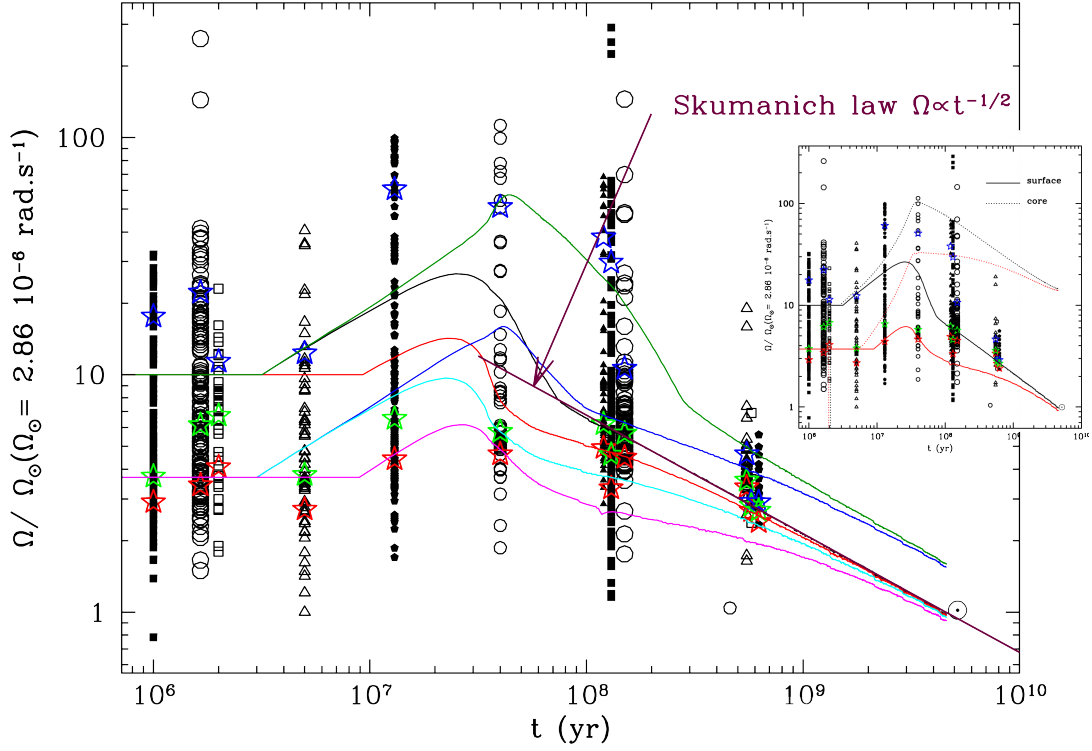


Figure 5.3: Surface angular velocity evolution as a function of time for different models including meridional circulation, turbulent shear and a torque according to Kawaler (1988). The points in the background are data from open clusters as presented in Gallet & Bouvier (2013). At each age, the red, green and blue stars represent the 25th percentile, the median and the 90th percentile of the observed distributions, respectively. The solid lines correspond to rotating $1 M_{\odot}$ models at solar metallicity including the transport of angular momentum and chemicals by the meridional circulation and the turbulent shear and a torque associated to the magnetized stellar wind following the prescription by Kawaler (1988) (Eq. 4.11). The varying parameters associated to each line are the initial rotation Ω_{ini} , the disk lifetime τ_{disk} , the parameter K from Eq. 4.11. In all cases, $\Omega_{sat} = 8\Omega_{\odot}$ in Eq. 4.11, and we consider the expression from Mathis et al. (2004) for the horizontal shear turbulent viscosity. Black : ($\Omega_{ini} = 10 \Omega_{\odot}$, $\tau_{disk} = 3 \text{ Myr}$, $K = 2.5 \cdot 10^{48}$); red : ($\Omega_{ini} = 10 \Omega_{\odot}$, $\tau_{disk} = 8 \text{ Myr}$, $K = 2.5 \cdot 10^{48}$); green : ($\Omega_{ini} = 10 \Omega_{\odot}$, $\tau_{disk} = 3 \text{ Myr}$, $K = 6.5 \cdot 10^{47}$); blue : ($\Omega_{ini} = 3.8 \Omega_{\odot}$, $\tau_{disk} = 3 \text{ Myr}$, $K = 6.5 \cdot 10^{47}$); magenta : ($\Omega_{ini} = 3.8 \Omega_{\odot}$, $\tau_{disk} = 8 \text{ Myr}$, $K = 2.5 \cdot 10^{48}$), cyan : ($\Omega_{ini} = 3.8 \Omega_{\odot}$, $\tau_{disk} = 3 \text{ Myr}$, $K = 2.5 \cdot 10^{48}$). These models do not take the microscopic diffusion of nuclides into account. The classical Skumanich law (Skumanich 1972) is also plotted as indicated on the figure. The small-sized included picture reproduces the rotation of the surface (solid line) and of the core (dotted line) for the black (in black) and the magenta (in red) models of the main plot.

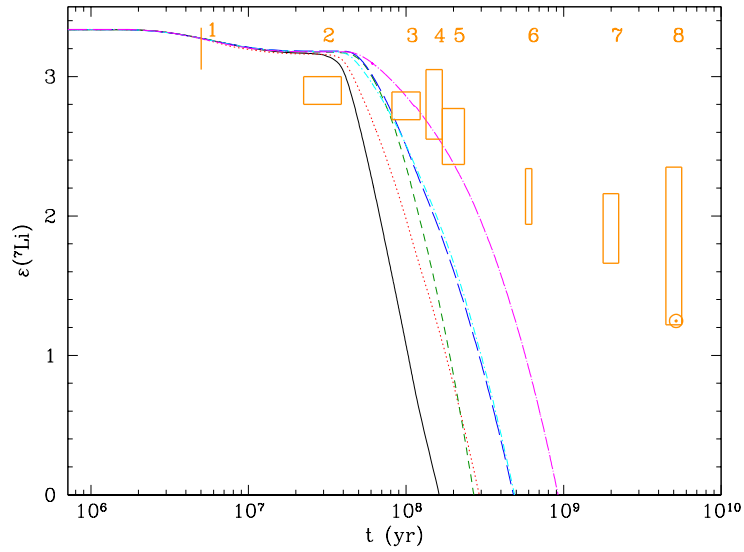


Figure 5.4: Evolution of the surface lithium abundance $\varepsilon(\text{Li}) = \log(N(\text{Li})/N(\text{H})) + 12$ as a function of time for the models plotted on Fig. 5.3. The orange rectangles indicate the lithium abundance dispersion in the T_{eff} range centred around the value predicted by the models at the corresponding age ± 100 K, for the following groups of open clusters according to [Sestito & Randich \(2005\)](#): (1) NGC 2264, 5 Myr, (2) IC2391 / IC2602 / IC4665, 30 Myrs, (3) Pleiades / Blanco 1, 100 Myrs, (4) NGC 2516, 150 Myrs, (5) M34 / M35 / NGC6475, 250 Myrs, (6) Hyades / Praesepe / Coma Ber / NGC 6633, 600 Myrs, (7) NGC 752 / NGC 3680 / IC 4651, 2 Gyrs, (8) M67, 5 Gyrs. The Sun is also represented with its lithium abundance of $\varepsilon(\text{Li}) \approx 1.2$ dex.

in Fig. 5.2. For instance for the fast rotators, the model that reproduces best the high velocity at the ZAMS (around 40 Myr), is computed with a value of the K parameter (from the [Kawaler \(1988\)](#) torque prescription, Eq. 4.11) such that the braking induced on the main sequence is not efficient enough to lead to the slow rotation of the Sun at the solar age.

Looking at what happens in the interior, we see from the small-sized insertion, that a strong differential rotation is maintained during the entire evolution from the PMS to the age of the Sun, which indicates that meridional circulation (which is the main process transporting the angular momentum in the radiative interior together with the non-stationary terms associated with the contraction on the PMS) cannot couple the surface to the internal regions.

Turning to the evolution of the lithium abundances which are a good tracer of the depth and efficiency of extra-mixing processes occurring in radiative interiors, these rotating models completely fail to reproduce the observations beyond the ZAMS as shown in Fig. 5.4. The vertical shear is the dominant transport process for the chemicals. Due to the absence of efficient angular momentum transport, the strong braking applied at the stellar surface does not modify the deep rotation and only reduces the rotation of the outer regions, leading to strong differential rotation. Then, the larger the torque the more efficient the mixing and the larger the lithium depletion.

As in [Decressin et al. \(2009\)](#), the processes transport angular momentum and chemicals are

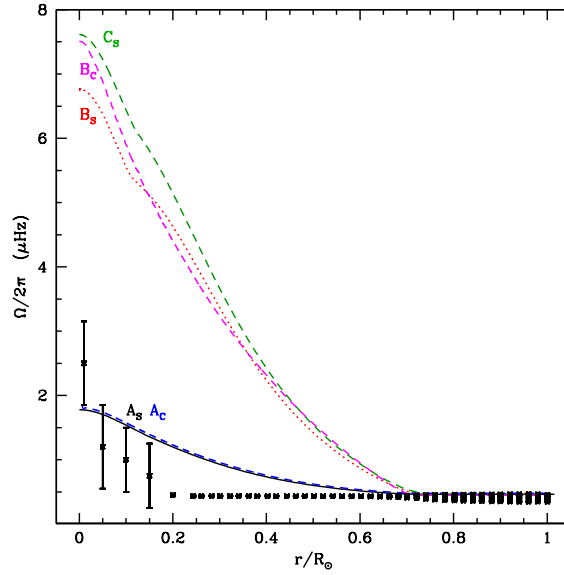


Figure 5.5: Comparison between the solar internal profile predicted by the different models and that deduced from helioseismology. Models A,B and C are computed from the ZAMS assuming $v \sin i = 2.2, 20$ and 50 km.s^{-1} . For models B_S and C_S , the plotted value is $\Omega/2\pi - 0.2325$ rather than $\Omega/2\pi$ in order for the surface value they reach to match that reached by model B_C . The data points down to $r/R_\odot = 0.2$ are deduced from the acoustic mode splittings determined by the observations of GOLF, MDI, and GONG instruments. The data points in the core correspond to the supposed core rotation extracted from the potentially observed gravity modes. These values have still large error bars and need to be confirmed. From *Turck-Chièze et al. (2010)*.

different and as foreseen in *Charbonnel & Talon (2005)*, in the absence of microscopic diffusion, the evolution of the lithium surface abundance during the main sequence phase is fully dominated by the form of the angular velocity profile and the amount of turbulent shear, which is important in the models including *Maeder & Zahn (1998)* formalism with a *Kawaler (1988)* torque.

In *Turck-Chièze et al. (2010)*, I computed solar models including the same physical ingredients but starting at the ZAMS¹. Our main goal was to fully explore the transport "à la *Maeder & Zahn (1998)*" in the case of the solar (calibrated) model and to derive constraints on the rotational history of the Sun on the main sequence according to the ZAMS velocity. These computations were made in parallel with the CESTAM code (*Marques et al. 2013*), and served as a mutual validation of both codes. The main result is displayed in Fig. 5.5. This figure shows the rotation profiles achieved in the solar model at the age of the Sun assuming an initial velocity at the ZAMS of $v \sin i = 2.2 \text{ km.s}^{-1}$ (A models), 20 km.s^{-1} (B models) and 50 km.s^{-1} , this last value being the one assumed in previous evolution models of the rotating Sun (*Chaboyer et al. 1995; Eggenberger et al. 2005; Charbonnel & Talon 2005*). We see that the only way to obtain a rotation contrast between the surface and the core lower than one order of magnitude within the framework set up for these computations is to assume that the Sun has

¹The rotation evolution during the PMS was not considered and a solid-body rotation was assumed throughout the model at the ZAMS

been a slow rotator ever since it arrived on the ZAMS. This is essentially due to an inefficient torque at such velocities, and very slow meridional circulation (which is the process dominating the transport of angular momentum), which allow to maintain a small degree of differential rotation in the solar interior. However, even in this extreme configuration, the profile obtained for models A present a too large differential rotation between $r = 0.75$ and $r = 0.2 R_{\odot}$ to reproduce the helioseismic data.

The more recent and complete computations presented above only confirm these early results and the inefficiency of the transport "*à la Maeder & Zahn (1998)*" to reproduce the angular momentum and lithium abundances evolution in solar-type stars.

5.1.4 Self-consistent non-standard models of solar-type stars including rotation, rotation-induced mixing and IGW

Following this first approach, it is clear that we need to find a mechanism that efficiently transports angular momentum and reduces the differential rotation rate in the interior of solar-mass PMS stars, as indicated by the parametric models of [Bouvier \(2008\)](#); [Gallet & Bouvier \(2013\)](#).

Talon & Charbonnel (2008), in the fourth paper of a series where they have investigated the efficiency of internal gravity waves (IGW) as a transport mechanism for angular momentum, show that for a $3 M_{\odot}$, one may expect efficient generation of waves and important fluxes during the PMS evolution. As the internal structure of intermediate and solar-mass stars evolving down the Hayashi line and to the ZAMS is qualitatively the same, we expect IGW to be also efficient in solar-mass stars during this phase.

In Charbonnel et al. (2013), a first paper of a series to come, we have thus investigated the transport of angular momentum by meridional circulation, shear turbulence and IGW in low-mass stars as they evolve on the PMS. We use the formalism presented in [Talon & Charbonnel \(2005\)](#), we compute the IGW generation at each time-step, self-consistently with the fast evolving structure, and we follow both the prograde and retrograde waves propagation in the radiative interior. In these computations, we have neglected the torque exerted by the magnetized stellar wind may have during the PMS. The initial velocity considered is of about $\Omega = 3.7\Omega_{\odot}$.

In Fig. 5.6, we plot the angular momentum luminosity $\mathcal{L}_{\mathcal{J}}(\omega, \ell)$ at the base of the convective envelope of a $1 M_{\odot}$ for IGW generated by Reynolds-stress in the external convective layers as a function of the emission frequency ω and of the degree ℓ . At the considered convective edge (located at radius r_{cz}), the mean flux of angular momentum carried by a monochromatic wave of spherical order ℓ and local (i.e., emission frequency ω (m being the azimuthal order), i.e., the momentum flux per unit frequency, is related to the kinetic energy flux by

$$\mathcal{F}_{J,r_{cz}}(m, \ell, \omega) = \frac{2m}{\omega} \mathcal{F}_E(\ell, \omega) \quad (5.1)$$

The so-called angular momentum luminosity at the considered convective edge (envelope or core) is obtained after horizontal integration

$$\mathcal{L}_{J\ell,m}(r_{cz}) = 4\pi r_{cz}^2 \mathcal{F}_{J,r_{cz}}. \quad (5.2)$$

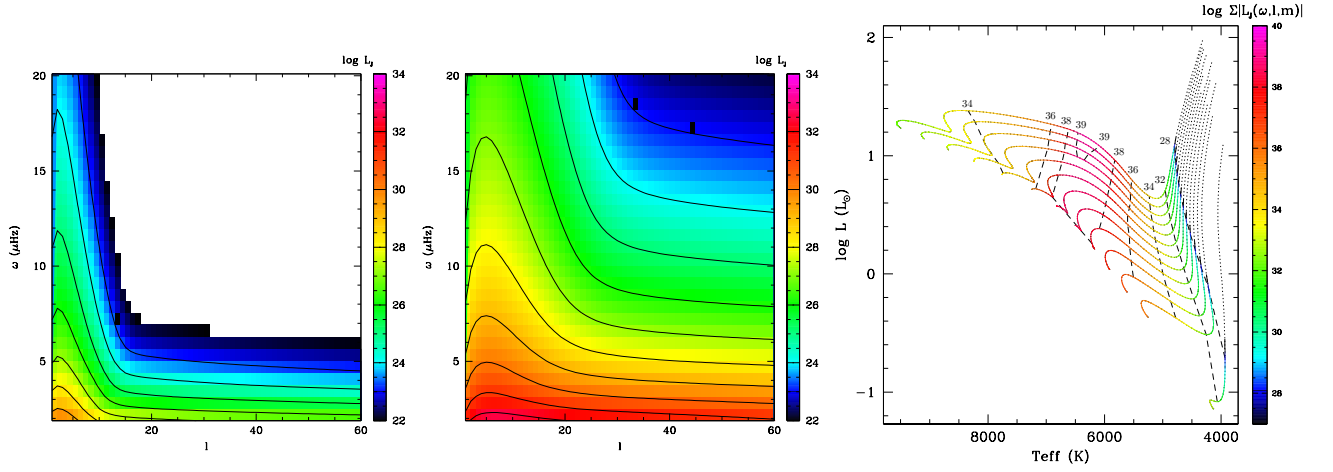


Figure 5.6: *Left and middle panels* Angular momentum luminosity $\mathcal{L}_J(\omega, \ell)$ at the base of the convective envelope of IGW generated by Reynolds-stress in the external convective layers as a function of the emission frequency ω and of the degree ℓ at two different ages on the PMS evolution of a $1 M_\odot$ model. *Right panel* total momentum flux carried by IGW generated by the convective envelope. Dotted lines indicate the region where the stars are fully convective so that no IGW can be generated. The vertical dashed lines connect models where the excitation has the same value. *From Charbonnel et al. (2013).*

$$\mathcal{L}_J(r) = \mathcal{L}_{J,\text{env}} + \mathcal{L}_{J,\text{core}}, \quad (5.3)$$

where each component is given by

$$\sum_{\sigma, \ell, m} \mathcal{L}_{J\ell, m}(r_{\text{cz}}) \exp[-\tau(r, \sigma, \ell)], \quad (5.4)$$

where ‘cz’ refers to the interface between the radiative region and the corresponding convection zone (i.e., envelope or core).

The local damping rate

$$\tau(r, \sigma, \ell) = [\ell(\ell + 1)]^{\frac{3}{2}} \int_r^{r_{\text{cz}}} (K_T + \nu_v) \frac{N N_T^2}{\sigma^4} \left(\frac{N^2}{N^2 - \sigma^2} \right)^{\frac{1}{2}} \frac{dr}{r^3} \quad (5.5)$$

takes the mean molecular weight stratification into account, as well as the thermal and the (vertical) turbulent viscosity (K_T and ν_v respectively), and directly depends on the Brunt-Väisälä frequency N^2 . Here, σ is the local Doppler-shifted frequency

$$\sigma(r) = \omega - m [\Omega(r) - \Omega_{\text{cz}}] \quad (5.6)$$

with ω the wave frequency in the reference frame of the corresponding emitting convection zone that rotates with the angular velocity Ω_{cz} .

In the $1 M_\odot$ we see that the angular momentum luminosity increases as the star evolves on the PMS, and the total momentum flux carried by IGW generated by the convective envelope is maximum at the ZAMS as also seen from the right panel of Fig. 5.6, where the $1 M_\odot$ model

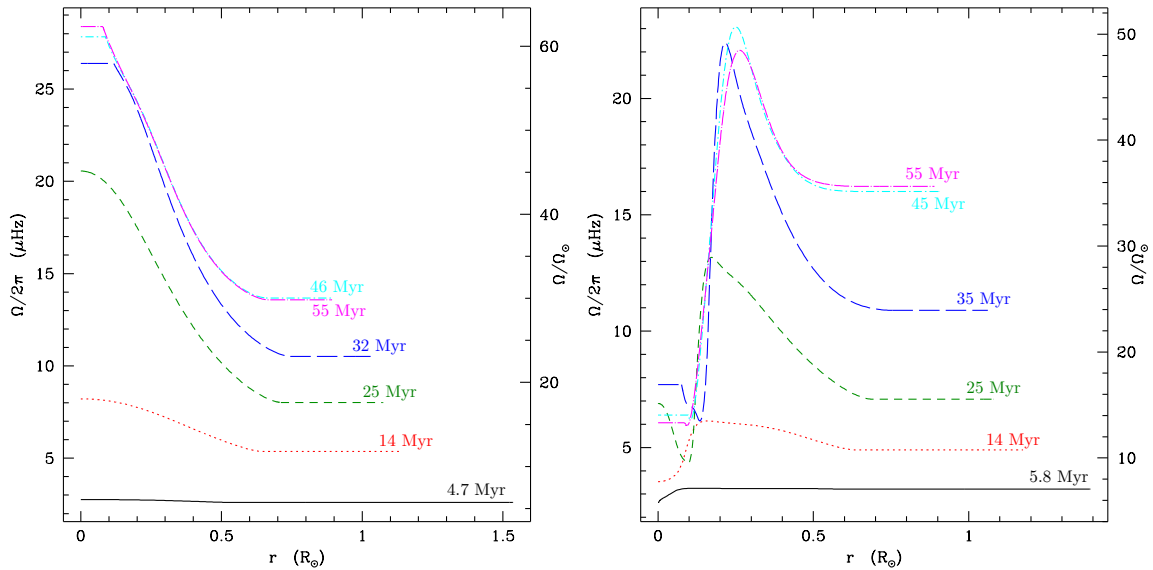


Figure 5.7: Internal profiles of angular velocity as a function of radius in a $1 M_{\odot}$ model including angular momentum transport by meridional circulation and shear turbulence (left) and by meridional circulation, shear turbulence and IGW (right), for different ages on the PMS evolution as indicated on the labels. *From Charbonnel et al. (2013).*

is the third track from the bottom. The waves having the smaller frequency and the lower ℓ are the most efficient in transporting angular momentum.

Not only is the net flux of angular momentum transport by IGW important in magnitude, it is also *actually* efficient to transport angular momentum and strongly modify the angular velocity profiles as evidenced in Fig. 5.7. The slight differential rotation that builds up at the end of the disk-coupling phase as a result of stellar contraction along the Hayashi track, induces a Doppler shift between the emission and local IGW spectra. As a consequence, low-frequency low-degree waves, which undergo the largest differential damping between retrograde and prograde components (see Eq. 5.6), soon penetrate all the way to the central regions where they deposit their negative momentum and very efficiently spin down the core. This configuration is further maintained until the model reaches the ZAMS, with a profile of angular velocity completely different from that obtained when IGW are not taken into account.

These results are very encouraging since IGW actually generate a stronger coupling between the core and the envelope. They are however only the first step of a more detailed study that will include the effect of magnetized stellar wind and will be evolved up to the age of the Sun to be confronted to observations.

IGW represent a very good candidate to explain the chemical and rotational evolution of solar-type stars. The PMS study presented is one of the hints of this statement, the other being given by the results already obtained in Charbonnel & Talon (2005). In this early work, the transport of angular momentum was only considered starting at the ZAMS, and the spectrum of the IGW excited at the edge of the convective envelope was assumed to be the same during the

entire evolution from the ZAMS to the age of the Sun, based on the fact that the structure and the properties of convection and of thermal diffusivity do not vary sufficiently so as to modify the excitation of IGW at this phase. The rotation profiles they obtained for a model with $v \sin i = 50 \text{ km.s}^{-1}$ and a torque from magnetized stellar winds extracting angular momentum at the surface so as to reach the solar surface mean rotation period at 4.57 Gyr are presented in Fig. 5.8b. The different wave fronts of IGW create a depletion in the rotation profile as the star evolves on the main sequence, leading to a mostly flat profile by the age of the Sun. These models also lead to a good fit to the surface lithium abundances evolution as evidenced from data in open clusters (see Fig. 2 in Charbonnel & Talon (2005)).

5.1.5 Self-consistent non-standard models of solar-type stars including rotation, rotation-induced mixing and Tayler-Spruit dynamo

As it has become clear that meridional circulation and rotation-driven instabilities can not alone explain the observed rotation and chemical evolution of solar-type stars, additional transport processes have been proposed as candidates to reduce the discrepancy between the rotating models and the observations. I have described the work we do among the STAREVOL team and within the TOUPIES project to explore the impact of IGW. Another good candidate and yet not fully explored process is the magnetic driven instabilities.

In Chap. 3 we have seen that magnetic fields are detected in low-mass and solar-type stars at all evolutionary phases, and knowing that it may induce modifications in the stellar structure and induce transport processes in rotating stars, it is natural to check the impact of such a physical ingredient on the rotational evolution of solar-type stars.

Such a work has been done by Eggenberger et al. (2005); Yang & Bi (2006); Eggenberger et al. (2010a) who have explored the impact of the Tayler-Spruit dynamo (Spruit 1999, 2002) on the evolution of a solar-type star. Eggenberger et al. (2005) used the Taylor-Spruit dynamo formalism in addition to a transport "à la Maeder & Zahn (1998)", assuming a ZAMS velocity of 50 km/s, a torque from magnetized stellar winds and an azimuthal field of 100 Gauss, and focused on the rotation profile that could be achieved in a $1 M_{\odot}$ model. The result is presented in Fig. 5.8a and turns out to be very encouraging since the very large magnetic diffusivity obtained with the formalism they use rapidly enforces quasi solid-body rotation and allows to obtain a profile at the age of the Sun that fits very nicely the helioseismic data. In Eggenberger et al. (2010a), following the same path as the one I described for IGW, they use the same formalism but now compute a self-consistent evolution from the PMS phase. The results obtained in the first place for the MS evolution are maintained : the magnetic diffusivity is also dominant during the PMS phase, enforcing a solid-body rotation that prevents shear mixing to be efficient in rapid rotators compared to the slow rotators in which they imagine that the Tayler-Spruit instability does not develop. This allows a much better fit to both the rotational and the chemical evolution of solar-type stars as evidenced from the observations presented previously, as shown in Fig. 5.9.

The efficiency and development of this very same process has however been challenged by theoretical and numerical simulations (Zahn et al. 2007), and these results need to be confirmed using a formalism which is not as controversial.

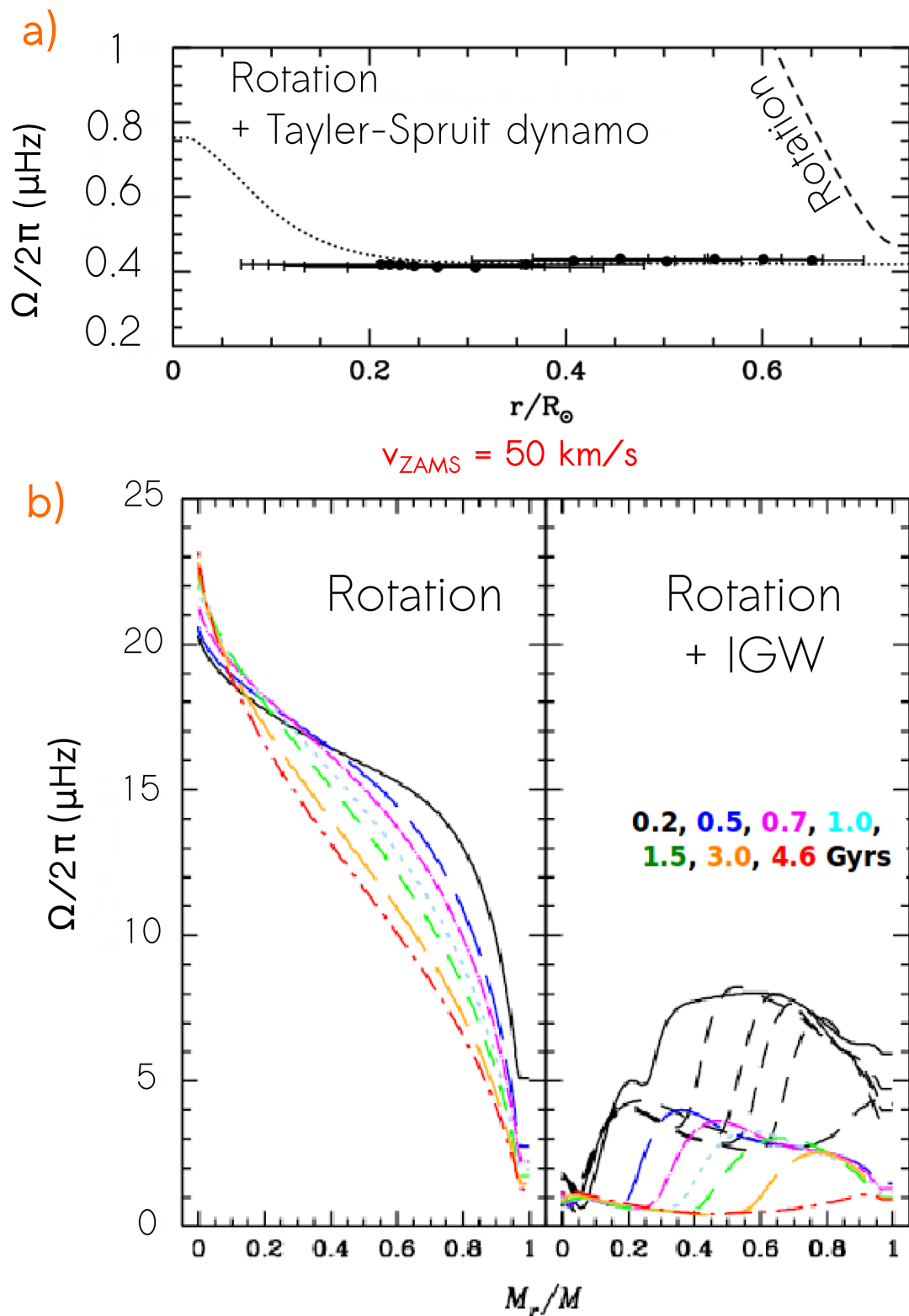


Figure 5.8: Internal rotation profile of $1 M_{\odot}$ models at the age of the Sun obtained by Eggenberger et al. (2005) (a) and Charbonnel & Talon (2005) (b) when adding the effect of the Tayler-Spruit instability and of the IGW respectively to that of meridional circulation and turbulent shear to compute the transport of angular momentum and chemicals.

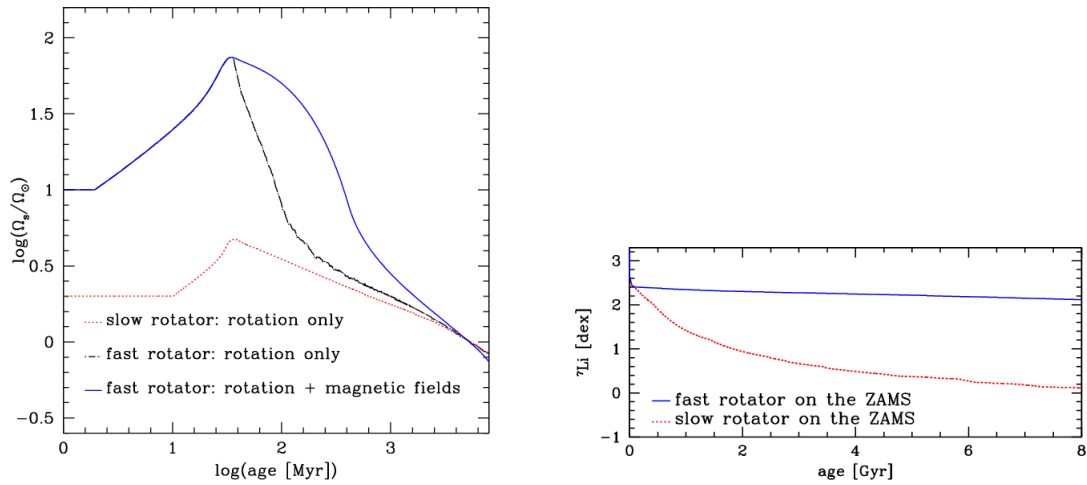


Figure 5.9: *Left* Variation with time of the surface angular velocity of $1 M_{\odot}$ models for fast and slow rotators on the ZAMS. *Right* Surface abundance of lithium $\epsilon(Li)$ during the evolution of $1 M_{\odot}$ models. The model of a slow rotator on the ZAMS is computed with rotation only, while the model of a fast rotator on the ZAMS is computed with both rotation and magnetic fields. From *Eggenberger et al. (2010a)*.

5.2 Red Giant Branch stars

Beyond the turn-off, the low-mass (and thus solar-type) stars evolve through the Hertzsprung gap and up the giant branch at the base of which they undergo the first dredge-up that induces a modification of their surface abundance pattern. As already mentioned in Chap. 3, unexpected variations of the abundance of light elements participating to H burning are observed at the surface of most of low-mass RGB stars, evidencing the action of some extra-mixing process able to connect the deep convective envelope with the periphery of the hydrogen burning shell. On the other hand, due to the strong expansion of the outer regions, the stars inflate while still maintaining a small mass loss rate, which should lead to a significant decrease of the surface rotation due to angular momentum conservation. This is actually observed in most cases (*de Medeiros 2004*).

Based on this analysis of the observational constraints, rotation-induced mixing was rapidly considered as a potential origin for the abundance anomalies encountered.

5.2.1 Rotating models of low-mass RGB stars

In *Palacios et al. (2006)*, I explored the efficiency of the transport "à la *Maeder & Zahn (1998)*" in low-mass low-metallicity RGB stars in different configurations, in particular assuming both solid-body rotation and specific angular momentum conservation for the convective envelope. These models showed that the transport of angular momentum by meridional circulation and turbulent shear do not dominate the overall evolution of the angular velocity profile which is instead shaped by the contraction of the radiative core. The differential rotation built in these models is extremely important as shown in Fig. 5.10, about 2 orders of magnitude at the bump, but the diffusion coefficient are strongly limited by the mean molecular gradients existing in the hydrogen burning shell, and they are far too slow to allow for an efficient

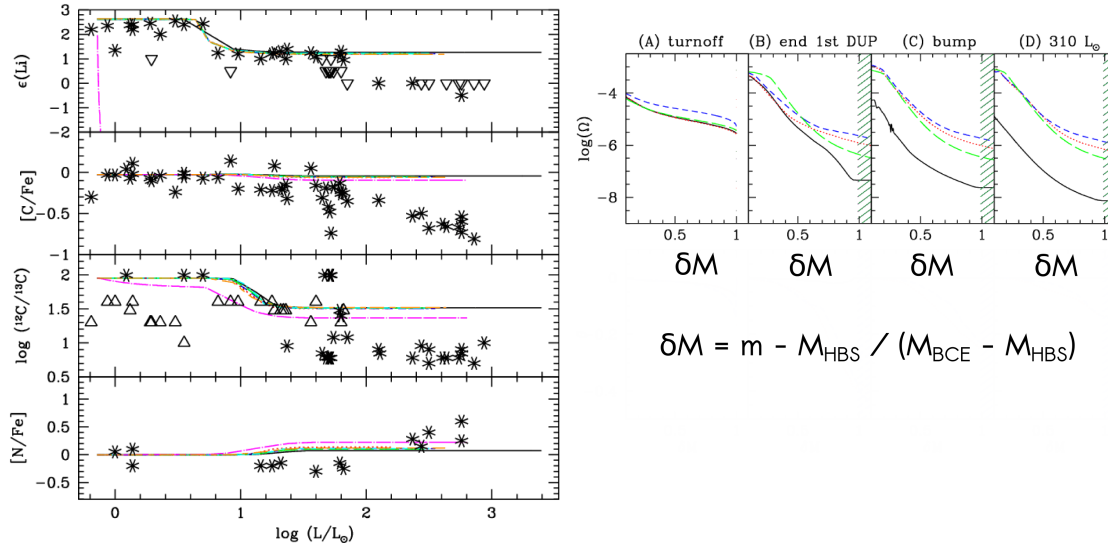


Figure 5.10: *Left* Comparison of the surface abundance evolution of Li, C, and N compared to the data from Gratton et al. (2000). *Right* Angular velocity Ω profiles for different models of a $0.8 M_\odot$ model at low metallicity. The solid lines are for a model with solid-body rotation in the convective envelope and the other lines are for models assuming constant specific angular momentum in the convective envelope with different initial rotation rates. The scaled mass coordinate δM allows a blow-up of the region of interest ($\delta M = 0$ at the base of the HBS and $\delta M = 1$ at the base of the CE). The long dashed lines represent the Ω profiles that one gets when the angular momentum evolution only results from the structural readjustments beyond the turn-off (i.e. no AM transport). From Palacios et al. (2006).

modification of the surface abundances of light elements.

A large improvement was achieved by the inclusion of the thermohaline instability in the models (Charbonnel & Zahn 2007; Charbonnel & Lagarde 2010), since in the hydrogen burning shell, the inversion of mean molecular weight generated by the ${}^3\text{He}({}^3\text{He}, 2p){}^4\text{He}$ induces the favourable conditions for its growth. In the absence of any interaction between the shear and this instability, and thus assuming that the finger structures associated to this double diffusive instability have an aspect ratio smaller than 1, Charbonnel & Zahn (2007) and Charbonnel & Lagarde (2010); Lagarde et al. (2012) showed that this instability is much more efficient than the shear and the meridional circulation to transport nuclides and that it could actually lead to variations of Li, ${}^{12}\text{C}$, ${}^{12}\text{C}/{}^{13}\text{C}$ and ${}^{14}\text{N}$ in very good agreement with the observations as shown in Fig. 5.11.

This instability is however inefficient in the angular momentum transport and the problem of the very large differential rotation achieved in the RGB models still remains.

5.2.2 News from asteroseismology

The angular momentum evolution of solar-type stars is globally only constrained by the variations of the surface velocity and until very recently this was true from the PMS to the end

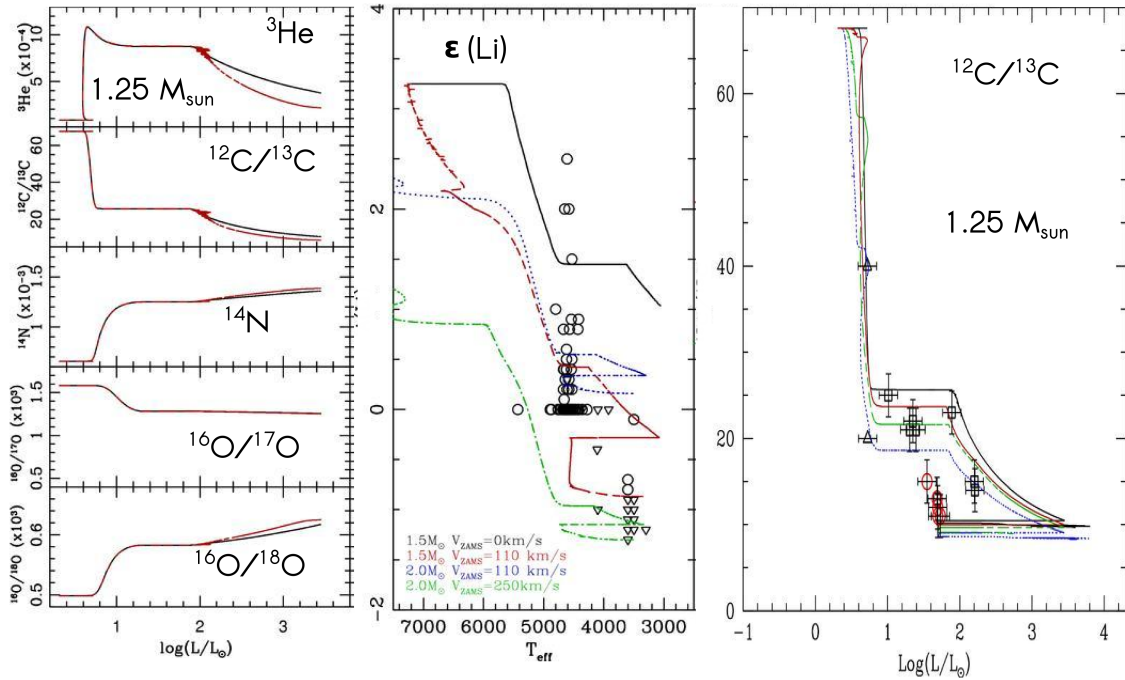


Figure 5.11: *Left* Abundance variation with respect to luminosity for a $1.25 M_\odot$ model including rotation and thermohaline mixing with two distinct efficiencies (black and red lines). *Middle* Lithium abundance variation in models with diverse masses and rotation all including thermohaline mixing compared to abundances measured in evolved stars of the galactic field. *Right* Carbon isotopic ratio as a function of luminosity for $1.25 M_\odot$ models with different rotation velocities all including thermohaline mixing compared to data from the M67 open cluster. The triangle is a subgiant star, the squares are RGB stars and red circles are clump stars. From Charbonnel & Lagarde (2010).

of the AGB phase, with the sole exception of the Sun for which helioseismology gives access to the internal rotation profile down to $0.2 R_\odot$. As already mentioned in Chap. 3, the CoRoT and Kepler missions allowed to detect solar-like oscillations in red giant stars and revealed that the modes propagating in their interior are mixed p and g modes, which allows to probe the very core of the red giants to which we were completely blind before (see e.g. Chaplin & Miglio 2013, for a recent review).

These results carry the promise of great new developments for stellar physics and stellar evolution models as they bring unprecedented constraints for the transport processes mechanisms operating in the radiative interior of low and intermediate mass stars.

The inversion of the rotation profile for the red giants is still complicated, but Deheuvels et al. (2012) have completed such analysis for the Kepler star Otto, and the main result is that the inversion is compatible with differential rotation between the envelope and the core, but to a much lesser extent than what is predicted from rotating models by several orders of magnitude. This work indicates that some mechanism is at play that allows for efficient transfer of angular

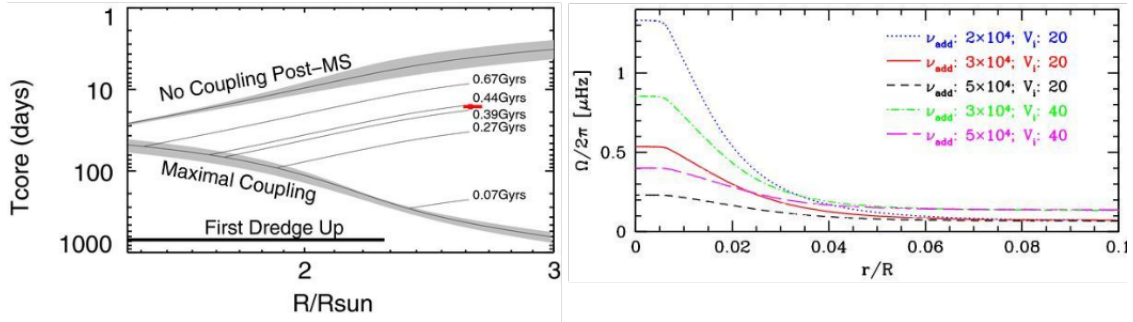


Figure 5.12: *Left* Best fit low-mass model using PMS rotation data as a starting point. Tracks between the solid body and no post-main sequence coupling explore the effects of relaxing solid-body rotation at different points on the subgiant branch. From [Tayar & Pinsonneault \(2013\)](#). *Right* Rotation profiles achieved for the model of Otto including rotation and an additional uniform viscosity profile ν_{add} for the transport of angular momentum only. From [Eggenberger et al. \(2012\)](#).

momentum between the core and the envelope, and more importantly that this mechanism is efficient enough so as to counteract the effect of core contraction during the post main sequence evolution up to the RGB tip.

[Eggenberger et al. \(2010c,b\)](#); [Lagarde et al. \(2012\)](#); [Marques et al. \(2013\)](#) have put some efforts to evaluate the impact of transport processes on the asteroseismic quantities from rotating stellar evolution models so as to provide directly comparable quantities to the observers.

Considering that rotating models (without magnetic fields nor IGW) fail to reproduce the rotation contrast found in the subgiant Otto, [Eggenberger et al. \(2012\)](#); [Tayar & Pinsonneault \(2013\)](#) have performed parametric investigations coupled to rotating models in order to quantify the needed efficiency of the missing transport process and their results are presented in Fig. 5.12.

According to [Tayar & Pinsonneault \(2013\)](#), to match observations, low-mass stars require significant decoupling between the core and the envelope during the subgiant evolution, and it seems that this decoupling would occur when the first dredge-up begins and builds up a mean molecular weight gradient.

On the other hand, [Eggenberger et al. \(2012\)](#) find that to counterbalance the core contraction and the associated angular momentum transport, a diffusive process with an equivalent diffusivity of about $3 \times 10^4 \text{ cm}^2 \cdot \text{s}^{-1}$ is necessary to be efficient in the *entire radiative region*.

Both conclusions open the door for testing at this phase other transport processes as magnetic fields and IGW that have been shown to be promising candidates to explain observations during the earlier evolution of solar-type stars, and in particular during the PMS, where the structure is similar to that found in subgiant branch stars.

Conclusion

Contents

6.1 Summary	73
6.2 Future prospects	74

6.1 Summary

Stellar evolution and stellar evolution models are a cornerstone not only for stellar astrophysics but also for galactic physics, planet formation, cosmology ... Stellar evolution models are used in many aspects of astrophysics, to evaluate masses, radii and ages of stars but also of their surrounding planets, to constrain the formation and structure of the associations, clusters and galaxies they are found in, to evaluate galactic and extragalactic distances and ages, to understand the cosmic evolution of nuclides. Understanding how stars evolved from their birth to their state of remnant is thus of prime importance.

We have seen that despite the great success of standard stellar evolution models developed in the early 1950's and improved in the 1970's with the inclusion of microscopic diffusion processes, the increasing number of discrepancies between the predictions of these models and observational results, have impuled the need to *go beyond* that zero order representation.

To move to the next level of accuracy in stellar evolution models, it appeared necessary to introduce physical ingredients that are completely overlooked in standard models, being considered as having a second order effect on stellar evolution, as rotation or magnetic fields. The increasing number of detections of magnetic fields in stars throughout the HR diagram and the ubiquitous existence of rotation indicate that these phenomena should be taken into account to build more realistic stellar evolution models. In addition, they are known from theory to directly impact the structure of stars and to trigger instabilities in stellar plasmas, all aspects that could lead to differences in the outcome of stellar evolution models that would incorporate them.

Other indicators as unpredicted abundance patterns, population counts or rotation contrasts inside other stars that the Sun point to the existence of transport processes occurring in stellar interiors in addition to convection, and able to modify both the angular momentum distribution and the chemical stratification.

From an observational point of view, we are gaining insight on real stars to a level that was previously only possible for the Sun, and the developments started within the framework of solar physics and the solar models should now be spread to all the categories of spectral types.

The formalisms developed to account for rotation and rotation-induced transport processes were the first to be implemented in new generation stellar evolution codes and are now the best spread into non-standard stellar evolution codes that separate into two families according to the used formalism. These two families of models have been shown to produce very similar results when used to model the main sequence evolution of both massive and low and intermediate mass stars¹, but the codes predictions strongly differ (it is already the case for standard models) for massive stars beyond the turn-off (Martins & Palacios 2013; Brott et al. 2011; Ekström et al. 2012) and also need to be improved for the advances evolutionary stages of low and intermediate-mass stars.

Magnetic fields and IGW marginally accounted for either due to the complexity of their implementation, the lack of self-consistent formalism for their generation process or to the lack of observational constraints which leads to a large parameters space. Hydrodynamical instabilities as the double-diffusive so called *thermohaline* instability are also accounted for in some non-standard models as they may generate important transport of nuclides that may be associated with the observed abundance anomalies.

In parallel to these efforts of improving the models of secular evolution of stars, some efforts have sprung in the last decade to move to another level by assembling the building blocks that will lead in the future to stellar evolution models including the non spherical nature of stars. This direct approach is however still in its infancy, essentially limited by computing power (but not exclusively), and the use of 3-D direct simulations of stars at a given evolutionary point are also being computed in order to use 3-D experiments as guidelines to 1-D evolutionary models.

Rotating stellar evolution models have improved the comparison with observations in many aspects, in particular in the case of massive stars and of intermediate mass stars (see e.g. the review by Maeder & Meynet 2000) . Rotation and the rotation-driven instabilities alone as included them in stellar evolution codes are however not sufficient to account for the rotational and chemical evolution of solar-type stars.

For these stars, it is necessary to introduce processes that more efficiently transport angular momentum, and the first attempts made using IGW or magneto-rotational instabilities are more than encouraging.

6.2 Future prospects

From the review given in Chap. 4, new standards are arising in the domain of stellar evolution modelling, and I intend to continue my effort as a full actor of this evolution in the coming years. Indeed, the context of modern astrophysics is an open path to explore and push the

¹<http://www.mpa-garching.mpg.de/stars/SCC/StarCode.html>
<http://www.astro.up.pt/corot/>
 Martins & Palacios (2013)

limits of our understanding of stars, thanks to the better and more systematic exploitation of observational techniques as spectropolarimetry, asteroseismology and interferometry.

In addition to the need to account for the new constraints coming from such types of observational data, a lot of theoretical work still needs to be done, either via analytical analysis or using numerical experiments, to improve the way non-standard transport processes are accounted for in stellar evolution codes.

In order to improve our understanding of stars, it is thus necessary to continue to tightly bridge theoretical, heavy numerical and observational approaches together with stellar evolution modelling. I have worked in such manners up to now and intend to continue doing so in the coming future. More specifically, in the years to come I intend to pursue in the following directions :

- I have started doing 3-D numerical experiments to constrain the interplay between convection, rotation and magnetic fields in red giant stars, and I will continue in this direction together with A.S. Brun. Our main mid-term objective is to be able to constrain the evolution of the rotation profile in the convective envelope of solar-type stars as they evolve from the turn-off to the upper red giant branch. Such simulations are heavy and long to perform, but this has been improved by the developers of the ASH code, and makes our objective reachable. Moreover, it is now also possible to simulate an entire star, including both convective and radiative regions (Brun et al. 2011), and thus to actually probe the connection and angular momentum transfer between them for different structural setups.
- As mentioned in Chap. 4, most of the transport processes in radiative regions are included as separate ingredients that do not directly interact with each other. This is an idealized view in many ways, which needs to be improved. For instance, the thermohaline instability efficiency as described in Chap. 5 relies on the aspect ratio of the finger structure that may develop in regions with an inversion of mean-molecular weight. In presence of strong shear mixing, one may wonder whether such structures would remain or would be erased. Turning to IGW, the spectrum of waves and the total angular momentum flux they may carry depend on the excitation mechanism which is partially described in the current adopted formalisms. Moreover, IGW and magnetic fields are seen as equally efficient processes to transport angular momentum in stars, but are treated in concurrent models as of present. Maeder et al. (2013) have recently proposed a new definition of the instability criteria for several hydrodynamical instabilities when assuming a direct interaction between them, and this is a path I wish to explore within stellar evolution models in the future.
- In Chap. 5, I have presented the present status of state-of-the-art models for the evolution of solar-type stars. The main challenge is to understand and manage to reproduce the evolution of their angular momentum content with physically grounded models, from the PMS where surface rotation periods are the only available constraints, to the age of the Sun and the red giant branch, where asteroseismology now gives access to the core rotation and thus in some cases to the contrast of angular velocity between the core and the surface. I will be involved in the modelling of the early phases within the TOUPIES project until

2016, and I will hopefully also contribute to bring new constraints on the rotation of solar-type stars at the age of the Sun by leading observational proposals as the proposal 093.D-0567 submitted at the end of 2013 to determine the age of solar analogs for which rotation periods are available from CoRoT luminosity curves.

Of course, I will also continue my early efforts to self-consistently model the angular momentum evolution of low-mass stars up to the AGB phase.

In addition to these research mid to long term prospects, I wish to continue my involvement in the development of tools that will facilitate the access, the exploitation and the visualization of the data produced by models. I am involved with Dr. N. Rodriguez, a computer scientist specialized in visualization and rendering, in a project to build visualization concepts and tools for highly multi-dimensional data, and I will continue this collaboration in the years to come.

In parallel, with my duties as an astronomer, I will increase my involvement in the development of data models and tools to make theoretical stellar data (spectra and stellar evolution models outputs) available and interoperable within the framework of the Virtual Observatory.

Constants and Formulae

Contents

A.1 Units and Constants	77
A.2 Nomenclature	78

A.1 Units and Constants

The set of equations solved in stellar evolution codes is written in *cgs* units.

Unit	Value
1 Å	0.1 nm = 10^{-8} cm
1 erg	10^{-7} Joule
1 dyne.cm ⁻²	0.1 Pascal = 10^{-6} bar = 9.8693×10^{-7} atm.
1 eV	1.60219×10^{-12} erg

Table A.1: Units

Constant	Unit	Value
E_ν	eV	$12398.55 / \lambda$ (Å)
c	cm.s ⁻¹	2.99792×10^{10}
h	erg.s	6.62607×10^{-27}
G		
m_A (or <i>a.m.u.</i>)	g	1.66054×10^{-24}
a_0	cm	0.529178×10^{-9}
a	erg.cm ⁻³ .K ⁻⁴	$\frac{4\sigma}{c} = 7.5657 \times 10^{-15}$
σ	erg.cm ⁻² .s ⁻¹ .K ⁻⁴	5.6704×10^{-8}
M_\odot	g	1.9891×10^{33}
R_\odot	cm	6.9599×10^{10}

Table A.2: Useful Constants

A.2 Nomenclature

Name	Meaning
ρ	density
v	macroscopic velocity of the plasma
m	mass of the concentric sphere of radius r
P	total pressure
Φ	gravitational potential derived from the Poisson equation $\nabla^2\Phi = 4\pi G\rho$
s	specific entropy (defined by the second principle of thermodynamics)
T	local temperature
L	local luminosity
ε_n	nuclear energy
ε_ν	nutrinic energy
ε_g	gravitational energy
δ	$:= \left(\frac{d\ln\rho}{d\ln T}\right)_P$ coefficient for the generalized equation of state :
$\frac{d\rho}{\rho} = \alpha \frac{dP}{P} - \delta \frac{dT}{T} + \phi \frac{d\mu}{\mu}$	
X_i	mass fraction of the nuclide i
c_p	specific heat at constant pressure
a	radiation constant
σ	Stefan-Boltzmann constant
m_i	mass of nuclide i
r_{ji}	rate for the nuclear reaction between nuclide j and i
∇	real temperature gradient
∇_{rad}	radiative temperature gradient
∇_{ad}	adiabatic temperature gradient
κ	mean Rosseland opacity
g	local gravity
g_{eff}	effective gravity
G	gravitation constant
T_{eff}	effective temperature at $\tau = 2/3$
τ	optical depth
H_p	$:= -\frac{dr}{d\ln P}$ pressure scale height
α_{MLT}	mixing length parameter

Table A.3: Nomenclature

Selected papers

NUMERICAL SIMULATIONS OF A ROTATING RED GIANT STAR. I. THREE-DIMENSIONAL MODELS OF TURBULENT CONVECTION AND ASSOCIATED MEAN FLOWS

A. S. BRUN¹ AND A. PALACIOS^{2,3}

¹ DSM/IRFU/SAp, CEA-Saclay & UMR AIM, CEA-CNRS-Université Paris 7, 91191 Gif-sur-Yvette, France; sacha.brun@cea.fr

² DSM/IRFU/SAp, CEA-Saclay, 91191 Gif-sur-Yvette cedex, France; palacios@graal.univ-montp2.fr

³ GRAAL, Université Montpellier II, CNRS, place Eugène Bataillon, 34095 Montpellier, France

Received 2009 April 3; accepted 2009 July 21; published 2009 August 18

ABSTRACT

With the development of one-dimensional stellar evolution codes including rotation and the increasing number of observational data for stars of various evolutionary stages, it becomes more and more possible to follow the evolution of the rotation profile and angular momentum distribution in stars. In this context, understanding the interplay between rotation and convection in the very extended envelopes of giant stars is very important considering that all low- and intermediate-mass stars become red giants after the central hydrogen burning phase. In this paper, we analyze the interplay between rotation and convection in the envelope of red giant stars using three-dimensional numerical experiments. We make use of the Anelastic Spherical Harmonics code to simulate the inner 50% of the envelope of a low-mass star on the red giant branch. We discuss the organization and dynamics of convection, and put a special emphasis on the distribution of angular momentum in such a rotating extended envelope. To do so, we explore two directions of the parameter space, namely, the bulk rotation rate and the Reynolds number with a series of four simulations. We find that turbulent convection in red giant stars is dynamically rich, and that it is particularly sensitive to the rotation rate of the star. Reynolds stresses and meridional circulation establish various differential rotation profiles (either cylindrical or shellular) depending on the convective Rossby number of the simulations, but they all agree that the radial shear is large. Temperature fluctuations are found to be large and in the slowly rotating cases, a dominant $\ell = 1$ temperature dipole influences the convective motions. Both baroclinic effects and turbulent advection are strong in all cases and mostly oppose one another.

Key words: convection – hydrodynamics – methods: numerical – stars: evolution – stars: interiors – stars: rotation

Online-only material: color figures

1. OBSERVATIONS AND MODELS OF RGB STARS

1.1. What are Observations and Stellar Evolution Models Telling Us?

Almost all, if not all stars rotate, and the distribution of their angular momentum appears to change along the course of their evolution as can be seen from the $v \sin i$ data collected during the last decades for stars all over the HR diagram (e.g., see for instance Pilachowski & Milkey 1984, 1987; de Medeiros & Mayor 1999; Glebocki & Stawikowski 2000; Royer et al. 2002a, 2002b; Barnes et al. 2005; Karl et al. 2005; Carney et al. 2008).

To constrain the internal angular momentum profile at each evolutionary phase, the easiest approach would be to probe stellar interiors in order to derive the angular velocity profile. Helioseismology allows us to invert the inner solar rotation profile down to $r = 0.25 R_{\odot}$ (Schou et al. 1998; Antia & Basu 2000; Antia et al. 2008; García et al. 2008). Asteroseismology should soon offer similar opportunities for other stellar spectral types thanks to the CoRoT (Goupil et al. 2006; Baglin et al. 2007) and Kepler satellites. In the meantime, however, we are left with indirect probes of the internal angular momentum distribution in all stars: (1) the surface velocity measurements for stars of similar initial mass at different evolutionary stages; (2) the surface abundance anomalies resulting from the action of internal transport processes, in part due to rotation, that connect the stellar envelopes to the nuclearly processed internal regions. These indirect probes can be compared to the results of one-dimensional rotating stellar evolution models (Pinsonneault et al. 1989; Fliegner & Langer 1994; Meynet & Maeder 1997;

Talon et al. 1997; Maeder & Meynet 2000; Heger et al. 2000, 2005; Palacios et al. 2003, 2006; Chanamé et al. 2005; Suijs et al. 2008) in order to guess the angular velocity profile evolution. The introduction of rotation and associated transport processes in one-dimensional stellar evolution models leads indeed to a clear improvement of the comparison between theoretical predictions and observations, in particular from the point of view of chemical abundances. However, a number of points, in particular concerning the evolution of the surface rotation velocities, remain to be elucidated. It is the case for the differences between predicted and observed spin rates for white dwarfs and neutron stars (Heger et al. 2005; Suijs et al. 2008), or the interpretation of the surface velocities distribution of horizontal branch stars (Sills & Pinsonneault 2000; Recio-Blanco et al. 2002, 2004).

While important theoretical developments have been devoted to the description of the one-dimensional angular momentum transport in the radiative stellar interiors (Zahn 1992; Maeder & Zahn 1998; Mathis & Zahn 2004), the transport of angular momentum in convective regions, and in particular in extended convective envelopes, is poorly described in one-dimensional models. This is of particular importance for the case of giant stars that possess very extended convective envelopes, occupying up to 80% and more of the total stellar radius. These stars are expected to have very slow surface rotation due to their large radius, which is confirmed by observations (de Medeiros & Mayor 1999; Carney et al. 2008), but may also have a rapidly rotating core (Sills & Pinsonneault 2000).

Understanding the angular momentum distribution during the giant evolutionary phases is crucial to understand the subsequent

Diagnoses to unravel secular hydrodynamical processes in rotating main sequence stars

T. Decressin^{1,2}, S. Mathis^{3,8}, A. Palacios⁴, L. Siess⁵, S. Talon⁶, C. Charbonnel^{1,7}, and J.-P. Zahn⁸

¹ Geneva Observatory, University of Geneva, chemin des Maillettes 51, 1290 Sauverny, Switzerland

² Argelander Institute for Astronomy (AIfA), Auf dem Hügel 71, 53121 Bonn, Germany
e-mail: decressin@astro.uni-bonn.de

³ Laboratoire AIM, CEA/DSM-CNRS-Université Paris Diderot, IRFU/SAP Centre de Saclay, 91191 Gif-sur-Yvette, France
e-mail: stephane.mathis@cea.fr

⁴ GRAAL, Université Montpellier II, CNRS, Place E. Bataillon, 34095 Montpellier Cedex 05, France

⁵ IAA-ULB, Université Libre de Bruxelles, Boulevard du Triomphe, CP 26, 1050 Bruxelles, Belgium

⁶ Réseau Québécois de Calcul de Haute Performance, Université de Montréal (DGTIC), CP 6128, succ. Centre-ville, Montréal H3C 3J7, Canada

⁷ LATT, CNRS UMR 5572, Université de Toulouse, 14 Av. Edouard Belin, 31400 Toulouse Cedex 04, France

⁸ LUTH, Observatoire de Paris-CNRS-Université Paris-Diderot, Place Jules Janssen, 92195 Meudon, France

Received 24 July 2008 / Accepted 18 November 2008

ABSTRACT

Context. Recent progress and constraints brought by helio and asteroseismology call for a better description of stellar interiors and an accurate description of rotation-driven mechanisms in stars.

Aims. We present a detailed analysis of the main physical processes responsible for the transport of angular momentum and chemical species in the radiative regions of rotating stars. We focus on cases where meridional circulation and shear-induced turbulence all that are included in the simulations (i.e., no either internal gravity waves nor magnetic fields). We put special emphasis on analysing the angular momentum transport loop and on identifying the contribution of each of the physical process involved.

Methods. We develop a variety of diagnostic tools designed to help disentangle the role of the various transport mechanisms. Our analysis is based on a 2-D representation of the secular hydrodynamics, which is treated using expansions in spherical harmonics. By taking appropriate horizontal averages, the problem reduces to one dimension, making it implementable in a 1D stellar evolution code, while preserving the advective character of angular momentum transport. We present a full reconstruction of the meridional circulation and of the associated fluctuations of temperature and mean molecular weight, along with diagnosis for the transport of angular momentum, heat, and chemicals. In the present paper these tools are used to validate the analysis of two main sequence stellar models of 1.5 and 20 M_{\odot} , for which the hydrodynamics has previously been extensively studied in the literature.

Results. We obtain a clear visualisation and a precise estimation of the different terms entering the angular momentum and heat transport equations in radiative zones of rotating stars. This enables us to corroborate the main results obtained over the past decade by Zahn, Maeder, and collaborators concerning the secular hydrodynamics of such objects. We focus on the meridional circulation driven by angular momentum losses and structural readjustments. We confirm quantitatively for the first time through detailed computations and separation of the various components that the advection of entropy by this circulation is balanced very well by the barotropic effects and the thermal relaxation during most of the main sequence evolution. This enables us to simplify for the thermal relaxation on this phase. The meridional currents in turn advect heat and generate temperature fluctuations that induce differential rotation through thermal wind, thus closing the transport loop. We plan to make use of our refined diagnosis tools in forthcoming studies of secular (magneto-)hydrodynamics of stars at various evolutionary stages.

Key words. hydrodynamics – turbulence – stars: evolution – stars: rotation

1. The impact of rotation on stellar evolution

Rotation, and more precisely differential rotation, has a major impact on the internal dynamics of stars, in several ways. It induces large-scale circulations both in radiative and convective zones that simultaneously advect angular momentum, nuclides, and magnetic fields (Eddington 1925; Vogt 1925; Sweet 1950; Mestel 1953; Busse 1982; Zahn 1992; Talon 1997; Talon et al. 1997; Maeder & Zahn 1998; Meynet & Maeder 2000; Garaud 2002b; Palacios et al. 2003, 2006; Mathis & Zahn 2004, 2005; Rieutord 2006a; Espinosa Lara & Rieutord 2007; Mathis et al. 2007). When the star rotates differentially, various instabilities develop (secular and dynamical shear instabilities, baroclinic,

and multidiffusive instabilities) that generate hydrodynamical turbulence in radiative zones, in addition to these circulations. Just as in the terrestrial atmosphere and in laboratory experiments, this turbulence acts to reduce its cause, namely the gradients of angular velocity and of chemical composition. This explains why its effect may be described as a diffusion process (Talon & Zahn 1997; Maeder 2003; Mathis et al. 2004; Talon 2007, and references therein).

Rotating stars have an equator that is cooler than the poles, which has a strong effect on radiatively driven stellar winds and hence on the loss of mass and angular momentum (Maeder 1999). If rotation is large enough, the stars can even reach the break-up limit, when centrifugal force balances the gravity, and

Rotational mixing in low-mass stars

II. Self-consistent models of Pop II RGB stars

A. Palacios¹, C. Charbonnel^{2,3}, S. Talon⁴, and L. Siess¹

¹ Institut d’Astronomie et d’Astrophysique, Université Libre de Bruxelles Campus de la Plaine, Boulevard du Triomphe, CP 226, 1050 Bruxelles, Belgium

e-mail: apalacio@ulb.ac.be; ana.palacios@cea.fr

² Observatoire de Genève, 51 chemin des Maillettes, 1290 Sauverny, Switzerland

³ Laboratoire d’Astrophysique de Toulouse-Tarbes, Observatoire Midi-Pyrénées, 14 Av. E. Belin, 31400 Toulouse, France

⁴ Département de Physique, Université de Montréal, Montréal PQ H3C 3J7, Canada

Received 15 March 2005 / Accepted 21 February 2006

ABSTRACT

Aims. In this paper we study the effects of rotation in low-mass, low-metallicity RGB stars.

Methods. We present the first evolutionary models taking into account self-consistently the latest prescriptions for the transport of angular momentum by meridional circulation and shear turbulence in stellar interiors as well as the associated mixing processes for chemicals computed from the ZAMS to the upper RGB. We discuss the uncertainties associated with the physical description of the rotational mixing in detail and carefully study their effects on the rotation profile, diffusion coefficients, structural evolution, lifetimes, and chemical signatures at the stellar surface. We focus in particular on the various assumptions concerning the rotation law in the convective envelope, the initial rotation velocity distribution, the presence of μ -gradients, and the treatment of the horizontal and vertical turbulence.

Results. This exploration leads to two main conclusions. (1) After completion of the first dredge-up, the degree of differential rotation (and hence mixing) is maximised in the case of a differentially rotating convective envelope (i.e., $j_{CE}(r) = \text{const.}$), as anticipated in previous studies. (2) Even with this assumption, and contrary to some previous claims, the present treatment for the evolution of the rotation profile and associated meridional circulation and shear turbulence does not lead to enough mixing of chemicals to explain the abundance anomalies in low-metallicity field and globular cluster RGB stars observed around the *bump* luminosity.

Conclusions. This study raises questions that need to be addressed in the near future. These include, for example, the interaction between rotation and convection and the trigger of additional hydrodynamical instabilities.

Key words. stars: evolution – stars: interiors – stars: rotation – stars: abundances – hydrodynamics – turbulence

1. Abundance anomalies in RGB stars

The standard theory of stellar evolution¹ predicts that the chemical composition on the surface of low-mass stars is modified on the way to the red giant branch (RGB) during the so-called first dredge-up (hereafter 1st DUP; Iben 1965). There, the expanding stellar convective envelope (hereafter CE) deepens in mass, leading to dilution of the surface material within regions that have undergone partial hydrogen burning in the earlier main sequence. Qualitatively, this leads to a decrease in the surface abundances of the fragile LiBeB elements and of ¹²C, while those of ³He, ¹³C, and ¹⁴N increase. Abundances of O and heavier elements essentially remain unchanged. Quantitatively, these abundance variations depend on the stellar mass and metallicity (e.g., Sweigart et al. 1989; Charbonnel 1994; Boothroyd & Sackmann 1999). After the 1st DUP, the CE withdraws, while the hydrogen burning shell (hereafter HBS) moves outward in mass. Within the standard framework no more variations of the surface abundance pattern are expected until the star reaches the asymptotic giant branch (hereafter AGB).

Observations sampling the evolution from the turn-off to the base of the RGB in open clusters and in the galactic field stars have validated these predicted surface abundance variations up to the completion of the 1st DUP² (e.g. Gratton et al. 2000). However, observational evidence has accumulated of a second and distinct mixing episode that is not predicted by standard models and that occurs in low-mass stars after the end of the 1st DUP and, more precisely, at the RGB *bump*.

The determination of the carbon isotopic ratio ¹²C/¹³C (hereafter *CIR*) for RGB stars in open clusters with various turn-off masses (Gilroy 1989) has provided the first pertinent clue to this process. It was indeed shown that bright RGB stars with initial masses lower than $\sim 2\text{--}2.5 M_{\odot}$ exhibit considerably lower *CIR* than predicted by standard models after the 1st DUP. Thanks to data collected in stars sampling the RGB of M 67 (Gilroy & Brown 1991), it clearly appeared that observations deviate from standard predictions just at the so-called RGB *bump* (Charbonnel 1994). The Hipparcos parallaxes allowed the evolutionary phase of large samples of field stars with known *CIR* to

¹ By this we refer to the modelling of non-rotating, non-magnetic stars, in which convection and atomic diffusion are the only transport processes considered.

² One has, of course, to consider possible variations in the surface abundance of lithium occurring in some cases already on the main sequence (hereafter MS). This discussion is, however, beyond the scope of this paper (see e.g. Charbonnel et al. 2000; and Palacios et al. 2003, Paper I).

Rotational mixing in low-mass stars

I Effect of the μ -gradients in main sequence and subgiant Pop I stars

A. Palacios¹, S. Talon², C. Charbonnel¹, and M. Forestini³

¹ Laboratoire d'Astrophysique de Toulouse, CNRS UMR5572, OMP, 14 Av. E. Belin, 31400 Toulouse, France

² Département de Physique, Université de Montréal, Montréal PQ H3C 3J7, Canada; CERCA, 5160 Boul. Décarie, Montréal PQ H3X 2H9, Canada

³ Laboratoire d'Astrophysique de l'Obs. de Grenoble, 414 rue de la Piscine, 38041 Grenoble Cedex 9, France

Received 22 August 2002 / Accepted 22 October 2002

Abstract. We present a first set of results concerning stellar evolution of rotating low-mass stars. Our models include fully consistent transport of angular momentum and chemicals due to the combined action of rotation induced mixing (according to Maeder & Zahn 1998) and element segregation. The analysis of the effects of local variations of molecular weight due to the meridional circulation on the transport of angular momentum and chemicals are under the scope of this study. We apply this mechanism to low mass main sequence and subgiant stars of population I.

We show that the so-called μ -currents are of major importance in setting the shape of the rotation profile, specially near the core. Furthermore, as shown by Talon & Charbonnel (1998) and Charbonnel & Talon (1999) using models without μ -currents, we confirm that rotation-induced mixing in stars braked via magnetic torquing can explain the blue side of the Li dip, as well as the low Li abundances observed in subgiants even when μ -currents are taken into account. We emphasize that μ variations are not to be neglected when treating rotation-induced mixing, and that they could be of great importance for latter evolutionary stages.

Key words. stars: interiors – stars: rotation – stars: abundances – hydrodynamics – turbulence

1. Introduction

Whereas standard stellar evolution models (allowing solely for mixing in convective regions) represent a good tool for a zeroth order description of stellar observations, they cannot account for series of abundance patterns observed in various locations of the Hertzsprung-Russell diagram.

While some abundance anomalies are best explained in terms of surface features (as is the case of Am stars for example; see Turcotte et al. 2000), others probably involve deep mixing (as the He overabundances in O stars; see Maeder & Meynet 2000 for details). Rotation induced mixing, in the form of meridional circulation, baroclinic and shear instabilities, in conjunction with microscopic diffusion has been extensively used in order to reduce the discrepancies between standard models and observations, and has proved to be quite promising.

However, following rotation induced mixing in stellar evolution codes is challenging and, up to now, many of the theoretical results from numerical computations have assumed some hypothesis that could be too restrictive. Here, we wish to

further examine the role of horizontal chemical inhomogeneities in the evolution of meridional circulation.

As first pointed out by Mestel (1953), meridional circulation is generated by a departure from spherical symmetry, and settles to restore it, but in turn generates itself a new dissymmetry: the meridian currents transport material with different mean molecular weights from one place to another of the radiative zone, so that a non-spherical μ -distribution is set up which retroacts on the circulation, diminishing its magnitude. In this early description, assuming that the radiative zone does not suffer any local turbulent mixing and that the star remains in solid body rotation, this retroaction was actually shown to inhibit totally the circulation in chemically inhomogeneous regions.

Kippenhahn (1974) pointed out the importance of taking into account the changes in molecular weight, particularly because a strong ∇_{μ} may represent a barrier that hinders mixing. In the models he proposes to explain the Am phenomenon, Vauclair (1977) emphasizes also the important role of the μ -barrier and underlines the fact that it can considerably delay mixing below the convective envelope of slow rotators. This point, and more precisely the retroaction effect of the μ -currents

Send offprint requests to: A. Palacios,
e-mail: apalacio@ast.obs-mip.fr

Bibliography

- Abia, C., Domínguez, I., Gallino, R., et al. 2002, *ApJ*, 579, 817 (Quoted page 36.)
- Abney, W. D. W. 1877, *MNRAS*, 37, 278 (Quoted page 21.)
- Abt, H. A., Levato, H., & Grosso, M. 2002, *ApJ*, 573, 359 (Quoted page 22.)
- Allain, S. 1998, *A&A*, 333, 629 (Quoted page 57.)
- Angelou, G. C., Church, R. P., Stancliffe, R. J., Lattanzio, J. C., & Smith, G. H. 2011, *ApJ*, 728, 79 (Quoted page 39.)
- Arnould, M., Goriely, S., & Jorissen, A. 1999, *A&A*, 347, 572 (Quoted page 34.)
- Auriere, M., Konstantinova-Antova, R., Espagnet, O., et al. 2013, *ArXiv e-prints* (Quoted page 52.)
- Aurière, M., Wade, G. A., Konstantinova-Antova, R., et al. 2009, *A&A*, 504, 231 (Quoted page 52.)
- Babcock, H. W. & Babcock, H. D. 1955, *ApJ*, 121, 349 (Quoted page 31.)
- Bahcall, J. N. & Pinsonneault, M. H. 1992, *Reviews of Modern Physics*, 64, 885 (Quoted page 16.)
- Baraffe, I., Chabrier, G., & Gallardo, J. 2009, *ApJ*, 702, L27 (Quoted page 56.)
- Barnbaum, C., Morris, M., & Kahane, C. 1995, *ApJ*, 450, 862 (Quoted page 22.)
- Baumann, P., Ramírez, I., Meléndez, J., Asplund, M., & Lind, K. 2010, *A&A*, 519, A87 (Quoted page 33.)
- Bazán, G., Dearborn, D. S. P., Dossa, D. D., et al. 2003, in *Astronomical Society of the Pacific Conference Series*, Vol. 293, *3D Stellar Evolution*, ed. S. Turcotte, S. C. Keller, & R. M. Cavallo, 1–58381 (Quoted page 47.)
- Beck, P. G., Montalban, J., Kallinger, T., et al. 2012, *Nature*, 481, 55 (Quoted page 25.)
- Boesgaard, A. M. 2005, in *Astronomical Society of the Pacific Conference Series*, Vol. 336, *Cosmic Abundances as Records of Stellar Evolution and Nucleosynthesis*, ed. T. G. Barnes, III & F. N. Bash, 39 (Quoted page 34.)
- Boesgaard, A. M. & Budge, K. G. 1989, *ApJ*, 338, 875 (Quoted page 33.)
- Boesgaard, A. M., Deliyannis, C. P., & Steinhauer, A. 2005, *ApJ*, 621, 991 (Quoted page 34.)
- Boesgaard, A. M. & Krugler Hollek, J. 2009, *ApJ*, 691, 1412 (Quoted page 34.)
- Boesgaard, A. M. & Tripicco, M. J. 1986, *ApJ*, 303, 724 (Quoted page 33.)
- Böhm-Vitense, E. 1958, *ZAp*, 46, 108 (Quoted page 14.)
- Bouvier, J. 2008, *A&A*, 489, L53 (Quoted pages 57 et 63.)
- Bouvier, J., Matt, S. P., Mohanty, S., et al. 2013, *ArXiv e-prints* (Quoted page 56.)
- Bragança, G. A., Daflon, S., Cunha, K., et al. 2012, *AJ*, 144, 130 (Quoted page 22.)

- Brott, I., de Mink, S. E., Cantiello, M., et al. 2011, *A&A*, 530, A115 (Quoted pages 43 et 74.)
- Browning, M. K. 2008, *ApJ*, 676, 1262 (Quoted page 30.)
- Brun, A. S., Browning, M. K., & Toomre, J. 2005, *ApJ*, 629, 461 (Quoted page 28.)
- Brun, A. S., Miesch, M. S., & Toomre, J. 2004, *ApJ*, 614, 1073 (Quoted page 49.)
- Brun, A. S., Miesch, M. S., & Toomre, J. 2011, *ApJ*, 742, 79 (Quoted page 75.)
- Brun, A. S. & Palacios, A. 2009, *ApJ*, 702, 1078 (Quoted pages 48, 49 et 51.)
- Brun, A. S., Turck-Chièze, S., & Morel, P. 1998, *ApJ*, 506, 913 (Quoted pages 16, 17 et 18.)
- Burgers, J. M. 1969, *Flow Equations for Composite Gases* (Quoted page 16.)
- Canto Martins, B. L., Lèbre, A., Palacios, A., et al. 2011, *A&A*, 527, A94 (Quoted pages 33 et 46.)
- Carlberg, J. K., Cunha, K., Smith, V. V., & Majewski, S. R. 2012, *ApJ*, 757, 109 (Quoted page 22.)
- Carlberg, J. K., Majewski, S. R., Patterson, R. J., et al. 2011, *ApJ*, 732, 39 (Quoted pages 22 et 24.)
- Carretta, E., Gratton, R. G., Lucatello, S., Bragaglia, A., & Bonifacio, P. 2005, *A&A*, 433, 597 (Quoted pages 34 et 35.)
- Cattaneo, F., Brummell, N. H., Toomre, J., Malagoli, A., & Hurlburt, N. E. 1991, *ApJ*, 370, 282 (Quoted page 50.)
- Chaboyer, B., Demarque, P., & Pinsonneault, M. H. 1995, *ApJ*, 441, 865 (Quoted page 62.)
- Chaboyer, B. & Zahn, J.-P. 1992, *A&A*, 253, 173 (Quoted page 44.)
- Chan, K. L. & Sofia, S. 1989, *ApJ*, 336, 1022 (Quoted page 50.)
- Chaplin, W. J. & Miglio, A. 2013, *ARA&A*, 51, 353 (Quoted page 70.)
- Chapman, S. & Cowling, T. G. 1970, *The mathematical theory of non-uniform gases. an account of the kinetic theory of viscosity, thermal conduction and diffusion in gases* (Quoted pages 16 et 17.)
- Charbonnel, C. & Balachandran, S. C. 2000, *A&A*, 359, 563 (Quoted page 34.)
- Charbonnel, C., Decressin, T., Amard, L., Palacios, A., & Talon, S. 2013, *A&A*, 554, A40 (Quoted pages 39, 45, 63, 64 et 65.)
- Charbonnel, C. & Do Nascimento, Jr., J. D. 1998, *A&A*, 336, 915 (Quoted page 34.)
- Charbonnel, C. & Lagarde, N. 2010, *A&A*, 522, A10 (Quoted pages 39, 45, 69 et 70.)
- Charbonnel, C. & Talon, S. 2005, *Science*, 309, 2189 (Quoted pages 57, 62, 65, 66 et 67.)
- Charbonnel, C. & Zahn, J.-P. 2007, *A&A*, 467, L15 (Quoted pages 39, 40, 45 et 69.)
- Chieffi, A. & Limongi, M. 2013, *ApJ*, 764, 21 (Quoted page 39.)
- Christensen-Dalsgaard, J., Dappen, W., Ajukov, S. V., et al. 1996, *Science*, 272, 1286 (Quoted page 16.)
- Clayton, D. D. 1984, *Principles of stellar evolution and nucleosynthesis*. (Quoted page 32.)

- Cline, K. S. 2005, PRIMUS, 15, 274 (Quoted page 10.)
- de Medeiros, J. R. 2004, in IAU Symposium, Vol. 215, Stellar Rotation, ed. A. Maeder & P. Eenens, 144 (Quoted pages 22 et 68.)
- De Ridder, J., Barban, C., Baudin, F., et al. 2009, Nature, 459, 398 (Quoted page 25.)
- Dearborn, D. S. P., Lattanzio, J. C., & Eggleton, P. P. 2006, ApJ, 639, 405 (Quoted page 47.)
- Decressin, T., Mathis, S., Palacios, A., et al. 2009, A&A, 495, 271 (Quoted pages 13, 14, 39, 46 et 61.)
- Deheuvels, S., García, R. A., Chaplin, W. J., et al. 2012, ApJ, 756, 19 (Quoted pages 25, 26 et 70.)
- Deupree, R. G. 1990, ApJ, 357, 175 (Quoted page 47.)
- Deupree, R. G. 1995, ApJ, 439, 357 (Quoted page 47.)
- Deupree, R. G. 1998, ApJ, 499, 340 (Quoted page 47.)
- Deupree, R. G. 2011, ApJ, 735, 69 (Quoted page 47.)
- Donati, J.-F. 2001, in Lecture Notes in Physics, Berlin Springer Verlag, Vol. 573, Astrotomography, Indirect Imaging Methods in Observational Astronomy, ed. H. M. J. Boffin, D. Steeghs, & J. Cuypers, 207 (Quoted page 27.)
- Donati, J.-F., Gregory, S. G., Alencar, S. H. P., et al. 2011, MNRAS, 417, 472 (Quoted page 55.)
- Donati, J.-F., Gregory, S. G., Alencar, S. H. P., et al. 2013, MNRAS, 436, 881 (Quoted page 55.)
- Donati, J.-F., Jardine, M. M., Gregory, S. G., et al. 2007, MNRAS, 380, 1297 (Quoted page 55.)
- Donati, J.-F., Jardine, M. M., Gregory, S. G., et al. 2008, MNRAS, 386, 1234 (Quoted page 55.)
- Donati, J.-F. & Landstreet, J. D. 2009, ARA&A, 47, 333 (Quoted pages 27, 29 et 30.)
- Donati, J.-F., Skelly, M. B., Bouvier, J., et al. 2010, MNRAS, 409, 1347 (Quoted page 55.)
- Duez, V., Mathis, S., & Turck-Chièze, S. 2010, MNRAS, 402, 271 (Quoted pages 40 et 41.)
- Eggenberger, P., Maeder, A., & Meynet, G. 2005, A&A, 440, L9 (Quoted pages 57, 62, 66 et 67.)
- Eggenberger, P., Maeder, A., & Meynet, G. 2010a, A&A, 519, L2 (Quoted pages 66 et 68.)
- Eggenberger, P., Meynet, G., Maeder, A., et al. 2008, Ap&SS, 316, 43 (Quoted page 39.)
- Eggenberger, P., Meynet, G., Maeder, A., et al. 2010b, A&A, 519, A116 (Quoted page 71.)
- Eggenberger, P., Miglio, A., Montalbán, J., et al. 2010c, A&A, 509, A72 (Quoted page 71.)
- Eggenberger, P., Montalbán, J., & Miglio, A. 2012, A&A, 544, L4 (Quoted page 71.)
- Ekström, S., Georgy, C., Eggenberger, P., et al. 2012, A&A, 537, A146 (Quoted page 74.)
- Endal, A. S. & Sofia, S. 1976, ApJ, 210, 184 (Quoted pages 37, 38, 40 et 42.)
- Endal, A. S. & Sofia, S. 1978, ApJ, 220, 279 (Quoted pages 38 et 39.)
- Espinosa Lara, F. & Rieutord, M. 2007, A&A, 470, 1013 (Quoted page 47.)
- Espinosa Lara, F. & Rieutord, M. 2011, A&A, 533, A43 (Quoted page 47.)
- Espinosa Lara, F. & Rieutord, M. 2013, A&A, 552, A35 (Quoted page 47.)

- Feiden, G. A. & Chaboyer, B. 2012, *ApJ*, 761, 30 (Quoted pages 39, 40 et 41.)
- Feiden, G. A. & Chaboyer, B. 2013, *ApJ*, 779, 183 (Quoted page 41.)
- Fowler, A. 1900, *MNRAS*, 60, 579 (Quoted page 21.)
- Frebel, A., Aoki, W., Christlieb, N., et al. 2005, *Nature*, 434, 871 (Quoted page 35.)
- Galilei, G., Welsler, M., & de Filiis, A. 1613, *Istoria E dimostrazioni intorno alle macchie solari E loro accidenti comprese in tre lettere scritte all'illvstrissimo signor Marco Velseri ...* (Quoted page 21.)
- Gallet, F. & Bouvier, J. 2013, *A&A*, 556, A36 (Quoted pages 56, 57, 58, 59, 60 et 63.)
- García, R. A., Salabert, D., Ballot, J., et al. 2011, *Journal of Physics Conference Series*, 271, 012046 (Quoted pages 25, 26 et 57.)
- Goldreich, P. & Kumar, P. 1990, *ApJ*, 363, 694 (Quoted page 45.)
- Goldreich, P., Murray, N., & Kumar, P. 1994, *ApJ*, 424, 466 (Quoted page 45.)
- Gratton, R. G., Sneden, C., Carretta, E., & Bragaglia, A. 2000, *A&A*, 354, 169 (Quoted pages 33, 34, 35 et 69.)
- Hartigan, P., Edwards, S., & Ghandour, L. 1995, *ApJ*, 452, 736 (Quoted page 46.)
- Heap, S. R., Lanz, T., & Hubeny, I. 2006, *ApJ*, 638, 409 (Quoted pages 33 et 35.)
- Heger, A., Langer, N., & Woosley, S. E. 2000, *ApJ*, 528, 368 (Quoted pages 37, 39 et 43.)
- Heger, A., Woosley, S. E., & Spruit, H. C. 2005, *ApJ*, 626, 350 (Quoted page 43.)
- Henyey, L. G., Lelevier, R., & Levee, R. D. 1959a, *ApJ*, 129, 2 (Quoted page 14.)
- Henyey, L. G., Wilets, L., Böhm, K. H., Lelevier, R., & Levee, R. D. 1959b, *ApJ*, 129, 628 (Quoted page 14.)
- Hui-Bon-Hoa, A. 2008, *Ap&SS*, 316, 55 (Quoted page 39.)
- Hunter, I., Brott, I., Lennon, D. J., et al. 2008, *ApJ*, 676, L29 (Quoted page 22.)
- Irwin, J. & Bouvier, J. 2009, in *IAU Symposium*, Vol. 258, *IAU Symposium*, ed. E. E. Mamajek, D. R. Soderblom, & R. F. G. Wyse, 363–374 (Quoted pages 24 et 56.)
- Karakas, A. & Lugaro, M. 2010, in *Nuclei in the Cosmos* (Quoted page 36.)
- Kawaler, S. D. 1988, *ApJ*, 333, 236 (Quoted pages 45, 60, 61 et 62.)
- Kippenhahn, R., Ruschenplatt, G., & Thomas, H.-C. 1980, *A&A*, 91, 175 (Quoted page 39.)
- Kippenhahn, R. & Thomas, H.-C. 1970, in *IAU Colloq. 4: Stellar Rotation*, ed. A. Slettebak, 20 (Quoted pages 37, 38 et 40.)
- Kippenhahn, R., Weigert, A., & Weiss, A. 2013, *Stellar Structure and Evolution* (Quoted pages 14, 16 et 28.)
- Kochukhov, O. & Wade, G. A. 2010, *A&A*, 513, A13 (Quoted page 29.)
- Korn, A. J., Grundahl, F., Richard, O., et al. 2006, *Nature*, 442, 657 (Quoted page 33.)
- Kosovichev, A. G., Schou, J., Scherrer, P. H., et al. 1997, *Sol. Phys.*, 170, 43 (Quoted page 49.)

- Kushwaha, R. S. 1957, *ApJ*, 125, 242 (Quoted page 14.)
- Lagarde, N., Decressin, T., Charbonnel, C., et al. 2012, *A&A*, 543, A108 (Quoted pages 69 et 71.)
- Lambert, D. L., Smith, V. V., Busso, M., Gallino, R., & Straniero, O. 1995, *ApJ*, 450, 302 (Quoted page 36.)
- Landin, N. R., Ventura, P., D'Antona, F., Mendes, L. T. S., & Vaz, L. P. R. 2006, *A&A*, 456, 269 (Quoted page 39.)
- Lèbre, A., Palacios, A., Do Nascimento, Jr., J. D., et al. 2009, *A&A*, 504, 1011 (Quoted page 34.)
- Li, L., Sofia, S., Ventura, P., et al. 2009, *ApJS*, 182, 584 (Quoted page 47.)
- Li, L. H., Ventura, P., Basu, S., Sofia, S., & Demarque, P. 2006, *ApJS*, 164, 215 (Quoted page 47.)
- Lignières, F., Petit, P., Böhm, T., & Aurière, M. 2009, *A&A*, 500, L41 (Quoted page 28.)
- Lind, K., Primas, F., Charbonnel, C., Grundahl, F., & Asplund, M. 2009, *A&A*, 503, 545 (Quoted page 35.)
- Livingston, W., Wallace, L., White, O. R., & Giampapa, M. S. 2007, *ApJ*, 657, 1137 (Quoted page 31.)
- Lydon, T. J. & Sofia, S. 1995, *ApJS*, 101, 357 (Quoted pages 37, 39, 40 et 41.)
- MacGregor, K. B. & Cassinelli, J. P. 2003, *ApJ*, 586, 480 (Quoted page 28.)
- Maeder, A. 1997, *A&A*, 321, 134 (Quoted page 44.)
- Maeder, A. & Meynet, G. 2000, *ARA&A*, 38, 143 (Quoted page 74.)
- Maeder, A. & Meynet, G. 2004, *A&A*, 422, 225 (Quoted page 45.)
- Maeder, A., Meynet, G., Lagarde, N., & Charbonnel, C. 2013, *A&A*, 553, A1 (Quoted page 75.)
- Maeder, A. & Zahn, J.-P. 1998, *A&A*, 334, 1000 (Quoted pages 37, 38, 39, 44, 62, 63, 66 et 68.)
- Maehara, H., Shibayama, T., Notsu, S., et al. 2012, *Nature*, 485, 478 (Quoted page 31.)
- Marques, J. P., Goupil, M. J., Lebreton, Y., et al. 2013, *A&A*, 549, A74 (Quoted pages 39, 62 et 71.)
- Martins, F., Hillier, D. J., Bouret, J. C., et al. 2009, *A&A*, 495, 257 (Quoted page 35.)
- Martins, F. & Palacios, A. 2013, *A&A*, 560, A16 (Quoted page 74.)
- Mathis, S., Decressin, T., Eggenberger, P., & Charbonnel, C. 2013, *A&A*, 558, A11 (Quoted pages 45 et 46.)
- Mathis, S., Duez, V., & Braithwaite, J. 2011, in *IAU Symposium*, Vol. 271, *IAU Symposium*, ed. N. H. Brummell, A. S. Brun, M. S. Miesch, & Y. Ponty, 270–278 (Quoted page 28.)
- Mathis, S., Palacios, A., & Zahn, J.-P. 2004, *A&A*, 425, 243 (Quoted pages 44, 46 et 60.)
- Mathis, S., Palacios, A., & Zahn, J.-P. 2007, *A&A*, 462, 1063 (Quoted page 46.)
- Matt, S. P., MacGregor, K. B., Pinsonneault, M. H., & Greene, T. P. 2012, *ApJ*, 754, L26 (Quoted pages 45, 46 et 59.)

- Mendes, L. T. S., D'Antona, F., & Mazzitelli, I. 1999, *A&A*, 341, 174 (Quoted page 39.)
- Mendes, L. T. S., Landin, N. R., & Vaz, L. P. R. 2013, in *IAU Symposium*, Vol. 302, IAU Symposium, ed. P. Petit, M. Jardine, & H. C. Spruit (Quoted page 39.)
- Meynet, G. & Maeder, A. 1997, *A&A*, 321, 465 (Quoted pages 39 et 40.)
- Meynet, G. & Maeder, A. 2003, *A&A*, 404, 975 (Quoted pages 33 et 45.)
- Michaud, G., Charland, Y., Vauclair, S., & Vauclair, G. 1976, *ApJ*, 210, 447 (Quoted page 17.)
- Mishenina, T. V., Soubiran, C., Kovtyukh, V. V., Katsova, M. M., & Livshits, M. A. 2012, *A&A*, 547, A106 (Quoted page 33.)
- Mokiem, M. R., de Koter, A., Evans, C. J., et al. 2006, *A&A*, 456, 1131 (Quoted pages 22, 23, 32 et 33.)
- Monck, W. H. S. 1890, *The Observatory*, 13, 180 (Quoted page 21.)
- Montmerle, T. & Michaud, G. 1976, *ApJS*, 31, 489 (Quoted page 17.)
- Morgenthaler, A., Petit, P., Morin, J., et al. 2011, *Astronomische Nachrichten*, 332, 866 (Quoted pages 29 et 30.)
- Morin, J., Delfosse, X., Donati, J.-F., et al. 2011, in *SF2A-2011: Proceedings of the Annual meeting of the French Society of Astronomy and Astrophysics*, ed. G. Alecian, K. Belkacem, R. Samadi, & D. Valls-Gabaud, 503–508 (Quoted page 30.)
- Morin, J., Donati, J.-F., Petit, P., et al. 2008, *MNRAS*, 390, 567 (Quoted page 31.)
- Mosser, B., Goupil, M. J., Belkacem, K., et al. 2012a, *A&A*, 548, A10 (Quoted pages 25 et 26.)
- Mosser, B., Goupil, M. J., Belkacem, K., et al. 2012b, *A&A*, 540, A143 (Quoted page 25.)
- Nordlander, T., Korn, A. J., Richard, O., & Lind, K. 2012, *Memorie della Societa Astronomica Italiana Supplementi*, 22, 110 (Quoted page 33.)
- Palacios, A. 2013, in *EAS Publications Series*, Vol. 62, *EAS Publications Series*, 227–287 (Quoted pages 40 et 43.)
- Palacios, A. & Brun, A. S. 2007, *Astronomische Nachrichten*, 328, 1114 (Quoted page 48.)
- Palacios, A. & Brun, A. S. 2013, *ArXiv e-prints* (Quoted pages 48 et 52.)
- Palacios, A., Charbonnel, C., Talon, S., & Siess, L. 2006, *A&A*, 453, 261 (Quoted pages 38, 39, 68 et 69.)
- Palacios, A., Talon, S., Charbonnel, C., & Forestini, M. 2003, *A&A*, 399, 603 (Quoted page 38.)
- Palla, F. & Stahler, S. W. 1992, *ApJ*, 392, 667 (Quoted page 56.)
- Palla, F. & Stahler, S. W. 1993, *ApJ*, 418, 414 (Quoted page 56.)
- Pantillon, F. P., Talon, S., & Charbonnel, C. 2007, *A&A*, 474, 155 (Quoted page 40.)
- Paquette, C., Pelletier, C., Fontaine, G., & Michaud, G. 1986, *ApJS*, 61, 177 (Quoted pages 17 et 18.)
- Paxton, B., Cantiello, M., Arras, P., et al. 2013, *ApJS*, 208, 4 (Quoted page 39.)
- Penny, L. R. 1996, *ApJ*, 463, 737 (Quoted page 22.)

- Penny, L. R. & Gies, D. R. 2009, *ApJ*, 700, 844 (Quoted pages 22 et 23.)
- Petit, P., Lignières, F., Aurière, M., et al. 2011, *A&A*, 532, L13 (Quoted page 28.)
- Petit, P., Lignières, F., Wade, G. A., et al. 2010, *A&A*, 523, A41 (Quoted page 28.)
- Pinsonneault, M. H., Kawaler, S. D., Sofia, S., & Demarque, P. 1989, *ApJ*, 338, 424 (Quoted pages 39 et 43.)
- Porter, D. H. & Woodward, P. R. 2000, *ApJS*, 127, 159 (Quoted page 50.)
- Potter, A. T. 2012, PhD thesis, University of Cambridge (Quoted page 41.)
- Reiners, A. & Mohanty, S. 2012, *ApJ*, 746, 43 (Quoted pages 45 et 46.)
- Richard, O. 2012, *Memorie della Societa Astronomica Italiana Supplementi*, 22, 211 (Quoted page 34.)
- Richard, O., Michaud, G., & Richer, J. 2001, *ApJ*, 558, 377 (Quoted pages 17 et 18.)
- Richard, O., Michaud, G., & Richer, J. 2005, *ApJ*, 619, 538 (Quoted page 34.)
- Richard, O., Vauclair, S., Charbonnel, C., & Dziembowski, W. A. 1996, *A&A*, 312, 1000 (Quoted page 16.)
- Richer, J., Michaud, G., & Turcotte, S. 2000, *ApJ*, 529, 338 (Quoted page 18.)
- Royer, F., Zorec, J., & Gómez, A. E. 2007, *A&A*, 463, 671 (Quoted pages 22 et 23.)
- Rucinski, S. M. 1990, *PASP*, 102, 306 (Quoted page 22.)
- Sagert, I., Hempel, M., Greiner, C., & Schaffner-Bielich, J. 2006, *European Journal of Physics*, 27, 577 (Quoted page 10.)
- Semel, M. 1989, *A&A*, 225, 456 (Quoted page 27.)
- Sestito, P. & Randich, S. 2005, *A&A*, 442, 615 (Quoted pages 57, 58 et 61.)
- Siess, L. & Forestini, M. 1996, *A&A*, 308, 472 (Quoted page 56.)
- Siess, L., Forestini, M., & Bertout, C. 1997, *A&A*, 326, 1001 (Quoted page 56.)
- Siess, L., Forestini, M., & Bertout, C. 1999, *A&A*, 342, 480 (Quoted page 56.)
- Skumanich, A. 1972, *ApJ*, 171, 565 (Quoted pages 45 et 60.)
- Soderblom, D. R., Jones, B. F., Balachandran, S., et al. 1993, *AJ*, 106, 1059 (Quoted page 57.)
- Souleyre, A. 1898, *Bulletin de la Societe Astronomique de France et Revue Mensuelle d'Astronomie, de Meteorologie et de Physique du Globe*, 12, 304 (Quoted page 21.)
- Spruit, H. C. 1999, *A&A*, 349, 189 (Quoted pages 38, 43 et 66.)
- Spruit, H. C. 2002, *A&A*, 381, 923 (Quoted pages 38, 39, 43 et 66.)
- Stancliffe, R. J. & Eldridge, J. J. 2009, *MNRAS*, 396, 1699 (Quoted page 39.)
- Stancliffe, R. J., Glebbeek, E., Izzard, R. G., & Pols, O. R. 2007, *A&A*, 464, L57 (Quoted pages 39 et 43.)
- Takeda, Y., Sato, B., & Murata, D. 2008, *PASJ*, 60, 781 (Quoted page 52.)
- Talon, S. & Charbonnel, C. 1998, *A&A*, 335, 959 (Quoted page 33.)

- Talon, S. & Charbonnel, C. 2003, *A&A*, 405, 1025 (Quoted pages 39 et 40.)
- Talon, S. & Charbonnel, C. 2004, *A&A*, 418, 1051 (Quoted page 40.)
- Talon, S. & Charbonnel, C. 2005, *A&A*, 440, 981 (Quoted page 63.)
- Talon, S. & Charbonnel, C. 2008, *A&A*, 482, 597 (Quoted pages 40, 45 et 63.)
- Talon, S. & Zahn, J.-P. 1997, *A&A*, 317, 749 (Quoted page 44.)
- Tayar, J. & Pinsonneault, M. H. 2013, *ApJ*, 775, L1 (Quoted page 71.)
- Tayler, R. J. 1954, *ApJ*, 120, 332 (Quoted page 14.)
- Tayler, R. J. 1973, *MNRAS*, 165, 39 (Quoted page 49.)
- Théado, S., Alecian, G., LeBlanc, F., & Vauclair, S. 2012, *A&A*, 546, A100 (Quoted page 18.)
- Tout, C. A., Livio, M., & Bonnell, I. A. 1999, *MNRAS*, 310, 360 (Quoted page 56.)
- Turck-Chièze, S., Palacios, A., Marques, J. P., & Nghiem, P. A. P. 2010, *ApJ*, 715, 1539 (Quoted pages 57 et 62.)
- Turcotte, S., Richer, J., Michaud, G., Iglesias, C. A., & Rogers, F. J. 1998, *ApJ*, 504, 539 (Quoted page 17.)
- Vauclair, S. 2004, *ApJ*, 605, 874 (Quoted pages 39 et 40.)
- Vauclair, S. & Théado, S. 2003, *ApJ*, 587, 777 (Quoted page 39.)
- Vauclair, S. & Théado, S. 2012, *ApJ*, 753, 49 (Quoted page 39.)
- Viallet, M., Baraffe, I., & Walder, R. 2011, *A&A*, 531, A86 (Quoted page 47.)
- Viallet, M., Baraffe, I., & Walder, R. 2013, *A&A*, 555, A81 (Quoted page 47.)
- Wade, G. A., Grunhut, J., Alecian, E., et al. 2013, *ArXiv e-prints* (Quoted page 27.)
- Walborn, N. R., Maíz Apellániz, J., Sota, A., et al. 2011, *AJ*, 142, 150 (Quoted page 22.)
- Weiss, A., Hillebrandt, W., Thomas, H.-C., & Ritter, H. 2004, *Cox and Giuli's Principles of Stellar Structure* (Quoted page 14.)
- Woodward, P. R., Porter, D. H., & Jacobs, M. 2003, in *Astronomical Society of the Pacific Conference Series*, Vol. 293, *3D Stellar Evolution*, ed. S. Turcotte, S. C. Keller, & R. M. Cavallo, 45 (Quoted pages 50 et 51.)
- Wright, N. J., Drake, J. J., Mamajek, E. E., & Henry, G. W. 2011, *ApJ*, 743, 48 (Quoted page 31.)
- Yang, W. M. & Bi, S. L. 2006, *A&A*, 449, 1161 (Quoted page 66.)
- Zahn, J.-P. 1992, *A&A*, 265, 115 (Quoted pages 37, 38, 39, 44, 46, 49 et 59.)
- Zahn, J.-P., Brun, A. S., & Mathis, S. 2007, *A&A*, 474, 145 (Quoted page 66.)
- Zahn, J.-P., Talon, S., & Matias, J. 1997, *A&A*, 322, 320 (Quoted page 45.)
- Zhao, M., Monnier, J. D., & Che, X. 2011, in *IAU Symposium*, Vol. 272, *IAU Symposium*, ed. C. Neiner, G. Wade, G. Meynet, & G. Peters, 44–55 (Quoted page 22.)